

Reviews of Geophysics®

REVIEW ARTICLE

10.1029/2021RG000754

Key Points:

- We provide a review of glacier evolution studies in which mass transfer through ice flow is explicitly modeled (ice-dynamical modeling)
- We highlight recent advances, including the incorporation of ice dynamics when modeling glaciers at regional to global scales
- Recommendations are given concerning the steps to be considered when modeling the evolution of glaciers with an ice-dynamical setup

Supporting Information:

Supporting Information may be found in the online version of this article.

Correspondence to:

H. Zekollari,
zharry@ethz.ch;
harry.zekollari@ulb.be

Citation:

Zekollari, H., Huss, M., Farinotti, D., & Lhermitte, S. (2022). Ice-dynamical glacier evolution modeling—A review. *Reviews of Geophysics*, 60, e2021RG000754. <https://doi.org/10.1029/2021RG000754>

Received 12 JUL 2021
Accepted 5 APR 2022

Ice-Dynamical Glacier Evolution Modeling—A Review

H. Zekollari^{1,2,3,4} , M. Huss^{3,4,5}, D. Farinotti^{3,4} , and S. Lhermitte¹ 

¹Department of Geoscience and Remote Sensing, Delft University of Technology, Delft, The Netherlands, ²Laboratoire de Glaciologie, Université libre de Bruxelles, Brussels, Belgium, ³Laboratory of Hydraulics, Hydrology and Glaciology (VAW), ETH Zürich, Zürich, Switzerland, ⁴Swiss Federal Institute for Forest, Snow and Landscape Research (WSL), Birmensdorf, Switzerland, ⁵Department of Geosciences, University of Fribourg, Fribourg, Switzerland

Abstract Glaciers play a crucial role in the Earth System: they are important water suppliers to lower-lying areas during hot and dry periods, and they are major contributors to the observed present-day sea-level rise. Glaciers can also act as a source of natural hazards and have a major touristic value. Given their societal importance, there is large scientific interest in better understanding and accurately simulating the temporal evolution of glaciers, both in the past and in the future. Here, we give an overview of the state of the art of simulating the evolution of individual glaciers over decadal to centennial time scales with ice-dynamical models. We hereby highlight recent advances in the field and emphasize how these go hand-in-hand with an increasing availability of on-site and remotely sensed observations. We also focus on the gap between simplified studies that use parameterizations, typically used for regional and global projections, and detailed assessments for individual glaciers, and explain how recent advances now allow including ice dynamics when modeling glaciers at larger spatial scales. Finally, we provide concrete recommendations concerning the steps and factors to be considered when modeling the evolution of glaciers. We suggest paying particular attention to the model initialization, analyzing how related uncertainties in model input influence the modeled glacier evolution and strongly recommend evaluating the simulated glacier evolution against independent data.

Plain Language Summary Glaciers are permanent bodies of ice that move under their own weight. In contrast with ice sheets, glaciers directly affect their downstream environment through their role as natural water suppliers and their potential to generate natural hazards. Despite their limited total ice volume with respect to ice sheets (ca. 0.3 m for glaciers vs. ca. 65 m in ice sheets), glaciers are currently major sea-level rise contributors and are projected to remain so in the coming century. Given their large societal importance, there is a wide scientific interest in accurately representing the dynamics and evolution of glaciers through time. To simulate glaciers evolution over time, a wide variety of techniques exist, where the most detailed techniques account for ice-dynamical processes, that is, the movement of glaciers and mass transfer. In this review, we specifically focus on model studies that incorporate ice-dynamical processes. Ice-dynamical glacier evolution models have to date mainly been used when simulating individual glaciers, but we here also highlight how such techniques are now also starting to be used when modeling glaciers at regional to global scales. We put particular emphasis on the decision-process when designing an ice-dynamical model study, how these decisions relate to data availability, and how the modeled glacier evolution should be interpreted and be presented.

1. Introduction

The ~200,000 glaciers on Earth play a crucial role within the Earth System. Meier (1984) was one of the first to recognize that glaciers outside the ice sheets are dominant contributors to sea-level rise. Glaciers were important sea-level rise contributors over the twentieth century (e.g., Frederikse et al., 2020; Parkes & Marzeion, 2018) and have contributed to sea-level rise at even greater rates through the twenty-first century to date (e.g., Ciraci et al., 2020; Hugonnet et al., 2021; Wouters et al., 2019; Zemp et al., 2019). In the coming decades, glaciers are projected to lose a substantial part of their remaining volume, maintaining their position as one of the main contributors to sea-level rise (Edwards et al., 2021; Hock et al., 2019; Marzeion et al., 2020).

Glaciers also directly affect their neighboring environment (Figure 1). They act as natural water reservoirs, and populations living downstream are dependent on glacier runoff for water consumption, agriculture and hydropower production (e.g., Anderson & Radic, 2020; Biemans et al., 2019; Haeberli & Weingartner, 2020; Huss & Hock, 2018; Immerzeel et al., 2020; Laurent et al., 2020; Lutz et al., 2019; Pritchard, 2019; Schaeffli et al., 2019). This water supply plays an important role for biodiversity, both locally and in downstream regions

© 2022. The Authors.

This is an open access article under the terms of the Creative Commons Attribution License, which permits use, distribution and reproduction in any medium, provided the original work is properly cited.

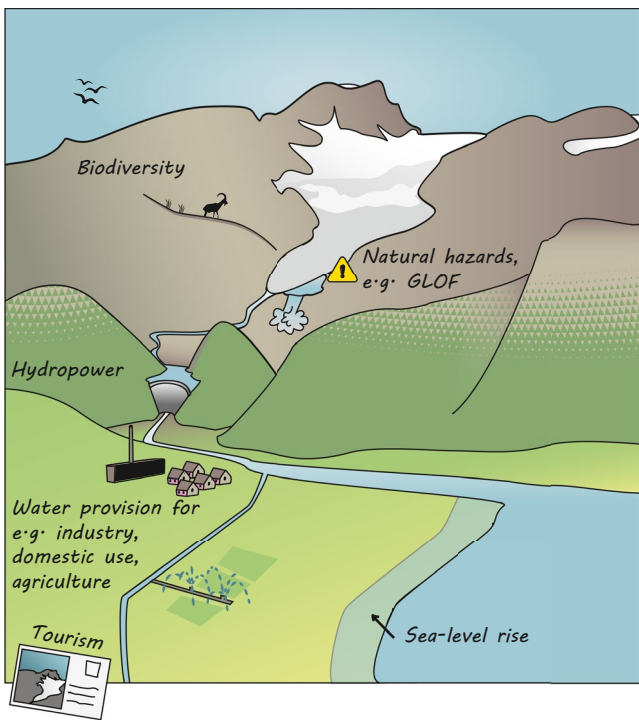


Figure 1. Schematic overview of the impact of a glacier on its direct vicinity and the downstream environment.

(e.g., Brown et al., 2018; Cauvy-Fraunié & Dangles, 2019; Fell et al., 2018; Milner et al., 2017; Yurkov et al., 2019). Glaciers furthermore have an important touristic value (e.g., Demiroglu et al., 2018; Purdie et al., 2020; Salim et al., 2021; Stewart et al., 2017; Watson & King, 2018) and can be source of major natural hazards, especially when undergoing large changes (e.g., Cook et al., 2018; Einhorn et al., 2015; Faillettaz et al., 2015; Harrison et al., 2018; Kääb et al., 2018; Veh et al., 2020). Among their many important aspects, glaciers also act as some of the clearest indicators of changing climatic conditions. Glaciers adapt their geometry to changing atmospheric and climatic conditions, and hence their changes can be used to better understand past climatic conditions (e.g., Balco, 2020; Mackintosh et al., 2017; Roe et al., 2017).

Given their paramount societal importance, there is thus major interest in simulating glacier evolution accurately over time. When modeling the temporal evolution of glaciers at regional to global scales, large-scale glacier evolution models are needed, which rely on various simplifications (see Hock et al., 2019; Marzeion et al., 2020 for overview). In turn, detailed ice-dynamical glacier evolution studies (IDGES) on individual glaciers are needed to assess the importance of these simplifications. In such detailed studies, the processes occurring at the surface, which determine the surface mass balance (SMB), are combined with ice flow processes that determine the mass transfer within glaciers. Detailed IDGES targeting individual glaciers are also important for specific applications (e.g., to forecast possible hazards, or to calculate evolution of runoff over time) and to obtain an enhanced insight in the role that physical processes have on glacier evolution (e.g., the role of debris cover, of frontal ablation and of changes in subglacial ice dynamics).

The field of ice-dynamical glacier evolution modeling has strongly evolved over recent decades. Whereas the pioneering studies from the 1980s relied on flowline approaches in which glacier motion was described based on a local stress balance (e.g., Huybrechts et al., 1989; Oerlemans, 1986), it is now common to model glaciers in 3-D while accounting for higher-order stress gradients (e.g., Jouvet & Huss, 2019; Réveillet et al., 2015). The level of sophistication for describing the mass balance has also evolved, with a shift from typically very simplified approaches (e.g., linear elevation-dependent SMB functions) to studies in which physically based melt models that include various terms of the energy balance are used.

Here, we give an overview of IDGES that simulate the temporal evolution of glaciers at decadal to centennial time scales and in which both ice dynamics and SMB processes are accounted for. The focus is on the modeling of individual glaciers, rather than on (outlet glaciers of) ice sheets (for this, refer for instance to Goelzer et al. (2017), Pattyn et al. (2017), Hindmarsh (2018), and Hanna et al. (2020)). Regional and global studies are not the focus of this review and are only addressed in the outlook, where the emphasis is mainly on their recent improvements, and how techniques and methods that were used for individual studies are now increasingly being utilized when modeling the evolution of a larger sample of glaciers. As the simulated glacier evolution depends strongly on observations (e.g., on glacier geometry) and boundary conditions (e.g., climate forcing), these model inputs are also addressed in detail in this review.

Our review (see Figure 2 for summary) aims to provide guidance when designing a glacier evolution study, taking into account the many decisions that need to be made (Table 1). For this, we review a wide range of IDGES that use flowline modeling (Table 2) and 3-D modeling (Table 3). We focus on how IDGES represent the modeling of glacier geometry (Section 2), mass balance (Section 3), and ice flow (Section 4), and how these are implemented from a numerical perspective (Section 5). Particular attention is also given to how to initialize, calibrate, and evaluate a glacier evolution model (Section 6). Next, we overview current research gaps and highlight the potential future developments for glacier evolution modeling (Section 7). Here, particular attention is given to the different types of input and how the related uncertainty should be accounted for when designing the model setup and when interpreting the model outcome. Based on this, we provide recommendations on the steps to follow when modeling the time evolution of glaciers (Section 8). Our goal is to provide a comprehensive overview, which could for

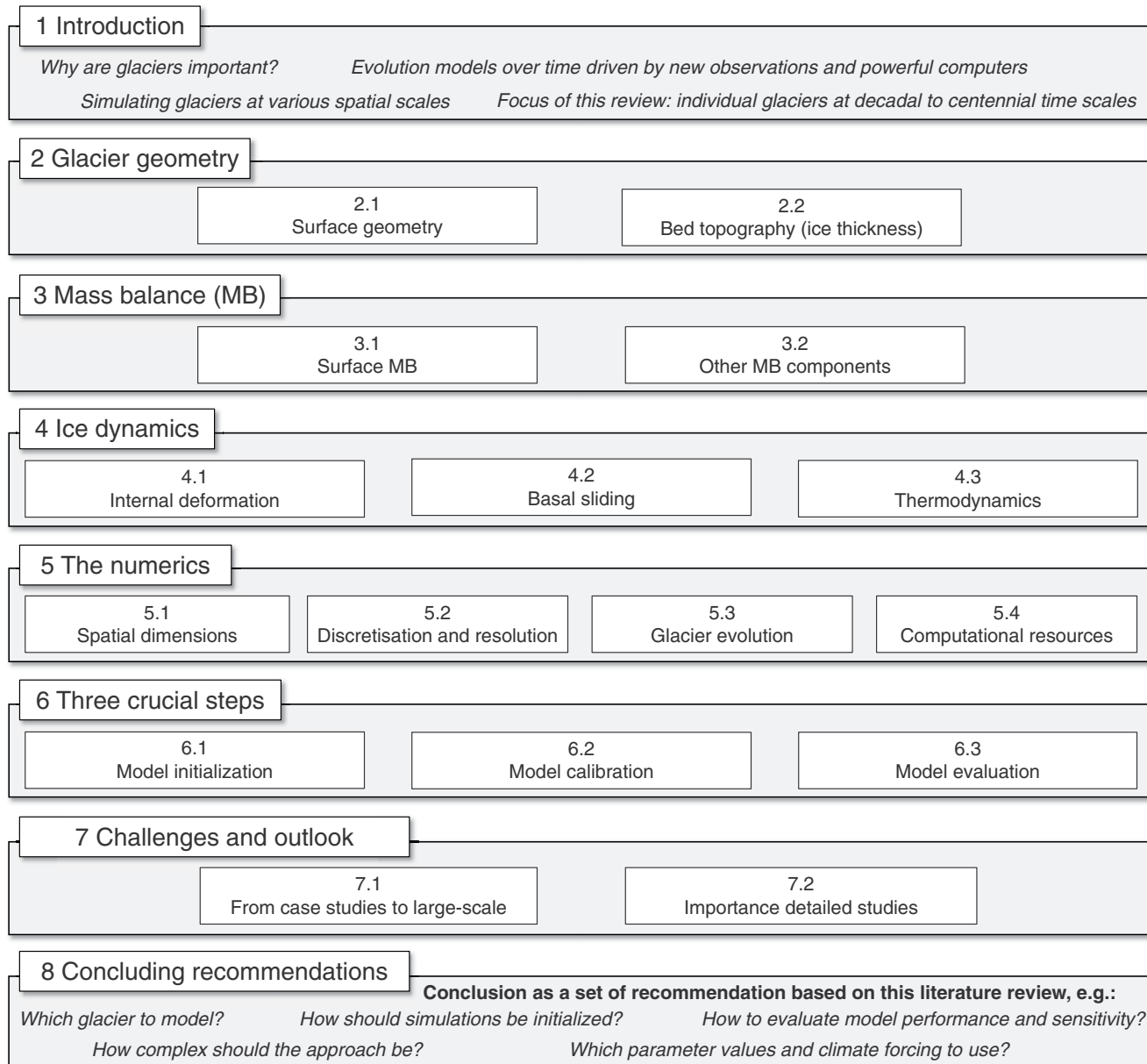


Figure 2. Overview of paper structure. The numbers refer to the sections. The wording here reflects the information contained in every section; the paper's section titles differ in some cases.

instance be used by students and early career researchers who are about to enter the field of ice-dynamical glacier evolution modeling.

2. What Is the Shape of the Glacier? Glacier Geometry Representation

When modeling the evolution of a glacier numerically, accurate information concerning the glacier geometry, that is, the surface topography and the underlying bed topography, is of crucial importance (Figure 3). Whereas the surface can be observed directly, the bed topography is more challenging to determine. Generally, the bed topography is derived by subtracting a reconstructed ice-thickness field from observations of the surface elevation.

Table 1

Comprehensive List of Statements Made in the Text and IDGES Where These Techniques Are Used/Where These Topics Are Treated

Refs	Statement	IDGES
1	Glacier geometry from topographic map	For example, Adhikari and Huybrechts (2009), De Smedt and Pattyn (2003), Hannesdóttir et al. (2015), Huybrechts et al. (1989), Jouvet et al. (2011), Laumann and Nesje (2009), Mackintosh et al. (2002), Oerlemans (1997a), Schmeits and Oerlemans (1997), Stroeven et al. (1989), and Zuo and Oerlemans (1997)
2	DEM based on airborne techniques (e.g., nation-wide DEMs)	For example, Anderson et al. (2008), Compagno et al. (2019), Giesen and Oerlemans (2010), Gilbert et al. (2017), Huss et al. (2007), Jouvet et al. (2011), Jouvet and Huss (2019), Le Meur and Vincent (2003), Réveillet et al. (2015), Schäfer et al. (2015), Zekollari et al. (2014), and Zwinger and Moore (2009)
3	Glacier geometry from SRTM	For example, Engelhardt et al. (2017), Leclercq et al. (2012), Wijngaard et al. (2019), and Ziemen et al. (2016)
4	Ice thickness measurements from radio-echo sounding	For example, Adhikari and Huybrechts (2009), Adhikari and Marshall (2013), Anderson et al. (2008), Aðalgeirs ðóttir et al. (2011, 2006), De Smedt and Pattyn (2003), Flowers et al. (2007), Gantayat et al. (2017), Giesen and Oerlemans (2010), Gilbert et al. (2020), Guðmundsson et al. (2009), Hannesdóttir et al. (2015), Huss et al. (2007), Jouvet et al. (2011), Jouvet and Huss (2019), Li et al. (2017), Mackintosh et al. (2002), Marshall et al. (2005), Réveillet et al. (2015), Rowan et al. (2015), Schlosser (1997), Schmidt et al. (2020), Sugiyama et al. (2007), Wang et al. (2019), Zekollari, Huybrechts, et al. (2017), Zekollari et al. (2014), Zhao et al. (2014), and Zwinger and Moore (2009)
5	Assuming plastic flow for ice thickness reconstruction	For example, Anderson et al. (2008), Giesen and Oerlemans (2010), Greuell (1992), Huybrechts et al. (1989), Laumann and Nesje (2009), Rowan et al. (2015), Stroeven et al. (1989), Wallinga and van de Wal (1998), Wijngaard et al. (2019), and Zekollari et al. (2013)
6	Reconstruct ice thickness by minimizing misfit with observations	For example, Kruss and Smith (1982), Laumann and Nesje (2009), Leclercq et al. (2012), Oerlemans (1997b), Schmeits and Oerlemans (1997), and Wallinga and van de Wal (1998)
7	Data collected by automatic weather stations	For example, Adhikari and Marshall (2013), Gantayat et al. (2017), Giesen and Oerlemans (2010), Gilbert et al. (2020), Li et al. (2017), and Zhao et al. (2014)
8	Data from meteorological stations and upscaling to the glacier level	For example, Aðalgeirs ðóttir et al. (2011 (2006), Compagno et al. (2019), Flowers et al. (2007 (2005), Gantayat et al. (2017), Giesen and Oerlemans (2010), Gilbert et al. (2017), Guðmundsson et al. (2009), Hannesdóttir et al. (2015), Huss et al. (2007), Johannesson (1997), Jouvet et al. (2011 (2009), Laumann and Nesje (2009), Li et al. (2017), Mackintosh et al. (2002), Marshall et al. (2005), Oerlemans (1997a), Schlosser (1997), Schneeberger et al. (2001), Wallinga and van de Wal (1998), Wijngaard et al. (2019), Zekollari, Huybrechts, et al. (2017), and Zekollari et al. (2014))
9	Past climatic conditions simulated from RCM or GCMs	For example, Engelhardt et al. (2017), Schmidt et al. (2020), Wijngaard et al. (2019), Zekollari, Huybrechts, et al. (2017), Zhao et al. (2014), and Ziemen et al. (2016)

Table 1
Continued

Refs	Statement	IDGES
10	Use of tree ring data	For example, Leclercq et al. (2012), Oerlemans (1986), Schlosser (1997), and Stroeven et al. (1989)
11	Future climate from (/inspired on) GCM simulation	For example, Adhikari and Marshall (2013), Anderson et al. (2008), Flowers et al. (2005), Giesen and Oerlemans (2010), Gilbert et al. (2017), Le Meur et al. (2007), Marshall et al. (2005), Réveillet et al. (2015), Schäfer et al. (2015), and Schneeberger et al. (2001)
12	Future climate from (/inspired on) RCM simulation	For example, Aðalgeirsdóttir et al. (2011, 2006), Engelhardt et al. (2017), Guðmundsson et al. (2009), Huss et al. (2007), Jouvet et al. (2011 (2009), Jouvet and Huss (2019), Laumann and Nesje (2009 (2014), Li et al. (2017), Schmidt et al. (2020), Zekollari et al. (2014), Zhao et al. (2014), and Ziemen et al. (2016)
13	SRES future climate scenarios	For example, Aðalgeirsdóttir et al. (2011 (2006), Duan et al. (2012), Giesen and Oerlemans (2010), Guðmundsson et al. (2009), Jouvet et al. (2011), Laumann and Nesje (2009 (2014), Le Meur et al. (2007), and Li et al. (2017)
14	RCP future climate scenarios	For example, Adhikari and Marshall (2013), Engelhardt et al. (2017), Gantayat et al. (2017), Gilbert et al. (2017), Jouvet and Huss (2019), Réveillet et al. (2015), Schäfer et al. (2015), Schmidt et al. (2020), Wang et al. (2019), Zekollari, Huybrechts, et al. (2017), and Ziemen et al. (2016)
15	Direct use of elaborate SMB observation	For example, Albrecht et al. (2000), Le Meur and Vincent (2003), Schneeberger et al. (2001), Vincent et al. (2000), and Zwinger and Moore (2009)
16	Elevation-dependent representation of the SMB	For example, Adhikari and Huybrechts (2009), Adhikari and Marshall (2013), Allison and Kruss (1977), De Smedt and Pattyn (2003), Gantayat et al. (2017), Huybrechts et al. (1989), Laumann and Nesje (2014), Letréguilly and Reynaud (1989), Li et al. (2017), Oerlemans (1986, 1997b), Réveillet et al. (2015), Rowan et al. (2015), Stroeven et al. (1989), Sugiyama et al. (2007), Wang et al. (2019), and Zhao et al. (2014)
17	Temperature threshold to distinguish between snow and rain accumulation	For example, Aðalgeirsdóttir et al. (2011, 2006), Duan et al. (2012), Engelhardt et al. (2017), Flowers et al. (2007, 2005), Gilbert et al. (2020), Hannesdóttir et al. (2015), Huss et al. (2007), Jouvet et al. (2011), Leclercq et al. (2012), Schäfer et al. (2015), Schmidt et al. (2020), Zekollari, Huybrechts, et al. (2017), Zekollari et al. (2014), and Ziemen et al. (2016).
18	Accounting for refreezing of meltwater	For example, Aðalgeirsdóttir et al. (2006), Duan et al. (2012), Flowers et al. (2005), Gilbert et al. (2020), Hannesdóttir et al. (2015), Schäfer et al. (2015), Zekollari, Huybrechts, et al. (2017), and Zwinger and Moore (2009)

Table 1
Continued

Refs	Statement	IDGES
19	PDD modeling for SMB	For example, Anderson et al. (2008), Aðalgeirsdóttir et al. (2011, 2006), Compagno et al. (2019), Duan et al. (2012), Flowers et al. (2007 (2005), Gilbert et al. (2020, 2017), Guðmundsson et al. (2009), Hannesdóttir et al. (2015), Huss et al. (2007), Johannesson (1997), Jouvet et al. (2011 (2009), Jouvet and Huss (2019), Li et al. (2017), Schäfer et al. (2015), Schneeberger et al. (2001), Wijngaard et al. (2019), Zekollari, Huybrechts, et al. (2017), Zhao et al. (2014), and Ziemen et al. (2016)
20	SMB modeled through simple energy balance model	For example, Engelhardt et al. (2017), Leclercq et al. (2012), Schmeits and Oerlemans (1997), and Zekollari et al. (2014)
21	SMB from full-energy balance modeling	For example, Giesen and Oerlemans (2010), Le Meur et al. (2007), Mackintosh et al. (2002), Oerlemans (1997a), and Schmidt et al. (2020)
22	Debris cover accounted for	For example, Huss et al. (2007), Jouvet et al. (2011), Rowan et al. (2015), and Wijngaard et al. (2019)
23	Basal mass balance modeled	For example, Flowers et al. (2005, 2007), Marshall et al. (2005), and Rowan et al. (2015)
24	Elevation threshold for basal sliding	For example, Aðalgeirsdóttir et al. (2006), De Smedt and Pattyn (2003), Jouvet et al. (2011 (2009), Réveillet et al. (2015), and Sugiyama et al. (2007)
25	Basal motion explicitly set to zero through no-slip boundary condition	For example, Adhikari and Marshall (2013), Li et al. (2017), Zhao et al. (2014), and Zwinger and Moore (2009)
26	Basal sliding related to third power of basal drag	For example, Oerlemans (1986, 1997a, 1997b), Adhikari and Huybrechts (2009), Anderson et al. (2008), Aðalgeirsdóttir et al. (2011, 2006), Compagno et al. (2019), De Smedt and Pattyn (2003), Engelhardt et al. (2017), Gantayat et al. (2017), Giesen and Oerlemans (2010), Hannesdóttir et al. (2015), Jouvet et al. (2011 (2009), Jouvet and Huss (2019), Laumann and Nesje (2009 (2014), Le Meur et al. (2007), Le Meur and Vincent (2003), Leclercq et al. (2012), Mackintosh et al. (2002), Schmeits and Oerlemans (1997), Stroeven (1996), Stroeven et al. (1989), Wallinga and van de Wal (1998), Zekollari, Huybrechts, et al. (2017), Zekollari et al. (2014), and Zuo and Oerlemans (1997)
27	Basal sliding related to third power of basal drag, divided by pressure	For example, De Smedt and Pattyn (2003), Greuell (1992), Oerlemans (1986), Schlosser (1997), Schmeits and Oerlemans (1997), Stroeven (1996), Stroeven et al. (1989), Wallinga and van de Wal (1998)
28	Linear relationship between basal drag and sliding	For example, Allison and Kruss (1977), Flowers et al. (2007 (2005), Gilbert et al. (2020 (2017), Marshall et al. (2005), Réveillet et al. (2015), Schäfer et al. (2015), Sugiyama et al. (2007), and Wang et al. (2019)
29	Basal sliding implicitly included in the treatment of internal deformation	For example, Adhikari and Marshall (2013), Albrecht et al. (2000), Aðalgeirsdóttir et al. (2011 (2006), Guðmundsson et al. (2009), Hannesdóttir et al. (2015), Huybrechts et al. (1989), Johannesson (1997), Schneeberger et al. (2001), and Wijngaard et al. (2019)

Table 1
Continued

Refs	Statement	IDGES
30	Glaciers in European Alps assumed to be isothermal	For example, Compagno et al. (2019), Huybrechts et al. (1989), Jouvet et al. (2011 (2009), Jouvet and Huss (2019), Le Meur et al. (2004), Schmeits and Oerlemans (1997), and Zekollari et al. (2014)
31	Glaciers in Scandinavia assumed to be isothermal	For example, Albrecht et al. (2000), Giesen and Oerlemans (2010), Laumann and Nesje (2014), Oerlemans (1986), and Schneeberger et al. (2001)
32	Glaciers in Iceland assumed to be isothermal	For example, Aðalgeirsdóttir et al. (2011), Flowers et al. (2007, 2005), Marshall et al. (2005), and Schmidt et al. (2020)
33	Thermodynamics through conservation of energy with heat fluxes	For example, Gilbert et al. (2020, 2017), Li et al. (2017), Zekollari, Huybrechts, et al. (2017), Zhao et al. (2014), and Zwinger and Moore (2009)
34	Thermodynamics at the glacier by accounting for geothermal heat flux	For example, Flowers et al. (2007 (2005), Gilbert et al. (2020), Li et al. (2017), Marshall et al. (2005), Rowan et al. (2015), Schäfer et al. (2015), Zekollari, Huybrechts, et al. (2017), Zhao et al. (2014), and Zwinger and Moore (2009)
35	First efforts glacier flowline modeling	For example, Allison and Kruss (1977), Bindschadler et al. (1977), Budd (1975), Budd and Jenssen (1975), Budd and McInnes (1974), Kruss (1983, 1984), Kruss and Smith (1982), Oerlemans (1986), and Untersteiner and Nye (1968)
36	Flowline modeling in the late 1980s and 1990s	For example, Greuell (1992), Huybrechts et al. (1989), Letréguilly and Reynaud (1989), Oerlemans (1997a, 1997b), Oerlemans et al. (1998), Schlosser (1997), Schmeits and Oerlemans (1997), Stroeven et al. (1989), Wallinga and van de Wal (1998), and Zuo and Oerlemans (1997)
37	Flowline modeling by connecting several independent flowlines	For example, Engelhardt et al. (2017), Gantayat et al. (2017), Schlosser (1997), Schmeits and Oerlemans (1997), Stroeven (1996), and Zuo and Oerlemans (1997)
38	Manual detection of flowlines	For example, Adhikari and Huybrechts (2009), Adhikari and Marshall (2013), De Smedt and Pattyn (2003), Gantayat et al. (2017), Huybrechts et al. (1989), Laumann and Nesje (2009), Mackintosh et al. (2002), Oerlemans (1997a), Schmeits and Oerlemans (1997), Stroeven et al. (1989), and Vincent et al. (2000)
39	Glacier cross section geometry represented as trapezoid	For example, Oerlemans (1986, 1997a, 1997b), Adhikari and Huybrechts (2009), Anderson et al. (2008), Engelhardt et al. (2017), Gantayat et al. (2017), Greuell (1992), Laumann and Nesje (2009), Leclercq et al. (2012), Schlosser (1997), Schmeits and Oerlemans (1997), Stroeven (1996), and Wallinga and van de Wal (1998)
40	Accounting for non-local stresses in flowline modeling	For example, Adhikari and Marshall (2011 (2012), Duan et al. (2012), Greuell (1992), and Hubbard (2000)
41	3-D model using the SIA	For example, Aðalgeirsdóttir et al. (2011, 2006), Flowers et al. (2007 (2005), Giesen and Oerlemans (2010), Guðmundsson et al. (2009), Hannesdóttir et al. (2015), Laumann and Nesje (2014), Le Meur et al. (2007), Le Meur and Vincent (2003), and Vincent et al. (2004)

Table 1
Continued

Ref	Statement	IDGES
42	3-D model accounting for higher-order/full-Stokes stresses	For example, Adhikari and Marshall (2013), Albrecht et al. (2000), Compagno et al. (2019), Gilbert et al. (2020) (2017), Jouvet et al. (2011) (2009), Jouvet and Huss (2019), Li et al. (2017), Réveillet et al. (2015), Schäfer et al. (2015), Schneeberger et al. (2001), Zekollari, Huybrechts, et al. (2017), Zekollari et al. (2014), Zhao et al. (2014), and Zwinger and Moore (2009)
43	Finite difference approaches	For example, Aðalgeirsdóttir et al. (2006), Flowers et al. (2007, 2005), Le Meur and Vincent (2003), Marshall et al. (2005), Wijngaard et al. (2019), and Zekollari et al. (2014)
44	Grid resolution of (few) hundreds of meters	For example, Oerlemans (1986, 1997a, 1997b), Allison and Kruss (1977), Greuell (1992), Huybrechts et al. (1989), Johannesson (1997), Kruss and Smith (1982), Letréguilly and Reynaud (1989), Schlosser (1997), Stroeven (1996), Stroeven et al. (1989), and Zuo and Oerlemans (1997)
45	Grid resolution of few tens of meters	For example, Le Meur et al. (2007), Le Meur and Vincent (2003), Wijngaard et al. (2019), and Zekollari et al. (2014)
46	Triangular elements used in finite elements methods	For example, Aðalgeirsdóttir et al. (2011), Duan et al. (2012), Gilbert et al. (2020), Hannesdóttir et al. (2015), Li et al. (2017), and Réveillet et al. (2015)
47	Finite elements on the order of few tens of meters	For example, Compagno et al. (2019), Gilbert et al. (2020), Jouvet et al. (2009), Li et al. (2017), Réveillet et al. (2015), Wang et al. (2019), and Zhao et al. (2014)
48	Grid elements fixed in size throughout simulation	For example, Jouvet et al. (2009), Jouvet and Huss (2019), Réveillet et al. (2015), Schäfer et al. (2015), and Zwinger and Moore (2009)
49	Finite element approaches in higher-order/full-Stokes models	For example, Adhikari and Marshall (2013), Duan et al. (2012), Gilbert et al. (2020, 2017), Jouvet et al. (2011, 2009), Jouvet and Huss (2019), Li et al. (2017), Réveillet et al. (2015), Schäfer et al. (2015), Zhao et al. (2014), and Zwinger and Moore (2009)
50	Ice density of 900 kg m^{-3}	For example, Aðalgeirsdóttir et al. (2011), Gantayat et al. (2017), Giesen and Oerlemans (2010), Huss et al. (2007), and Leclercq et al. (2012)
51	Ice density of 910 kg m^{-3}	For example, Adhikari and Marshall (2013), Anderson et al. (2008), Li et al. (2017), Wang et al. (2019), Zhao et al. (2014), and Zwinger and Moore (2009)
52	Ice density of 917 kg m^{-3}	For example, Gilbert et al. (2020), Le Meur and Vincent (2003), Réveillet et al. (2015), and Wijngaard et al. (2019)
53	Explicit numerical schemes in flowline studies	For example, Oerlemans (1986, 1992, 1997a, 1997b), Adhikari and Huybrechts (2009), Anderson et al. (2008), Gantayat et al. (2017), Greuell (1992), Laumann and Nesje (2009), Leclercq et al. (2012), Schlosser (1997), Schmeits and Oerlemans (1997), and Zuo and Oerlemans (1997)
54	Explicit numerical schemes in 3-D studies	For example, Albrecht et al. (2000), Laumann and Nesje (2014), Rowan et al. (2015), and Wijngaard et al. (2019)

Table 1
Continued

Refs	Statement	IDGES
55	Implicit numerical methods	For example, De Smedt and Pattyn (2003), Jouvet et al. (2009), Schäfer et al. (2015), and Zwinger and Moore (2009)
56	(sub)daily (ca. 0.00025–0.003 a) time step	(sub)daily (ca. 0.00025–0.003 a), for example, Gantayat et al. (2017), Huss et al. (2007), Leclercq et al. (2012), Rowan et al. (2015), Wijngaard et al. (2019), and Ziemen et al. (2016)
57	(half-)weekly (0.01–0.025 a) time step	For example, De Smedt and Pattyn (2003), Flowers et al. (2005), Giesen and Oerlemans (2010), Greuell (1992), Marshall et al. (2005), Oerlemans (1997b), Rowan et al. (2015), Schmeits and Oerlemans (1997), Sugiyama et al. (2007), and Zekollari et al. (2014)
58	(half-)monthly to half-yearly (0.05–0.5 a) time step	For example, Adhikari and Marshall (2013), Gilbert et al. (2017), Jouvet et al. (2011 (2009)), Le Meur and Vincent (2003), and Schäfer and Le Meur (2007)
59	Annual time steps	For example, Compagno et al. (2019), Gilbert et al. (2020), Johannesson (1997), Schäfer et al. (2015), and Zwinger and Moore (2009)
60	Mass balance updated once a year	For example, Giesen and Oerlemans (2010), Greuell (1992), Hannesdóttir et al. (2015), Marshall et al. (2005), Schäfer et al. (2015), Zekollari, Huybrechts, et al. (2017), and Zekollari et al. (2014)
61	Mass balance time step on the order of minutes to days	For example, Aðalgeirsdóttir et al. (2006), Huss et al. (2007), Jouvet et al. (2011, 2009), Jouvet and Huss (2019), Le Meur et al. (2007), Oerlemans (1997a), Schmidt et al. (2020), and Zekollari et al. (2014)
62	Starting geometry from observed state	For example, Albrecht et al. (2000), Compagno et al. (2019), Jouvet et al. (2011, 2009), Jouvet and Huss (2019), Li et al. (2017), Schneeberger et al. (2001), and Zwinger and Moore (2009)
63	Starting geometry is a steady state	For example, Aðalgeirsdóttir et al. (2006), Gilbert et al. (2017), Gilbert et al. (2020), Guðmundsson et al. (2009), Hannesdóttir et al. (2015), Johannesson (1997), Laumann and Nesje (2014), Rowan et al. (2015), Schmidt et al. (2020), Wang et al. (2019), and Zekollari, Huybrechts, et al. (2017)
64	Starting geometry is from historical run	For example, Allison and Kruss (1977), Anderson et al. (2008), Aðalgeirsdóttir et al. (2011), Engelhardt et al. (2017), Flowers et al. (2005), Gantayat et al. (2017), Huybrechts et al. (1989), Laumann and Nesje (2009), Mackintosh et al. (2002), Oerlemans (1997b), Schmeits and Oerlemans (1997), Stroeven (1996), Stroeven et al. (1989), Vincent et al. (2000), and Zekollari et al. (2014)
65	“Dynamic calibration” of model to match past observed glacier changes	For example, Adhikari and Huybrechts (2009), De Smedt and Pattyn (2003), Giesen and Oerlemans (2010), Leclercq et al. (2012), Mackintosh et al. (2002), Oerlemans (1997b), Oerlemans et al. (1998), Schmeits and Oerlemans (1997), Wallinga and van de Wal (1998), Zekollari et al. (2014), and Zuo and Oerlemans (1997)
66	Use of geodetic observations for SMB calibration	For example, Compagno et al. (2019), Gilbert et al. (2020, 2017), Huss et al. (2007), Jouvet et al. (2011, 2009), Jouvet and Huss (2019), and Sugiyama et al. (2007)

Table 1
Continued

Refs	Statement	IDGES
67	Calibration SMB to reproduce in situ observations	For example, Adhikari and Huybrechts (2009), Adhikari and Marshall (2013), Aðalgeirsdóttir et al. (2006, 2011), Engelhardt et al. (2017), Flowers et al. (2007), Giesen and Oerlemans (2010), Gilbert et al. (2017, 2020), Hannesdóttir et al. (2015), Jouvet et al. (2009, 2011), Jouvet and Huss (2019), Mackintosh et al. (2002), Réveillet et al. (2015), Zekollari et al. (2014), and Ziemen et al. (2016)
68	Calibration SMB to match geometry at a given date	For example, Flowers et al. (2007, 2005), Gantayat et al. (2017), Oerlemans (1997a), and Rowan et al. (2015)
69	Calibration of SMB model parameters	For example, Adhikari and Huybrechts (2009), Adhikari and Marshall (2013), Aðalgeirsdóttir et al. (2011, 2006), Compagno et al. (2019), Engelhardt et al. (2017), Flowers et al. (2007), Giesen and Oerlemans (2010), Gilbert et al. (2020, 2017), Hannesdóttir et al. (2015), Huss et al. (2007), Johannesson (1997), Jouvet et al. (2011 (2009)), Jouvet and Huss (2019), Mackintosh et al. (2002), Oerlemans (1997a), Réveillet et al. (2015), Rowan et al. (2015), Schneeberger et al. (2001), Sugiyama et al. (2007), Zekollari, Huybrechts, et al. (2017), and Ziemen et al. (2016)
70	Modification of precipitation to match SMB	For example, Flowers et al. (2007), Giesen and Oerlemans (2010), Gilbert et al. (2020), Johannesson (1997), Laumann and Nesje (2009), Leclercq et al. (2012), Mackintosh et al. (2002), Schmeits and Oerlemans (1997), and Ziemen et al. (2016)
71	Ice flow model calibration to match observed surface velocities	For example, Albrecht et al. (2000), Anderson et al. (2008), Compagno et al. (2019), De Smedt and Pattyn (2003), Gilbert et al. (2020 (2017)), Jouvet et al. (2011 (2009)), Kruss and Smith (1982), Réveillet et al. (2015), Schaefer et al. (2015), Schmidt et al. (2020), Stroeven (1996), Sugiyama et al. (2007), Wang et al. (2019), and Zekollari et al. (2013)
72	Ice flow model calibration to match observed length or volume changes	For example, Aðalgeirsdóttir et al. (2011, 2006), Greuell (1992), Jouvet et al. (2009), Le Meur and Vincent (2003), and Schlosser (1997)
73	Ice flow model calibration to match observed geometry	For example, Adhikari and Huybrechts (2009), Compagno et al. (2019), De Smedt and Pattyn (2003), Gantayat et al. (2017), Hannesdóttir et al. (2015), Huybrechts et al. (1989), Mackintosh et al. (2002), Stroeven (1996), and Stroeven et al. (1989)

Table 1
Continued

Refs	Statement	IDGES
74	Calibration by modifying the rate factor	For example, Adhikari and Huybrechts (2009), Adhikari and Marshall (2013), Albrecht et al. (2000), Anderson et al. (2008), Aðalgeirsdóttir et al. (2011, 2006), Compagno et al. (2019), De Smedt and Pattyn (2003), Giesen and Oerlemans (2010), Greuell (1992), Hannesdóttir et al. (2015), Huybrechts et al. (1989), Jouvet et al. (2011, 2009), Laumann and Nesje (2009, 2014), Le Meur and Vincent (2003), Letréguilly and Reynaud (1989), Mackintosh et al. (2002), Schlosser (1997), Schmeits and Oerlemans (1997), Schmidt et al. (2020), Schneeberger et al. (2001), Stroeven (1996), Stroeven et al. (1989), Wallinga and van de Wal (1998), Wang et al. (2019), Wijngaard et al. (2019), Zekollari et al. (2014), and Zuo and Oerlemans (1997)
75	Calibration of sliding parameter	For example, Adhikari and Huybrechts (2009), Anderson et al. (2008), Aðalgeirsdóttir et al. (2011, 2006), Compagno et al. (2019), De Smedt and Pattyn (2003), Flowers et al. (2007, 2005), Gilbert et al. (2020, 2017), Greuell (1992), Jouvet et al. (2011, 2009), Laumann and Nesje (2014), Le Meur and Vincent (2003), Mackintosh et al. (2002), Réveillet et al. (2015), Schäfer et al. (2015), Schlosser (1997), Schmeits and Oerlemans (1997), Stroeven (1996), Sugiyama et al. (2007), Wallinga and van de Wal (1998), Wang et al. (2019), Zekollari et al. (2013), and Ziemen et al. (2016)
76	Calibration of spatially varying sliding parameter	For example, Sugiyama et al. (2007), Réveillet et al. (2015), Schäfer et al. (2015), and Gilbert et al. (2017, 2020)
77	Model evaluation by comparing to observed SMB	For example, Aðalgeirsdóttir et al. (2011), Engelhardt et al. (2017), Giesen and Oerlemans (2010), Guðmundsson et al. (2009), Huss et al. (2007), Johannesson (1997), Le Meur et al. (2007), Mackintosh et al. (2002), Schmidt et al. (2020), Vincent et al. (2000), and Zekollari (Huybrechts et al. 2017)
78	Model evaluation by comparing to observed surface velocities	For example, Allison and Kruss (1977), Aðalgeirsdóttir et al. (2011), Duan et al. (2012), Engelhardt et al. (2017), Gantayat et al. (2017), Huybrechts et al. (1989), Letréguilly and Reynaud (1989), Rowan et al. (2015), Schmidt et al. (2020), Stroeven et al. (1989), Vincent et al. (2000), Wallinga and van de Wal (1998), Wijngaard et al. (2019), Zekollari, Huybrechts, et al. (2017), Zuo and Oerlemans (1997), and Zwinger and Moore (2009)
79	Model evaluation by comparing to observed glacier geometries	For example, Adhikari and Huybrechts (2009), Albrecht et al. (2000), Compagno et al. (2019), Engelhardt et al. (2017), Gantayat et al. (2017), Giesen and Oerlemans (2010), Gilbert et al. (2020), Guðmundsson et al. (2009), Hannesdóttir et al. (2015), Huybrechts et al. (1989), Jouvet et al. (2011), Marshall et al. (2005), Rowan et al. (2015), Schmidt et al. (2020), Vincent et al. (2000), Wallinga and van de Wal (1998), Wang et al. (2019), Wijngaard et al. (2019), Zekollari, Huybrechts, et al. (2017) (Zekollari et al. (2014)), and Zuo and Oerlemans (1997)

Table 1
Continued

Refs	Statement	IDGES
80	Model evaluation by comparing to observed glacier geometry changes	For example, Anderson et al. (2008), Aðalgeirsdóttir et al. (2011), Compagno et al. (2019), Giesen and Oerlemans (2010), Greuell (1992), Hannesdóttir et al. (2015), Huss et al. (2007), Jouvet et al. (2011) (2009), Li et al. (2017), Réveillet et al. (2015), Rowan et al. (2015), Schmidt et al. (2020), Wallinga and van de Wal (1998), Wijngaard et al. (2019), Zekollari, Huybrechts, et al. (2017), Zekollari et al. (2014), Zhao et al. (2014), and Zwinger and Moore (2009)
81	Studies investigating the SMB—surface elevation feedback	For example, Giesen and Oerlemans (2010), Marshall et al. (2005), Oerlemans (1992), Schäfer et al. (2015), Schmidt et al. (2020), Zekollari, Huybrechts, et al. (2017), and Ziemen et al. (2016)
82	Studies investigating the effect of glacier changes on river runoff	For example, Aðalgeirsdóttir et al. (2011, 2006), Engelhardt et al. (2017), Flowers et al. (2007, 2005), Guðmundsson et al. (2009), Johannesson (1997), Li et al. (2017), and Wang et al. (2019)
83	Studies that provide insights in the glacier response time	For example, Adhikari et al. (2011), Adhikari and Huybrechts (2009), Adhikari and Marshall (2013), Anderson et al. (2008), De Smedt and Pattyn (2003), Gantayat et al. (2017), Greuell (1992), Huybrechts et al. (1989), Johannesson (1997), Jouvet et al. (2011), Jouvet and Huss (2019), Laumann and Nesje (2009), Le Meur and Vincent (2003), Leclercq et al. (2012), Letréguilly and Reynaud (1989), Oerlemans (1997a, 1997b), Rowan et al. (2015), Schmeits and Oerlemans (1997), Schmidt et al. (2020), Zekollari and Huybrechts (2015), Ziemen et al. (2016), and Zuo and Oerlemans (1997)
84	Studies deriving past climatic information from glacier simulations at decadal to centennial time scales	For example, Allison and Kruss (1977), Flowers et al. (2007), Huybrechts et al. (1989), Le Meur et al. (2004), Leclercq et al. (2012), Mackintosh et al. (2002), Oerlemans (1997a, 1997b), Smith and Budd (1979), and Stroeven et al. (1989)
85	Downscaling climatic data	For example, Engelhardt et al. (2017), Flowers et al. (2005), Gilbert et al. (2017), Hannesdóttir et al. (2015), Marshall et al. (2005), Schäfer et al. (2015), Schneeberger et al. (2001), Wijngaard et al. (2019), and Ziemen et al. (2016)

Note. For IDGES statements with three or fewer references, the references are immediately provided in the text; while for statements with four or more references, reference is made to this table. All the IDGES studies referenced here are included in Tables 2 and 3. IDGES, ice-dynamical glacier evolution study.

2.1. Surface Geometry

IDGES that consider older glacier geometries often rely on topographic maps, from which the information needs to be extracted (Table 1, refs 1). Airborne techniques are often used to create digital elevation models (DEMs) at regional scales, which can then be used directly in IDGES (Table 1, refs 2). More recently, DEMs derived from satellite products have become available, and such products have also been used in IDGES, including SRTM (Shuttle Radar Topography Mission, Table 1, refs 3), ASTER (Advanced Spaceborne Thermal Emission and Reflection Radiometer; used by Adhikari and Marshall (2013), Rowan et al. (2015), and Gantayat et al. (2017)) and SPOT5 (Satellite pour l'Observation de la Terre; used by e.g., Schmidt et al. (2020)). Some of these DEMs are not spatially complete (either by design or because of data gaps), an issue that is being solved through high-resolution DEMs such as WorldDEM and the related Copernicus DEM (Riegler et al., 2015), which will become valuable tools for future IDGES.

Table 2
Overview of Transient Flowline IDGES

Glacier and reference	Geometric information (DEM, ice thickness, flowline, ...)	Horizontal and time resolution	Time period	Ice flow (model type, parameters, ...)	Initialization and calibration	Validation	Additional notes
Argentière, France (Huybrechts et al., 1989)	Few measurements on ice thickness along flow line. Extended using plastic flow theory. Surface elevation from topographical map	$\Delta x = 250$ m. $\Delta t = 0.1$ a	1000–2000	SIA flowline model (parabolic cross section), basal sliding not explicitly modeled. Calibrated rate factor 0.8×10^{-16} Pa $^{-3}$ a $^{-1}$	Linear fit to observed mean mass balance for period 1976–1983. Different climatic series/proxies combined for transient run	Start with zero ice thickness in 1000 CE. Rate factor calibrated to have 1980 steady state length close to observation	Reproduce the observed ice thickness, surface elevation and velocities (slightly higher values obtained in modeling in general)
Glacier AX010, Nepal (Adhikari & Huybrechts, 2009)	Bed topography in parts known from radio echo sounding. DEM from 1996 topographic map	$\Delta x = 10$ m. $\Delta t = 0.01$ a	1200–2100	SIA flowline model with trapezoidal shape accounting for internal deformation and for basal motion: $a = 2.0 \times 10^{-18}$ Pa $^{-3}$ N $^{-3}$ a $^{-1}$. $a_s = 6.0 \times 10^{-14}$ m 8	Linear mass balance function, with perturbations obtained from temperature forcing. Past forcing from ice core and nearby meteorological stations	Starting point simulations is zero ice thickness in 1200 CE. Modeling glacier in 2006 as steady state for model calibration: ice flow parameters tuned to match observed glacier geometry.	Comparison modeled and observed present-day glacier geometry
Blanc, France (Leréguilly & Reynaud, 1989)	Ice thickness known close to front from drillings and in accumulation basin from seismic data	$\Delta x = 200$ m. $\Delta t = 0.1$ a	1882–1985, and beyond (constant MB forcing)	SIA flowline model, basal sliding not explicitly modeled. Solving continuity equation as diffusion-type equation. Rate factor of 0.2×10^{-16} Pa $^{-3}$ a $^{-1}$	Parabolic function to describe SMB. Time evolution based on time series from nearby glacier de Sarenne	Rate factor calculated for typical values in accumulation basin. Start from zero ice thickness and apply the 1882–1887 SMB during 600 years.	Qualitative comparison to the observed surface velocities and past glacier length fluctuations

Table 2
Continued

Glacier and reference	Geometric information (DEM, ice thickness, flowline, ...)	Horizontal and time resolution	Time period	Ice flow (model type, parameters, ...)	Initialization and calibration	Validation	Mass balance (model type, parameters, climatic info treatment, basal and frontal MB, ...)	Additional notes
Briksdalbreen (Laumann & Nesje, 2009)	Surface geometry from two topographic maps. Ice thickness measured in accumulation area, extrapolated to ablation area assuming a constant yield stress	$\Delta x = 100 \text{ m}$. $\Delta t = 0.05 \text{ a}$	1963–2085	SIA flowline model (trapezoidal cross section) with Weertman type of sliding law: $a = 2.0 \times 10^{-17} \text{ Pa}^{-3} \text{ a}^{-1}$. $a_{\text{sl}} = 1.8 \times 10^{-12} \text{ m}^8 \text{ N}^{-3} \text{ a}^{-1}$	Degree-day model used, calibrated to observations. For with climate data from nearby station (past) and temperature and precipitation derived from GCM-RCM simulations (SRES scenarios, future)	Modification of bed topography to match observed length changes	Analysis glacier length response time and reaction time. Role of calving is discussed to explain discrepancies between modeled and observed glacier retreat	
Carstensz and Meren, Indonesia (Allison & Kruss, 1977)	Bed topography from gravimetric surveys	$\Delta x = 100\text{--}150 \text{ m}$ (Carstensz and Meren glacier, respectively). $\Delta t = 0.1 \text{ a}$	1850s → 1970s	Flowline model. Basal sliding from linear flow law, ice deformation from quadratic relationship between stresses and deformation ($0.160 \text{ bar}^{-2} \text{ a}^{-1} = 1.6 \times 10^{-11} \text{ Pa}^{-2} \text{ a}^{-1}$): shape factor accounted for	Net balance as function of elevation	Start from zero ice thickness and evolve to steady state. Subsequently a perturbation to SMB-elevation profile (through steady net balance decrease or ELA increase) applied to fit the observed retreat	Compared to observed topography (in 1942 and 1972), surface velocities (in 1972)	Basal sliding was found to have almost negligible effect versus internal deformation. Goal: infer past climatic conditions and changes in net balance (ELA vs. SMB changes considered)
Chhota Shigri, India (Gantayat et al., 2017)	Bed topography from GPR measurements and modeling (with calibration to match present-day geometry). Surface from ASTER DEM	$\Delta x = 100 \text{ m}$. $\Delta t = 0.001 \text{ a}$	1876–2100	SIA flowline model with trapezoidal cross section. Flow parameters from Budd et al. (1979): $a = 1.9 \times 10^{-24} \text{ Pa}^{-3} \text{ s}^{-1}$ $(= 6.0 \times 10^{-17} \text{ Pa}^{-3} \text{ a}^{-1})$, $a_{\text{sl}} = 5.7 \times 10^{-20} \text{ m}^2 \text{ Pa}^{-3} \text{ s}^{-1}$	Polynomial fit with elevation for SMB. Meteorological observations from nearby station. For future: evolution under various RCPs	Creation of steady state with present-day glacier length to modifying flow parameters, bed topography and mass balance perturbation	Comparison modeled and observed ice thickness, surface elevation and surface velocities	Response time experiments also included

Table 2
Continued

Glacier and reference	Geometric information (DEM, ice thickness, flowline, ...)	Horizontal and time resolution	Time period	Ice flow (model type, parameters, ...)	Initialization and calibration	Validation	Additional notes
Chhota Shigri, India (Engelhardt et al., 2017)	Surface elevation from SRTM DEM. Bed topography derived from modeling (initialization procedure)	$\Delta x = 50 \text{ m}$	1951–2099	SIA flowline model with trapezoidal cross section. Flow parameters from Budd et al. (1979): $a = 1.9 \times 10^{-24} \text{ Pa}^{-3} \text{ s}^{-1}$ ($= 6.0 \times 10^{-17} \text{ Pa}^{-3} \text{ a}^{-1}$), $a_{\text{sI}} = 5.7 \times 10^{-20} \text{ m}^2 \text{ Pa}^{-3} \text{ s}^{-1}$	Distributed temperature-index approach including short-wave radiation (i.e. simple energy balance modeling). Climate from RCMs (5 km resolution; CORDEX South Asia), downscaled to 300 m. Forcing from ERA-Interim and GCMs (various RCPs). Debiasing with AWS data	Calibration of SMB model to match observed annual mass balances (through Monte Carlo simulation). Modification forcing before 1951 to match the 2000 glacier outline; repeated while varying bed (to match surface elevation)	Mass balance (model type, parameters, climatic info) treatment, basal and frontal (MB, ...)
Frans Josef, New Zealand (Oerlemans, 1997a)	Bed topography obtained by assuming perfect plasticity and yield stress of $2 \times 10^7 \text{ Pa}$ and corrected by accounting for basal sliding	$\Delta x = 100 \text{ m}$	1750–1995	SIA flowline model with trapezium cross section. Flow parameters from Budd et al. (1979): $a = 1.9 \times 10^{-24} \text{ Pa}^{-3} \text{ s}^{-1}$ ($= 6.0 \times 10^{-17} \text{ Pa}^{-3} \text{ a}^{-1}$), $a_{\text{sI}} = 5.7 \times 10^{-20} \text{ m}^2 \text{ Pa}^{-3} \text{ s}^{-1}$	Energy balance modeling, accounting for changes in albedo. 15-min time step for SMB component	Modify the albedo and the precipitation in order to match the observed geometry	Comparison of the modeled and the observed present-day geometry
Franz Josef, New Zealand (Anderson et al., 2008)	DEM derived from aerial photography. Bed topography from radio echo sounding	$\Delta x = 100 \text{ m}$	1894–2100	SIA flowline model with trapezoidal parameterization of cross section and shape factor. Weertman type of sliding law. $a = 1.5 \times 10^{-24} \text{ Pa}^{-3} \text{ s}^{-1}$ ($= 4.7 \times 10^{-17} \text{ Pa}^{-3} \text{ a}^{-1}$), $a_{\text{sI}} = 4.5 \times 10^{-20} \text{ m}^2 \text{ Pa}^{-3} \text{ s}^{-1}$	Degree-day mass balance model, which was previously calibrated and evaluated. Forcing from GCM simulations and additional idealized experiments	Initial geometry obtained from dynamic calibration procedure. Calibration of ice flow parameters to reproduce observed surface velocities. Adjustment of temperature series to reproduce observed length changes	Comparison present-day glacier length in model versus observations

Table 2
Continued

Glacier and reference	Geometric information (DEM, ice thickness, flowline, ...)	Horizontal and time resolution	Time period	Ice flow (model type, parameters, ...)	Initialization and calibration	Validation	Additional notes	
Friás, Argentina (Leclercq et al., 2012)	Surface DEM from SRTM. Bed is derived from ice flow model	$\Delta x = 25 \text{ m}$. $\Delta t = 0.00025 \text{ a}$ (approx. 2 hr)	1639–2100	SIA flowline model with a trapezoidal cross section. Flow parameters from Budd et al. (1979) $a = 6.0 \times 10^{-17} \text{ Pa}^{-3} \text{ a}^{-1}$, $a_{sl} = 5.7 \times 10^{-20} \text{ m}^2 \text{ Pa}^{-3} \text{ s}^{-1}$	Simplified surface energy-balance model forced with ERA-40 and ERA-I to create reference SMB field. Past climatic conditions from modeled length changes (dynamic calibration). Additional experiments with forcing from tree-ring and multi-proxy reconstructions.	Modification of bed topography to reproduce the observed glacier geometry. Observed changes in frontal position reproduced through dynamic calibration of mass balance forcing	Comparison of modeled surface mass balance to observations from nearby glaciers	Deriving past climatic conditions from modeled length changes. Response time experiments performed
Hintererisferner, Austria (Greuell, 1992)	Bed measured in lowest 2 km, for the rest extended through plastic flow assumption (assuming constant driving stress)	$\Delta x = 200 \text{ m}$. $\Delta t = 0.025 \text{ a}$	1894–1985 (also run starting in 1755)	SIA flowline model with trapezium like parameterization of cross section. Effect of longitudinal stresses and basal water pressure tested (found to be very limited): $a = 0.269 \times 10^{-16} \text{ Pa}^{-3} \text{ a}^{-1}$.	SMB derived from multiple linear regression analysis between SMB and temperature and precipitation series	Calibration of rate factor and sliding parameter to reproduce the geometry and velocities	Comparing observed and modeled past retreat	Shows limited effective flow model parameters. Response time also studied
Hintererisferner (Schlosser, 1997)	Several maps and DEMs (1855, 1894, 1920 and 1979). Bed topography from radar measurements and for upper part derived assuming constant basal shear stress	$\Delta x = 200 \text{ m}$	1850–1979	$a_{sl} = 1.028 \times 10^{-16} \text{ m}^5 \text{ N}^{-2} \text{ s}^{-1}$ $3.24 \times 10^{-9} \text{ m}^5 \text{ N}^{-2} \text{ a}^{-1}$	SIA flowline model with trapezoidal cross section. Accounting for several flowlines and friction of side walls (shape factor).	SMB model calibrated with on-site SMB measurements	Calibration rate factor and sliding parameter to reproduce observed front positions	Reconstruction from LIA extent to 1970s through two approaches to derive old SMB: from tree rings and by linking SMB to data from nearby stations. Both approaches work well

Table 2
Continued

Glacier and reference	Geometric information (DEM, ice thickness, flowline, ...)	Horizontal and time resolution	Time period	Ice flow (model type, parameters, ...)	Initialization and calibration	Validation	Mass balance (model type, parameters, climatic info treatment, basal and frontal MB, ...)
Hofsjökull ice cap (two outlet glaciers) (Johannesson, 1997)	Recent maps from which glacier width is determined. Bed topography from radio echo sounding	Δx between 100 m (near terminus) and 250 m (interior). $\Delta t = 1$ a	1990 (steady state) -2190 (200 years run)	SIA flowline model in which basal sliding is not explicitly calculated. $a = 5.3 \times 10^{-24} \text{ Pa}^{-3} \text{ s}^{-1}$ ($= 1.7 \times 10^{-16} \text{ Pa}^{-3} \text{ a}^{-1}$) according to study, the value is taken from Paterson, 1994; where the reference value is $2.1 \times 10^{-16} \text{ Pa}^{-3} \text{ a}^{-1}$)	PDD model, forced with data from nearby meteorological station. Future climate from projected climate trends for Iceland	Calibration SMB model with runoff data, Additional tuning of precipitation gradient to obtain a zero mass balance for period 1961–1990	SMB evaluated by comparing runoff from model and observed (for other time period than the calibration). Comparison modeled and measured SMB
Nigardsbreen, Norway (Oerlemans, 1986, 1992)	Bed unknown for large parts of the glacier: adjusted until agreement surface close to observed one	$\Delta x = \text{ca. } 150 \text{ m}$	1000 CE–1980s	SIA flowline model: $a = 0.95 \times 10^{-22} \text{ m}^6 \text{ s}^{-1} \text{ N}^{-3}$ ($= 3.0 \times 10^{-15} \text{ Pa}^{-3} \text{ a}^{-1}$), $a_{\text{sl}} = 2.8 \times 10^{-7} \text{ m}^5 \text{ N}^{-2} \text{ a}^{-1}$ ($= 0.9 \times 10^{-14} \text{ m}^5 \text{ s}^{-1} \text{ N}^{-2}$)	Parameterization with elevation based on linear fit to the observed mean mass balance for the period 1962–1975, which is perturbed over time. In Imposed values, within the literature range (Paterson, 1981)	SMB perturbed (and calving parameters also calibrated for some experiments) to reproduce maximum glacier length around 1,750	Steady state glacier length versus observation
Nigardsbreen, Norway (Oerlemans, 1997b)	Input from topographic map. Parts of bed topography known from hot water drilling, extended assuming perfect plasticity	$\Delta x = 100 \text{ m}$. $\Delta t = 0.01 \text{ a}$	1600–2100	SIA model. Values from (Budd et al., 1979): $= 1.9 \times 10^{-24} \text{ m}^6 \text{ s}^{-1} \text{ N}^{-3}$ ($= 6.0 \times 10^{-17} \text{ Pa}^{-3} \text{ a}^{-1}$), $a_{\text{sl}} = 5.7 \times 10^{-20} \text{ Pa}^{-3} \text{ m}^2 \text{ s}^{-1}$ ($= 1.8 \times 10^{-12} \text{ Pa}^{-3} \text{ m}^2 \text{ a}^{-1}$)	Parameterization as a function of elevation. Based on observations for the period 1962–1993	SMB—elevation function is perturbed to reproduce the observed historical glacier changes. Additionally, the bed topography is adjusted to reproduce present-day geometry after transient run	The numerical model was coded in Fortran-77, and a 1,000 years simulation took about 10 min on a Macintosh PowerPC 7100-66. Introducing concept of dynamic calibration

Table 2
Continued

Glacier and reference	Geometric information (DEM, ice thickness, flowline, ...)	Horizontal and time resolution	Time period	Ice flow (model type, parameters ...)	Initialization and calibration	Validation	Additional notes	
Pasterze (Zuo & Oerlemans, 1997)	Surface geometry from topographic map. Ice thickness derived assuming constant driving stress, adjusted to fit observed surface	$\Delta x = 200$ m	1851–2100	SIA flowline model, accounting for six tributaries also. Trapezium parameterization for cross section. Flow parameters: $a = 3.17 \times 10^{-25} \text{ m}^6 \text{ s}^{-1} \text{ N}^{-3}$ ($= 1.0 \times 10^{-17} \text{ Pa}^{-3} \text{ a}^{-1}$), $a_{\text{sI}} = 8.38 \times 10^{-17} \text{ m}^5 \text{ s}^{-1} \text{ N}^{-2}$	Reference SMB profile, perturbed based on dynamically calibrated term (to reproduce glacier length)	SMB calibrated in order to reproduce past length changes: “dynamic calibration” (Oerlemans, 1997b). Flow and sliding parameters were adjusted “to obtain realistic values”	Surface velocities modeled versus observed (period 1970–1990). Ice volumes modeled and measured for certain parts of the glacier for the 1970s. Area modeled versus observed in 1850, 1925, and 1969	Response time also analyzed
Rhone, Switzerland (Stroeven et al., 1989)	Surface elevation from topographic map. Some thickness measurements in ablation area, extrapolated to accumulation area assuming plastic flow	$\Delta x = 250$ m	1000–2000 CE	SIA flowline model of (Oerlemans, 1986) with trapezium shaped cross section. $a = 6 \times 10^{-25} \text{ m}^6 \text{ s}^{-1} \text{ N}^{-3}$ ($= 1.9 \times 10^{-17} \text{ Pa}^{-3} \text{ a}^{-1}$), $a_{\text{sI}} = 9.5 \times 10^{-17} \text{ m}^5 \text{ s}^{-1} \text{ N}^{-2}$	Rate factor and sliding coefficient chosen to reproduce ice thickness	Comparison to measured surface velocities of the period 1885–1910 SMB	Better understand past climatic conditions and how they affect the past SMB	
Rhone, Switzerland (Wallinga & van de Wal, 1998)	Surface geometry from topographic map. Bed topography for lower glacier part from seismic reflection. Extrapolated to accumulation area assuming plastic flow	$\Delta x = 250$ m. $\Delta t = 0.05$ a	1882–2100	SIA flowline model of with trapezium shaped cross section. $a = 3.17 \times 10^{-25} \text{ m}^6 \text{ s}^{-1} \text{ N}^{-3}$ ($= 1.0 \times 10^{-17} \text{ Pa}^{-3} \text{ a}^{-1}$), $a_{\text{sI}} = 9.51 \times 10^{-17} \text{ m}^5 \text{ s}^{-1} \text{ N}^{-2}$	Calibration of bed topography and flow parameters to reproduce the observed glacier length changes. Prior to 1882, dynamic calibration by adapting mass balance	Comparison to historical volume changes, observed profile (in 1969) and early twentieth century surface velocities	Several sensitivity tests performed for forcing parameters, flow parameters and bed profile	

Table 2
Continued

Glacier and reference	Geometric information (DEM, ice thickness, flowline, ...)	Horizontal and time resolution	Time period	Ice flow (model type, parameters, ...)	Initialization and calibration	Validation	Mass balance (model type, parameters, climatic info, treatment, basal and frontal MB, ...)
Rhone, Switzerland (Sugiyama et al., 2007)	Several DEMs. Bed topography from radar measurements	$\Delta x = 100 \text{ m}$. $\Delta t = 0.01 \text{ a}$	1878–2050	Flowline model including 2-D solving of flux along glacier cross section. Rate factor taken from Gudmundsson (1999): $a = 0.76 \times 10^{-16} \text{ Pa}^{-3} \text{ a}^{-1}$	Mass balance expressed as function of elevation	Starting point is observed geometry in 1878. Basal flow parameter calibrated to reproduce observed velocities. Mass balance gradients calibrated to reproduce observed elevation changes and length changes	Comparison of observed and modeled glacier volume and evolution over time
Saint Sorlin, France (Vincent et al., 2000)	Several DEMs. Ice thickness from boreholes, seismic soundings and gravimetric measurements	1905–1997	SIA flowline model Flow parameter $a = 1.3 \times 10^{-24} \text{ Pa}^{-3} \text{ s}^{-1}$ ($= 4.1 \times 10^{-17} \text{ Pa}^{-3} \text{ a}^{-1}$)	SMB derived from very dense network of mass balance observations	Reconstruction of glacier geometry in 1905 by perturbing present-day annual mass balance	Mass balance compared to geodetic volume changes. Compared modeled surface elevation and velocity to observations	Temporal change in surface velocity analyzed. Cannot be well represented throughflow parameter tuning; but uniform sliding helps resolving the discrepancy
Sofiyevskiy, Russia (De Smedt & Pattyn, 2003)	Bed topography from radio-echo sounding. Surface elevation from topographic map	$\Delta x = 100 \text{ m}$. $\Delta t = 0.01 \text{ a}$	1800–2100	SIA flowline model accounting for Weertman-type of basal sliding (for lower glacier part), internal deformation and lateral friction (through shape factor): $a = 0.8 \times 10^{-16} \text{ Pa}^{-3} \text{ a}^{-1}$, $a_{sl} = 1.0 \times 10^{-8} \text{ m}^5 \text{ N}^{-2} \text{ a}^{-1}$	Perturbation of mass-balance reference profiles	Dynamic calibration: SMB calibrated in order to reproduce past length changes.	Analysis of glacier response time and reaction time. Committed glacier loss also analyzed

Table 2
Continued

Glacier and reference	Geometric information (DEM, ice thickness, flowline, ...)	Horizontal and time resolution	Time period	Ice flow (model type, parameters, ...)	Initialization and calibration	Validation	Additional notes
Sólheimajökull, Iceland (Mackintosh et al., 2002)	Bed topography from radio-echo sounding. DEM for different moments in time	$\Delta x = 100$ m	1700–1990	SIA flowline model in which internal deformation and sliding are accounted for. $a = 6.0 \times 10^{-17} \text{ Pa}^{-3}$ $a^{-1}, a_{\text{sl}} = 1.8 \times 10^{-12} \text{ m}^8 \text{ N}^{-3} \text{ a}^{-1}$	Energy balance mode, used for reference mass-balance profile. Data from nearby meteorological station	Precipitation gradient and coefficient for turbulent heat fluxes calibrated to reproduce field measurements.	Comparison interannual variability mass balance with measurements on another glacier
Storglaciären, Sweden (Stroeven, 1996)	1980 glacier surface from 1:10,000 topographic maps, along steepest gradient. Ice thickness measured all along the flowline	$\Delta x = 100$ m	1915–1980	SIA flowline model with trapezium cross shape. Second flowline incorporated to represent southern branch of the accumulation area. $a = 1.0 \times 10^{-25} \text{ m}^6 \text{ s}^{-1} \text{ N}^{-3}$ ($= 3.2 \times 10^{-18} \text{ Pa}^{-3} \text{ a}^{-1}$), $a_{\text{sl}} = 1.1 \times 10^{-16} \text{ m}^5 \text{ N}^{-2} \text{ s}^{-1} (= 3.5 \times 10^{-9} \text{ m}^5 \text{ N}^{-2} \text{ a}^{-1})$	SMB is parameterized as a function of elevation, based on mass balance measurements and accounting for wind scouring and other effects at glacier tongue	Rate factor and sliding coefficient calibrated to reproduce the ice thickness and surface velocities. ELA adapted for glacier length	Tests robustness of the model through various simulations, including changes in bed topography
Unteraar, Switzerland (Huss et al., 2007)	Bed topography from dense network of radio-echo sounding profiles. Several surface DEMs	$\Delta x = 25$ m. $\Delta t = 0.003$ a (1 day)	2007–2050	SIA flowline model in which basal sliding accounts for 50% of the surface speed. Empirical relationship between ice thickness and local flux	Temperature-index model, accounting for debris cover, run at hourly resolution. Forcing from nearby meteorological station	Mass balance model calibrated with ice volume changes derived from DEM differencing. Future forcing from climate scenarios based on RCM modeling	Effect of debris cover on glacier evolution analyzed. Analysis of positioning planned future artificial lake versus modeled future glacier front position

Table 2
Continued

Glacier and reference	Geometric information (DEM, ice thickness, flowline, ...)	Horizontal and time resolution	Time period	Ice flow (model type, parameters, ...)	Initialization and calibration	Validation	Additional notes
Unter Grindelwald, Switzerland (Schneiteis and Oenlemans, 1997)	No ice thickness measurements, surface elevation from topographic map	$\Delta t = 0.02 \text{ a}$	1530–2100	SIA flowline model with trapezium cross shape. Second flowline incorporated to represent inflow from Ischmeergletscher. Calibrated flow parameters: $a = 9.5 \times 10^{-25} \text{ m}^6 \text{ s}^{-1} \text{ N}^{-3}$ ($= 3.0 \times 10^{-17} \text{ Pa}^{-3} \text{ a}^{-1}$), $a_{sl} = 2.51 \times 10^{-6} \text{ m}^5 \text{ N}^{-2} \text{ s}^{-1}$ ($= 7.9 \times 10^{-9} \text{ m}^5 \text{ N}^{-2} \text{ a}^{-1}$)	SMB parameterized as a function of elevation through polynomial. Inclusion of energy balance of ice-snow surface. Different climatic series/proxies combined for transient run to reproduce observed geometry (in 1987) and minimize difference between observed and modeled front positions	Ice flow model and SMB model calibrated through coupling (i.e. not individually). Adjusting various parameters (related to flow, basal stress, bed topography, and precipitation) to	Response time experiments conducted. Predicted a glacier advance in early 21st century due to high precipitation in 1970s and 1980s
Urumqi No. 1, China (Duan et al., 2012)	Triangular mesh, approx. 5,000 elements in total	2005–2070	Full-Stokes finite element flowline model. No explicit treatment of basal sliding. $a = 7.0 \times 10^{-17} \text{ Pa}^{-3} \text{ a}^{-1}$	Degree-day mass balance model. Linear increase in temperatures imposed based on IPCC B1 scenario	Modeled velocities are compared to observations	Note: IDGES, ice-dynamical glacier evolution study.	

Table 3
Overview of Transient 3-D IDGES

Glacier and reference	Geometric information (DEM, ice thickness, flowline, ...)	Horizontal and spatial resolution	Time period	Ice flow (model type, parameters, ...)	Initialization and calibration	Validation	Additional notes
Aletsch, Switzerland (Jouvet et al., 2011; Jouvet & Huss, 2019)	Several DEMs from topographic maps and aerial photography. Bed topography from radio-echo sounding	Finite element tetrahedrons about 100 m long and 30 m high. $\Delta t = 0.5$ a	Full-Stokes model for ice dynamics, with non-linear sliding law	Temperature index model. Future climate from ensemble of RCM simulations	Calibration flow parameter to match observed surface velocities. Calibration SMB parameters based on several DEMs, volume and length. Additional evaluation based on recent evolution in Jouvet and Huss (2019) performed by Jouvet and Huss (2019).	Comparison modeled and observed 20th century glacier geometry (based on several DEMs), sensitivity to ice-flow parameters and role of debris cover for future evolution is analyzed (Jouvet et al., 2011)	Analysis of committed glacier loss
Austre Lovénbreen, Svalbard (Wang et al., 2019)	Surface and bed topography DEM from GPS and radar measurements	Finite element triangles with side lengths of ca. 50 m	2010–2170	Full-Stokes ice flow model (Elmer) with linear relationship between basal friction and basal velocities	Initialization through creation of steady state glacier. Flow parameters obtained by comparing modeled and observed velocities	Additional simulation for time period 1962–2009 to compare modeled glacier in 2009 with observations. Differences used to estimate uncertainties in future modeled values	Glacier runoff is also analyzed

Table 3
Continued

Glacier and reference	Geometric information (DEM, ice thickness, flowline, ...)	Horizontal and spatial resolution	Time period	Ice flow (model type, parameters, ...)	Initialization and calibration	Validation	Additional notes
Barnes, Canada (Gilbert et al., 2017)	Surface DEM from Canadian Digital Elevation Model (CDEM). Bed topography from NASA IceBridge radar tracks	$\Delta t = 0.5 \text{ a}$	1960–2400	Finite element thermo-mechanically coupled full-Stokes model (Elmer), with sliding velocity linearly related to basal drag	Mass balance calculated from degree-day formulation Past forcing from nearby meteorological stations. Future forcing from CMIP5 GCM output	Creation of 1960 steady state with basal drag coefficients obtained from inversion of surface velocities. Mass balance calibrated to geodetic and in situ observations	Validation of SMB sensitivity to increasing air temperature Description of potential future catastrophically draining of ice dammed lakes. Comparison of glacier evolution to paleoclimatic evidence
Gauli, Switzerland (Compagno et al., 2019)	Bed topography from helicopter-borne radar measurements. Two DEMs for surface (1947 and 2010)	$\Delta x = 40 \text{ m}$ resolution. $\Delta t = 1 \text{ a}$	1946–2040	Full-Stokes ice flow model (Elmer/Ice). Basal velocities from Weertman-type sliding law. $a = 6.0 \times 10^{-17} \text{ Pa}^{-3} \text{ a}^{-1}$, $a_3 = 1.25 \times 10^{-14} \text{ m}^7 \text{ N}^{-3} \text{ a}^{-1}$	Mass balance from temperature index melt modeling and snow accumulation model. Forced with data from nearby stations. Future evolution based on mass balance of extreme years during observational period	Start from observed glacier geometry in 1947. Calibration of ice flow parameters to match glacier geometry in 2010 (from DEM) and observed velocities. Mass balance model calibrated based on observed volume changes	Goal of study is track trajectory of airplane in glacier and predict its reappearance at the surface
Gurenhekou, Tibet (Zhao et al., 2014)	Bed topography from radio echo sounding and from ice core	Finite elements with a horizontal resolution of ca. 30 m	2008–2057	Thermomechanically coupled Full-Stokes ice flow model (Elmer/Ice). No slip boundary condition	SMB parameterized as a function of elevation. For future climatic conditions, this function is perturbed based on SMB calculated from PDD approach.	Start from observed geometry (2007) with steady state thermodynamics	Modeled and observed glacier length changes are compared. Some SMB realization rejections based on this

Table 3
Continued

Glacier and reference	Geometric information (DEM, ice thickness, flowline, ...)	Horizontal and spatial resolution	Time period	Ice flow (model type, parameters, ...)	Initialization and calibration	Validation	Additional notes
Haig, Canada (Adhikari & Marshall, 2013)	Bed topography from radar measurements. Surface topography from ASTER DEM	DEM resolution of 25 m. Varying spatial resolution (finite elements). $\Delta t = 0.1$ a		Full-Stokes ice flow model (Elmer/Ice), assuming ice to be isothermal. Also experiments in which transverse and longitudinal stresses are neglected (i.e. SIA). No-slip basal boundary condition. $a = 1.25 \times 10^{-16} \text{ Pa}^{-3} \text{ a}^{-1}$	On-site SMB and meteorological measurements. SMB function of elevation. Future evolution based on trends from GCM simulation under RCP scenarios (CMIP5)		Many tests comparing the influence of ice flow model complexity on transient glacier evolution. Also experiments with step changes in climate (and committed loss)
Hans Tausen, Greenland (Zekollari, Huybrechts, et al., 2017)	DEM from radio-echo sounding (airborne and ground based)	$\Delta x = 250$ m	1990—multi-century evolution	Thermomechanically coupled higher-order ice flow model. Basal sliding from Weertman-type of sliding law. Rate factor is temperature-dependent following an Arrhenius-type function	PDD model forced with temperatures parameterized as function of elevation and latitude and elevation and precipitation from RCM. Model components calibrated based on SMB observations	Starting point future simulations is steady state ice cap. Geothermal heat flux is tuned to reproduce measured englacial temperatures	Comparison modeled and observed glacier geometry, 1961–1990 geometry changes, surface velocities and surface mass balance
Hardangerjøkulen, Norway (Giesen & Oerlemans, 2010)	DEMs from 1961 to 1995. Detailed radar measurements for ice thickness	$\Delta x = 100$ m. $\Delta t = 0.01$ a	1905–2100	2-D SIA model. $a = 2.4 \times 10^{-17} \text{ Pa}^{-3} \text{ a}^{-1}$, $a_{sl} = 3.0 \times 10^{-13} \text{ m}^8 \text{ N}^{-3} \text{ a}^{-1}$	Mass balance components calibrated to reproduce direct observations from AWS and mass balance to be in line with mass balance measurements.	Elaborate evaluation of modeled surface energy and mass balance with AWS measurements and MB measurements. 20th century glacier evolution compared to observations	Elaborate mass balance sensitivity tests performed. For future, influence climatic forcing analyzed and various feedback processes considered

Table 3
Continued

Glacier and reference	Geometric information (DEM, ice thickness, flowline, ...)	Horizontal and spatial resolution	Time period	Ice flow (model type, parameters, ...)	Initialization and calibration	Validation	Mass balance (model type, parameters, climatic info)
Hintererisferner, Austria (Wijngaard et al., 2019)	Various DEMs available, including recent EU-DEM. Bed topography from observations and modeling	$\Delta x = 30\text{ m}$. daily time step ($\Delta t = 0.003\text{ a}$)	1850–2016	SIA model, with correction factor to account for basal sliding and non-local stresses. $a = 1.7 \times 10^{-16}\text{ Pa}^{-3}\text{ a}^{-1}$ ($= 6.3 \times 10^{-16}\text{ Pa}^{-3}\text{ a}^{-1} \times 0.65/3$; where 0.65 is the correction factor, which in the study is formulated as a separate term, i.e. not included in flow parameter)	Melt based on degree-day approach. Role of avalanching also modeled. Forcing from CMIP5 GCMs (with and without anthropogenic forcing, and from nearby meteorological stations	Three-step approach for model calibration: (i) GCM selection based on modeled present-day area changes (ii) Flow and mass balance model parameters calibrated to match observed glacier velocities and recent elevation changes (iii) Manual calibration to enhance long-term model performance	Partly incorporated in multi-step calibration, complemented with additional analyses, such as area changes
Hoffellsjökull (part of Vatnajökull ice cap), Iceland (Aðalgeirsdóttir et al., 2011)	Bed topography from radio-echo sounding. Surface elevation maps and DEMs for 7 time periods (ca. 1890–2010)				PDD model. Past climate from nearby meteorological stations. Future climate forcing from 10 global and three regional climate models	Modeled melt compared to AWS measurements. Modeled past volume changes compared to observations. Comparison modeled and observed surface velocities	Analysis runoff changes in past and future. Tests with bed topography changes over time (trench filling) and effect on glacier evolution

Table 3
Continued

Glacier and reference	Geometric information (DEM, ice thickness, flowline, ...)	Horizontal and spatial resolution	Time period	Ice flow (model type, parameters, ...)	Initialization and calibration	Validation	Additional notes
Hofsjökull and southern part of Vatnajökull, Iceland (Aðalgeirsdóttir et al., 2006)	Bed topography from radio echo sounding	$\Delta x = 1 \text{ km}$	1990–2200	Finite difference SIA model. For Hofsjökull ice cap: sliding is not explicitly accounted for: $a = 1.9 \times 10^{-16} \text{ Pa}^{-3} \text{ a}^{-1}$	Degree day mass balance model. Future climate based on GCM output downscaled with RCM	SMB model calibrated with mass balance measurements. Calibration flow parameters to match observed geometry	Future runoff and sensitivity mass balance to climate change also analyzed
Juneau, Alaska (Ziemien et al., 2016)	Bed topography from worldwide glacier thickness reconstruction by Huss and Farinotti (2012). Surface elevation from SRTM	$\Delta x = 300 \text{ m}$. $\Delta t = \text{ca. } 0.001 \text{ a}$ (8 hr)	1971–2100	Ice flow calculated with the hybrid shallow ice–shallow shelf model: Parallel Ice Sheet Model (PISM). $a = 1.4 \times 10^{-16} \text{ Pa}^{-3} \text{ a}^{-1}$ (from Paterson and Budd (1982)). Basal sliding quadratic dependence on the basal stress: $a_{sl} = 2 \times 10^{-9} \text{ m}^5 \text{ N}^{-2} \text{ a}^{-1} (500 \text{ m a}^{-1}/(0.5 \text{ MPa})^2)$	Climatic forcing from RCM Weather Research and Forecasting Model (WRF). Ablation from positive degree day model	Multi-stage spinup (with three 30 years intervals) to derive initial 1971 ice thickness field. Calibration ice flow and SMB parameters to reproduce velocity and SMB observations, respectively.	Comparison modeled SMB to geodetic observations Tests also performed by using interpolated climate observations as forcing. Additional experiments starting from zero ice thickness and committed loss experiments. Elaborate uncertainty and sensitivity analyses ELA

Table 3
Continued

Glacier and reference	Geometric information (DEM, ice thickness, flowline, ...)	Horizontal and spatial resolution	Time period	Ice flow (model type, parameters, ...)	Initialization and calibration	Validation	Mass balance (model type, parameters, climatic info)
Khumbu, Nepal (Rowan et al., 2015)	Bed topography from radio echo sounding and gravity measurements. DEM from ASTER (ASTER GDEM 2011)	$\Delta x = 100$ m. Dynamic time step, typically on the order of 0.003–0.02 a	1000–2200	SIA ice flow model in which higher-order stresses are incorporated (second-order SIA). Basal sliding from relationship linking it to basal shear stress to the second power divided by effective pressure ($a_{sl} = 4 \times 10^{-4}$ m Pa $^{-1}$ a $^{-1}$). Englacial and supraglacial transport of debris cover is included. Thermodynamics included	SMB linked to surface elevation through linear relationship. ELA varied over time: for past to match present-day glacier geometry, for future based on CMIP5 RCP4.5 GCM simulations. SMB accounts for debris cover	Initial geometry from steady state simulation. Derivation of ELA values to match present-day glacier velocity, mean surface elevation change and geodetic mass balance	Comparison of present-day observed and modeled geometry (ice thickness), velocity, mean surface elevation change and geodetic mass balance
Langjökull, Iceland (Flowers et al., 2007)	DEM for ice cap in 2001. Bed topography from radio-echo sounding	$\Delta x = \text{ca. } 1$ km	1600–2000	Same model as used in Flowers et al. (2005): SIA with basal sliding coupled to basal hydrology. $a = 2.1 \times 10^{-16}$ Pa $^{-3}$ a $^{-1}$ (from Paterson, 1994); $a_{sl} = 1.5\text{--}3.5 \times 10^{-4}$ m Pa $^{-1}$ a $^{-1}$ (i.e. mean value of 2.5×10^{-4} m Pa $^{-1}$ a $^{-1}$)	Climatic information from weather station data and proxy-based reconstructions. Temperature-index modeling of melt	Degree-day factors calibrated to SMB measurements. Modification of basal flow coefficient, precipitation variation with temperature and scaling precipitation to reproduce present-day geometry	Comparison with observed surface velocities
Langjökull and Hofsjökull, Iceland (Guðmundsson et al., 2009)	Two DEMs for Hofsjökull and three for Langjökull. Bed topography from radio echo sounding		1990–2200	SIA model. Basal sliding implicitly included in Glen type of flow law (values taken from Aðalgeirsdóttir et al., 2006)	Degree-day mass balance model. Past forcing from nearby meteorological station. Future climate change scenario based on RCM simulation for Iceland under IPCC B2	Steady state in 1990	1990–2005 mass balance and glacier extent compared to observations

Table 3
Continued

Glacier and reference	Geometric information (DEM, ice thickness, flowline, ...)	Horizontal and spatial resolution	Time period	Ice flow (model type, parameters, ...)	Initialization and calibration	Validation	Mass balance (model type, parameters, climatic info treatment, basal and frontal MB, ...)	Additional notes
Langtang, Nepal (Wijngaard et al., 2019)	Surface from SRTM DEM. No direct bed topography measurements, derived from modeling	$\Delta x = 30 \text{ m}$. Daily time step ($\Delta t = 0.003 \text{ a}$)	1850–2016	SIA model, with correction factor to account for basal sliding and non-local stresses. $a = 8.7 \times 10^{-17} \text{ Pa}^{-3} \text{ a}^{-1}$ ($= 1.7 \times 10^{-16} \text{ Pa}^{-3} \text{ a}^{-1} \times 0.8^3$, where 0.8 is the correction factor, which in the study is formulated as a separate term, i.e. not included in flow parameter)	Melt based on degree-day approach. Role of avalanching also modeled. Forcing from CMIP5 GCMs (with and without anthropogenic forcing) and from nearby meteorological stations. Role of debris accounted for	Three-step approach for model calibration: (i) GCM selection based on modeled present-day (ii) Flow and mass balance model parameters calibrated to match observed glacier velocities and recent elevation changes (iii) Manual calibration to enhance long-term model performance	Partly incorporated in multi-step calibration, complemented with additional analyses, such as area changes	Analysis of changes in surface velocities over time, glacier response time and influence of debris cover and role of anthropogenic forcing in past evolution
Midre Lovénbre, Svalbard (Zwinger & Moore, 2009)	Bed topography measurements from ground penetrating radar. DEM from 1977 and two DEMs based on LiDAR (2003 and 2005)	$\Delta t = 1 \text{ a}$	1977–2030	Finite element thermo-mechanically coupled full-Stokes model (Elmer). No-slip condition for the velocity at the bed	Ablation/accumulation from field measurements. Kept constant for future simulations (without and with thermodynamic coupling) and transient simulations	Start from 1977 observed geometry. 3-step scheme with initialization based on steady state simulations (without and with thermodynamic coupling)	Comparison of modeled and observed basal thermal state, dip angles of isochrones, surface velocities and elevation changes	Accounts for formation of superimposed ice, which accounts for part of the net accumulation
Morteratsch glacier complex: Pers and Morteratsch, Switzerland (Zekollari et al., 2014)	Surface elevation from 25 m DEM. Ice thickness measured and extrapolated assuming plastic flow along central flowline	$\Delta x = 25 \text{ m}$. $\Delta t = 0.02 \text{ a}$	1865–2100	3-D Higher-order model. Flow parameters (taken from Zekollari et al., 2013): $a = 1.6 \times 10^{-16} \text{ Pa}^{-3} \text{ a}^{-1}$, $a_{\text{sl}} = 12 \times 10^{-16} \text{ m}^7 \text{ N}^{-3} \text{ a}^{-1}$	Simple-energy balance model	SMB model calibrated to field measurements.	Past volume changes. Present-day observed versus modeled geometry	Used for tests on the glacier response time (Zekollari and Huybrechts, 2015)

Table 3
Continued

Glacier and reference	Geometric information (DEM, ice thickness, flowline, ...)	Horizontal and spatial resolution	Time period	Ice flow (model type, parameters, ...)	Initialization and calibration	Validation	Additional notes
Qiantang No. 1, Tibet (Li et al., 2017)	Bed topography from radio echo sounding and from ice core	Finite elements with typical resolution around 50 m	2013–2050	Thermomechanically coupled Full-Stokes ice flow model (Elmer/Ice). No-slip basal boundary condition	Degree-day model, forced with observations from nearby stations (past) and on-site AWS. Based on this SMB versus elevation relationship is established and perturbed. For future linear trends are imposed and projections from RCM	Start from observed geometry with steady state thermodynamics	Comparison of modeled and observed front position and englacial temperatures
Rhone, Switzerland (Jouvet et al., 2009)	Bed topography measured at several locations. Several DEMs available from topographic maps	Variable spatial resolution, ca. 50 m (finite element). Higher resolution for solving transport equation	1874–2100	Full-Stokes model and sliding law relating basal velocity to third power of basal drag. For past, sliding is included: $a = 1.0 \times 10^{-16} \text{ Pa}^{-3} \text{ a}^{-1}$. $a_{\text{sl}} = 30,000 \text{ MPa}^{-3} \text{ m a}^{-1}$	PDD model (Huss et al., 2008). Based on meteorological measurements that are extended to the glacier. For future, by using RCM output	Compare to measured changes in glacier 3-D geometric evolution of glacier over century time scale and based on field measurements (Huss et al., 2008). Flow parameters calibrated to match past retreat and surface velocity measurements	Different calibration for past and future evolution: used different reference periods for calibration, resulting in different calibrated parameters

Table 3
Continued

Glacier and reference	Geometric information (DEM, ice thickness, flowline, ...)	Horizontal and spatial resolution	Time period	Ice flow (model type, parameters, ...)	Initialization and calibration	Validation	Mass balance (model type, parameters, climatic info treatment, basal and frontal MB, ...)	Additional notes
Rikha Samba, Nepal (Gilbert et al., 2020)	Bed topography from GPR measurements, which are extrapolated and corrected based on ice flow modeling. Surface DEM extracted from Pleiades tri-stereo imagery	$\Delta x = 50$ m (triangular elements). $\Delta t = 1$ a	1975–2100	Thermo-mechanical 3-D Full-Stokes model (Elmer/Ice). Basal sliding linearly correlated to basal drag. Firn model to determine the surface boundary conditions	Surface mass balance degree-day model. Meteorological data from AWS in proximity of the glacier. MB model forced with ERA-Interim for past and with linear trend for future	SMB model calibrated with field measurements and geodetic mass balance. Temperature and precipitation gradient to match observed mass balance. Bed topography is adapted and sliding parameter calibrated to reproduce observed surface elevation and velocities.	Comparison of modeled steady state geometry and thermal regime with observations	Particular focus on effect of water percolation on thermal structure of the glacier (with crevassed areas modeled based on Cauchy stresses)
Saint-Sorlin, France (Le Meur & Vincent, 2003)	Surface elevation from DEM. Bed topography from seismic data, boreholes and gravimetry	$\Delta x = 50$ m. $\Delta t = 0.05$ a	1905–1998	SIA model, $a = 6.3 \times 10^{-17} \text{ Pa}^{-3} \text{ a}^{-1}$, $a_{\text{sl}} = 5 \times 10^{-14} \text{ m}^8 \text{ N}^{-3} \text{ a}^{-1}$	Creation of 1905 steady state and subsequent calibration of flow parameters to fit observed thickness changes and changes in terminus position	2-D mass balance field based on 1957–1999 field-observations, forced with signal from linear mass-balance model for earlier periods	cf., Le Meur and Vincent (2003) for model calibration, but starting point is observed geometry in 1905	Discussion limitations SIA model. Response time analysis, committed loss experiments
Saint-Sorlin, France (Le Meur et al., 2007)	cf., Le Meur and Vincent (2003)	$\Delta x = 50$ m. Time step of 18 days ($\Delta t = 0.05$ a)	1905–2100	SIA, with same calibrated parameters as Le Meur and Vincent (2003)	Many field measurements used to reconstruct past SMB and cases where this is used to model the entire SMB with an energy balance model (Gerbaux et al., 2005). Future evolution: forced with GCM data	cf., Le Meur and Vincent (2003) for model calibration, but starting point is observed geometry in 1905	Comparing modeled and observed SMB. Comparing modeled and observed geometry deglaciating area	Test influence of forcing with ‘observed SMB’ (many observations + kriging) and modeled SMB

Table 3
Continued

Glacier and reference	Geometric information (DEM, ice thickness, flowline, ...)	Horizontal and spatial resolution	Time period	Ice flow (model type, parameters, ...)	Initialization and calibration	Validation	Additional notes	
Sportegreen, Norway (Laumann & Nesje, 2014)	Bed topography from radar measurements. Several DEMs	(also palaeo simulations starting 8ka BP)	2011–2200	SIA model, accounting for internal deformation and Weertman type of basal sliding: $a = 2.0 \times 10^{-17}$ $\text{Pa}^{-3} \text{a}^{-1}$, $a_{\text{sl}} = 0.68 \times 10^{-12} \text{ m}^8 \text{ N}^{-3} \text{ a}^{-1}$	Mass balance curve versus elevation. Future climate based on GCM-RCM run	Glacier assumed to be in steady state at present: match with observed geometry through calibration flow parameters	Compensating effect of precipitation increase versus temperature increase in coming decades	
Storglaciären, Sweden (Albrecht et al., 2000)	Several DEMs (four used in this study) and direct measurements of ice thickness	$\Delta x = 150 \text{ m}$	1959–1990	Blatter type of higher-order ice flow model, with implicit treatment of basal sliding. Also runs with SIA version (i.e. neglecting longitudinal stresses). Calibrate rate factor: $a = 22.2 \times 10^{-25} \text{ m}^6 \text{ s}^{-1} \text{ N}^{-3}$ ($= 7.0 \times 10^{-17} \text{ Pa}^{-3} \text{ a}^{-1}$) (test with SIA model): $28.5 \times 10^{-25} \text{ m}^6 \text{ s}^{-1} \text{ N}^{-3}$	Many field measurements used to construct annual mass-balance maps. Used as input for SMB model	Reproduce observed surface velocities through tuning of flow parameters	Comparing modeled and surveyed glacier geometry at present	Influence of frequency at which surface mass balance is updated. Comparison between model run with SIA and one run with HO
Storglaciären, Sweden (Schneebberger et al., 2001)	Same as Albrecht et al. (2000)	Δx mass balance: 30 m	1990–2050	Calibrated model of Albrecht et al. (2000); that is, Blatter type of higher-order ice flow model in which sliding is implicitly included (i.e. not explicitly accounted for)	Temperature index melt model, hourly time step. Optimized to SMB measurements on glacier.	See Albrecht et al. (2000) for details on model calibration	At that time, real state of the art in terms of forcing, SMB calculation and ice flow calculation	

Table 3
Continued

Glacier and reference	Geometric information (DEM, ice thickness, flowline, ...)	Horizontal and spatial resolution	Time period	Ice flow (model type, parameters, ...)	Initialization and calibration	Validation	Mass balance (model type, parameters, climatic info treatment, basal and frontal MB, ...)	Additional notes
Vatnajökull (Flowers et al., 2005; Marshall et al., 2005)	Bed topography from radar measurements. DEM over entire ice cap	$\Delta y = 1.85 \text{ km}$ ($1/60^\circ$), $\Delta x = 1.55\text{--}1.64 \text{ km}$ ($1/30^\circ$), $\Delta t = 0.02 \text{ a}$	1600–2300. Focus of study by Flowers et al. (2005) is on the next two centuries	SIA and longitudinal stress coupling (Marshall et al., 2005); SIA (Flowers et al., 2005). Coupled to subglacial hydrology. In Marshall et al. (2005): geothermal cauldrons under the ice cap are accounted for, and so is calving. $a = 7.4 \times 10^{-17} \text{ Pa}^{-3}$ a^{-1} (Aðalgeirsdóttir et al., 2000); $a_s = 6 \times 10^{-4} \text{ m}^3 \text{ N}^{-2}$ a^{-1} ($= \text{m Pa}^{-1} \text{ a}^{-1}$)	Steady states are considered, as well as modeled present-day state after transient simulation. Basal parameter and temperature offset degree day model. Future climate inspired from GCM runs	Comparison modeled ice cap and observed (both transient and steady state simulations). Elaborate comparisons when modifying flow parameter, sliding parameters, coupling to hydrology, climatic forcing and longitudinal stress coupling (Marshall et al., 2005)	Bed isostasy taken into account. Effect of subglacial hydrology and inclusion of longitudinal stress gradients on transient glacier evolution is investigated (Marshall et al., 2005).	Elaborate analyses future runoff and change basin divides (Flowers et al., 2005)
Vatnajökull (Schmidt et al., 2020)	DEM reconstructed from SPOT5 imagery. Bed topography based on radio echo sounding	$\Delta x = 500 \text{ m}$	1980–2300	Ice flow simulated with the Parallel Ice Sheet Model (PISM): SIA-SSA. Deformation at base accounting (SSA) for till properties and deformation. $a = 0.8 \times 10^{-16} \text{ Pa}^{-3}$ a^{-1} and varying values for sliding parameter	SMB calculated from snow-pack scheme from RCM HIRHAM5, accounting for various components energy balance. Forcing with data from HARMONIE-AROME (past) and EC-EARTH and CORDEX simulations	Several components of the snowpack scheme calibrated to reproduce AWS measurements. 1000-year spinup with 1980–1999 climate. Calibration of flow parameters to reproduce observed surface velocities	Comparison of measured versus observed SMB and velocities from mass balance stakes. 2010 geometry comparison: model versus observations: 2010 geometry, 1991–1992 to 2014–2015 volume changes	Effect of lapse rate on dynamic evolution is investigated. Surges not explicitly modeled, but used to explain discrepancies in modeled and observed velocities. Stabilization experiments under constant climate changes

Table 3
Continued

Glacier and reference	Geometric information (DEM, ice thickness, flowline, ...)	Horizontal and spatial resolution	Time period	Ice flow (model type, parameters, ...)	Initialization and calibration	Validation	Mass balance (model type, parameters, climatic info treatment, basal and frontal MB, ...)
Vatnajökull southeast outlet glaciers: Skálafellsjökull, Heinabergsjökull and Fláajökull (Hannesdóttir et al., 2015)	Bed topography from radio echo sounding DEMs for six time periods (1890–2010)	$\Delta x = 200$ m	1959–2100 (and also tests to reproduce 1890 geometry)	SIA on finite element grid. Implicit consideration of basal sliding (i.e. not explicitly accounted for; $a = 0.8 \times 10^{-16}$ $\text{Pa}^{-3} \text{a}^{-1}$)	Degree-day mass balance model accounting for refreezing. Data from nearby stations, atmospheric and linear theory of orographic precipitation models downscaled to high spatial resolution (up to 3 and 1 km respectively for precipitation)	Validation of simulated glacier evolution with observed geometries and area and volume changes in 2000, 1959 geometry simulated as steady state	Focus on downscaling of precipitation and how different techniques affect the modeled evolution
Vestfonna, Svalbard (Schäfer et al., 2015)	DEM from 1990 and bathymetric data for surrounding sea-floor	$\Delta x = 250$ –2,500 m (finite elements). $\Delta t = 1$ a	2006–2100	Finite element full-Stokes model (Elmer). Model not thermomechanically coupled: linear temperature profile imposed. Weertman-type of sliding law, with sliding parameter spatially varying	SMB calculated from temperature-net-radiation index model, accounting for refreezing. Model forced with ERA-Interim based data and CMIP5 GCM output under various RCPs. Downscaled to glacier level based multiple linear regression, variance-inflation techniques and local scaling techniques	Differences in surface elevation between modeled and observed topography analyzed after initial model relaxation	Detailed analysis of the importance of feedback between surface mass balance and elevation and how to incorporate this when modeling future evolution of strongly changing ice masses

Table 3
Continued

Glacier and reference	Geometric information (DEM, ice thickness, flowline, ...)	Horizontal and spatial resolution	Time period	Ice flow (model type, parameters, ...)	Initialization and calibration	Validation	Additional notes
Zongo, Bolivia (Réveillet et al., 2015)	Two DEMs (1997 and 2006) from stereo-pairs of aerial photographs. Bed topography from GPR measurements	$\Delta x = \text{ca. } 25 \text{ m}$ (finite element), 6 vertical layers	1997–2100	Finite element full-Stokes model (Elmer). $a = 1.6 \times 10^{-16} \text{ Pa}^{-3} \text{ a}^{-1}$	Mass balance by constructing mass balance elevation function and linking ELA to temperatures. Forcing from CMIP5 GCMs under various RCPs	Relaxation initial geometry over an 8-year time period. Calibration friction parameter ($=$ sliding parameter, which varies spatially) and surface mass balance	Comparison of modeled and observed changes in surface elevation and glacier length changes

Note: IDGES, ice-dynamical glacier evolution study.

In general, the uncertainty on these elevation products is very low compared to other model input, and ranges on the order of 1–10 m or less for recent studies. Thus, the use of higher-resolution and more accurate DEMs—for example, from UAVs, LIDAR (e.g., used in IDGES by Zwinger and Moore (2009), Aðalgeirsdóttir et al. (2011), and Hannesdóttir et al. (2015)) or remote sensing products—will generally have a limited influence on model results given other model uncertainties. In general, a larger issue in IDGES arises from the temporal mismatch between the DEM and other inputs, such as the glacier outline. With increasingly available and updated DEMs, this issue is likely to become less prominent for future IDGES.

2.2. Glacier Ice Thickness and Bed Topography

2.2.1. Observations

IDGES rely on a wide variety of bed topography reconstruction techniques. The most direct way of measuring the ice thickness is through borehole drilling. However, given the very high labor intensity of drilling boreholes, its application is limited to at most a few point measurements and the method is rarely used to derive the ice thickness in IDGES (e.g., Le Meur & Vincent, 2003; Li et al., 2017; Vincent et al., 2000).

The most widely used technique is to rely on ice thickness measurements from radio-echo sounding (Table 1, refs 4). These measurements are typically performed with systems deployed at the glacier surface, but some IDGES also use measurements from airplanes (e.g., Gilbert et al., 2017; Zekollari, Huybrechts, et al., 2017) and helicopters (e.g., Compagno et al., 2019). Other ice thickness reconstructions in IDGES rely on seismic data (e.g., Le Meur & Vincent, 2003; Vincent et al., 2000; Wallinga & van de Wal, 1998) or on gravimetric measurements (e.g., Rowan et al., 2015; Vincent et al., 2000).

2.2.2. Extension to Entire Glacier Domain

In ice flow modeling studies, discrete ice thickness observations (i.e., a collection of single points) need to be extended to obtain an ice thickness field covering the entire glacier area. For glaciers with a very high density of ice thickness measurements, techniques based on statistical interpolation can be used (e.g., Le Meur & Vincent, 2003; Vincent et al., 2000). However, in most IDGES, the glacierized area is covered with few ice thickness observations only. To estimate the ice thickness over glacierized areas for which no ice thickness observations exist, many IDGES rely on an inverse relationship between the local surface slope and the ice thickness (Table 1, refs 5).

More recently, new techniques have become available to derive the ice thickness from surface topography supported by models that consider the ice flow. These approaches can also consider other types of data, including surface velocities and SMB (Millan et al., 2022). For an overview of such techniques, refer to the Ice Thickness Models Intercomparison eXperiments (Farinotti et al., 2017, 2021). Most approaches derive the ice thickness independently from the glacier evolution, and for these cases the ice thickness can be seen as an input of the modeling. An alternative approach, which has been used in some IDGES, is to derive the ice thickness field as a part of the calibration procedure

by minimizing the misfit with observations on for example, surface elevation or surface velocities (Table 1, refs 6; Section 6.2.3).

2.2.3. Uncertainties

The uncertainty of the reconstructed ice thickness strongly relates to the number of thickness observations used to constrain the ice thickness field (e.g., Lapazaran et al., 2016; Martín-Español et al., 2016). Without any observations, typical uncertainties for the reconstructed ice thickness field are on the order of 20%–30% (Farinotti et al., 2017). For cases with observations, the uncertainty of the observations themselves needs to be accounted for, and the latter increases when extrapolating the measurements to the entire glacier. For example, a recent IDGES by Schmidt et al. (2020) assumes uncertainties on the order of 10–20 m for the observations, which results in uncertainties on the order of 50–100 m for the final reconstructed ice thickness field. It is thus clear that uncertainties of the ice thickness field are large in general and that these have an important effect on the modeled glacier evolution.

3. How Does Glacier Mass Change? Modeling the Mass Balance

An accurate representation of mass balance processes is crucial when modeling the evolution of a glacier, as it is through this process that a glacier gains or loses mass in response to changing climatic conditions. These processes occur at the glacier surface (Section 3.1), at the glacier front (Section 3.2.1), inside the glacier (Section 3.2.2), and at the glacier base (Section 3.2.2).

3.1. Surface Mass Balance

3.1.1. Forcing: The Atmospheric Data

When modeling the SMB of glaciers in IDGES, atmospheric data are needed at the glacier surface. For simplified SMB approaches, typically temperature and precipitation are needed, while more complex approaches often also use additional data (e.g., insolation, wind speed, humidity, or air pressure). The process of downscaling the data to the glacier level, which in some cases is as important as the choice of the atmospheric data itself, is addressed in Section 8 (recommendation (v)).

3.1.1.1. Past and Present-Day Climatic Conditions

The most detailed approach to represent atmospheric conditions over glaciers consists of using data collected by automatic weather stations on the glacier or in the direct vicinity (Table 1, refs 7). Unfortunately, in most cases such data are lacking. An alternative approach is then to use data collected from meteorological stations located in the vicinity of the glacier (Table 1, refs 8).

Several IDGES have used past climatic conditions simulated from regional and global circulation models (RCMs and GCMs, respectively) (Table 1, refs 9). Such simulations can be constrained by reanalysis products such as CRU (Harris et al., 2020) or ECMWF reanalysis project (ERA, as used in IDGES by Leclercq et al. (2012), Engelhardt et al. (2017), and Gilbert et al. (2020)). Some IDGES also estimate past climatic conditions from proxy data derived from for example, tree ring data (Table 1, refs 10), ice cores (Adhikari & Huybrechts, 2009) and in some cases even on more indirect approaches, such as wine harvest data (Stroeve et al., 1989).

3.1.1.2. Future Climatic Conditions

Future climatic conditions in IDGES are typically obtained from climate simulations, or simplified scenarios that are based on such simulations. Some IDGES use data from GCMs (Table 1, refs 11), while others have used climatic conditions simulated from high-resolution RCMs (Table 1, refs 12). CORDEX (Coordinated Regional Climate Downscaling Experiment) is a standardized framework for RCM simulations, and formed the starting point for simulating the future evolution of glaciers in some recent IDGES (e.g., Engelhardt et al., 2017; Schmidt et al., 2020).

The climate scenarios used in IDGES have evolved in pace with the various IPCC Assessment Reports (ARs). IPCC AR3 (2001) and AR4 (2007) mainly relied on SRES (Special Report on Emissions Scenarios; see Table 1, refs 13 for IDGES where these are used). IPCC AR5 replaced the SRES with representative concentration pathways (RCP2.6, RCP4.5, and RCP8.5 being the most commonly used; labeled after a possible range of radiative forcing values in W/m² in the year 2100), and many recent IDGES have used these RCPs for simulating the future evolution of glaciers (Table 1, refs 14). In the IPCC AR6 (IPCC, 2021), the new standard for forcing GCMs consists of Shared Socioeconomic Pathways (e.g., SSP1-26, SSP2-45, and SSP5-85), which will become the new reference scenarios for future IDGES.

3.1.2. Modeling the Surface Mass Balance

3.1.2.1. Direct Observations

When a large data set of observations that covers a sufficiently large fraction of a glacier area is available, the SMB in IDGES can be represented by directly extrapolating these observations to other locations on the glacier through kriging or simple statistical models. Very elaborate SMB observation networks have, for instance, been used directly in some IDGES (Table 1, refs 15). However, in most cases, the SMB needs to be extrapolated to the glacier area through more sophisticated techniques and/or through modeling.

3.1.2.2. SMB Representation Without Explicit Modeling of Accumulation and Ablation Processes

The simplest approach to represent the SMB in IDGES is to use an elevation-dependent representation of the SMB (Table 1, refs 16). Such relationships are typically based on observations of SMB and/or equilibrium line altitude (ELA). When using elevation-dependent SMB approaches, the temporal changes are usually modeled by shifting the ELA. Another approach consists of performing regression analyses between climatic data and SMB observations (e.g., Vincent et al., 2018; Zekollari & Huybrechts, 2018), and using these to simulate the temporal evolution of the SMB in IDGES (e.g., Greuell, 1992; Wallinga & van de Wal, 1998). Neural networks have also been used to link mass balance observations to climatic forcing (e.g., Steiner et al., 2005, 2008), and new advances in this field (e.g., Bolibar et al., 2020, 2022) will also be valuable tools for future IDGES.

3.1.2.3. SMB Representation With Explicit Modeling of Accumulation and Ablation Processes

The processes of mass gain (accumulation) and mass loss (ablation) can also be modeled explicitly. For most glaciers, the mass gain occurs through accumulation of snow, with threshold temperatures used to distinguish between rain and snowfall (Table 1, refs 17). The refreezing of meltwater can also play an important role, and is explicitly accounted for in various IDGES (Table 1, refs 18), while some IDGES also account for other mass supply processes, for example, through avalanching (e.g., Wijngaard et al., 2019).

Ablation occurs through various processes, such as snow and ice melt, wind drift and sublimation. A common approach to represent ablation consists of linking it to atmospheric temperatures. This is done through so called “positive degree day” (PDD) or “temperature-index” modeling, or through enhanced versions of this concept (e.g., Braithwaite, 1995; Hock, 2003; Pellicciotti et al., 2005). PDD modeling has been used in many IDGES (Table 1, refs 19).

In contrast to PDD approaches, “simplified energy balance models” also take into account short-wave radiation, and parameterize both long-wave radiation and turbulent heat fluxes as a function of temperature (Table 1, refs 20). The most detailed approaches solve the full energy balance by accounting for the various terms of the heat balance (e.g., latent and sensible heat, short- and long-wave radiation). These approaches are typically used in studies specifically dedicated to SMB modeling on glaciers (i.e., without time evolution) (e.g., Fitzpatrick et al., 2017; Gabbi et al., 2014; Sicart et al., 2011), but have also been applied a few times in IDGES (Table 1, refs 21). The role of debris on the ice surface has also been accounted for in some IDGES (Table 1, refs 22).

Instead of modeling the SMB as a part of IDGES, another possibility is to use the SMB that is directly calculated from a RCM. In such cases, the RCM does not provide the atmospheric forcing for the SMB model (cf., Section 3.1.1), but instead directly supplies the SMB. This approach is commonly used when modeling the SMB for polar ice sheets (see Fettweis et al., 2020; Mottram et al., 2020 for recent model intercomparison efforts), but is also applicable for IDGES focusing on large glaciers and ice caps (e.g., Schmidt et al., 2020).

3.2. Other Mass Balance Components

3.2.1. Frontal Mass Balance

When a glacier front is in contact with water (e.g., with an ocean, a sea, or a lake), an important fraction of mass loss can occur through frontal ablation and calving. A trivial approach to represent glacier calving in IDGES consists of setting the ice thickness to zero at the coastline/lakeshore or treating the front as land-terminating (e.g., Schäfer et al., 2015; Zekollari, Huybrechts, et al., 2017). Such approaches can be justified for cases where the frontal mass loss is small compared to other ablation processes. Other simplified approaches have been used in IDGES, in which calving fluxes are proportional to the water depth and/or the local ice thickness at the glacier front (e.g., Marshall et al., 2005; Oerlemans, 1986). More complex and comprehensive approaches exist to represent the frontal mass balance, but such approaches have not, to date, been applied in IDGES. These more complex approaches are typically used in theoretical studies and when modeling outlet glaciers of ice sheets (e.g., Nick et al., 2013; Todd et al., 2019; Ultee & Bassis, 2017; van Dongen et al., 2020).

3.2.2. Basal and Internal Mass Balance

Besides the surface and frontal mass balance, basal and internal mass balance processes can also affect the overall glacier mass balance (Jóhannesson et al., 2020). A few IDGES take into account mass loss and gain at the base, through melt and refreezing, respectively (Table 1, refs 23), and internal melting (Flowers et al., 2005, 2007; Marshall et al., 2005). However, the related uncertainties tend to be large, as direct observations are limited (e.g., Boulton & Hindmarsh, 1987; Copland et al., 1997; Goodman et al., 1979; Iverson et al., 2007; Rea & Whalley, 1994). Consequently, most IDGES do not consider these basal and internal MB processes, instead assuming that their contribution is small when compared to processes occurring at the glacier surface and front.

4. How Does the Glacier Flow? Modeling the Ice Dynamics

An accurate representation of glacier flow processes is of vast importance, as it is through this process that mass is transferred through a glacier by gravity.

4.1. Internal Deformation

4.1.1. Linking Stresses to Deformation: Flow Law

To describe stresses within glaciers, a force balance is used that is underpinned by the conservation of momentum (second law of Newton). Due to the high viscosity of ice, inertial and acceleration effects are negligible, and the conservation of momentum can be reduced to an equilibrium of stresses. These stresses are then linked directly to strain rates through a flow law. The most common approach is to express the flow law as a non-linear viscous power law (Glen, 1955; Nye, 1957; Steinemann, 1958). In such a flow law, the stiffness of the ice is described through a rate factor, sometimes termed the “deformation factor” or “creep parameter.” This rate factor depends on ice properties such as temperature (strongest dependence) and impurities (e.g., Budd & Jacka, 1989; Budd et al., 1979). However, as most IDGES do not consider thermodynamics and often assume all ice to be at the pressure melting point (see also Section 4.3), the rate factor is often used for model calibration (see details in Section 6.2.2). For a comprehensive overview of the relationship between stresses acting on glaciers and their deformation, refer to for example, Hooke (2005, chapter 4), Greve and Blatter (2009, chapter 4), and Cuffey and Paterson (2010, chapter 3).

4.1.2. Describing Stresses in Glaciers: Force Balance

4.1.2.1. Full-Stokes and Higher-Order Approaches

Full-Stokes models account for all terms in the force balance (Figure 4a). The full-Stokes approach is thus the most complete one but is computationally expensive. In contrast with full-Stokes models, higher-order models rely on a hydrostatic approximation in which vertical resistive stresses are neglected. Different types of higher-order models exist (Hindmarsh, 2004), some of which assume the horizontal gradients in the vertical velocities to be negligibly small compared to the vertical gradients of horizontal velocities. As a result, the computation of

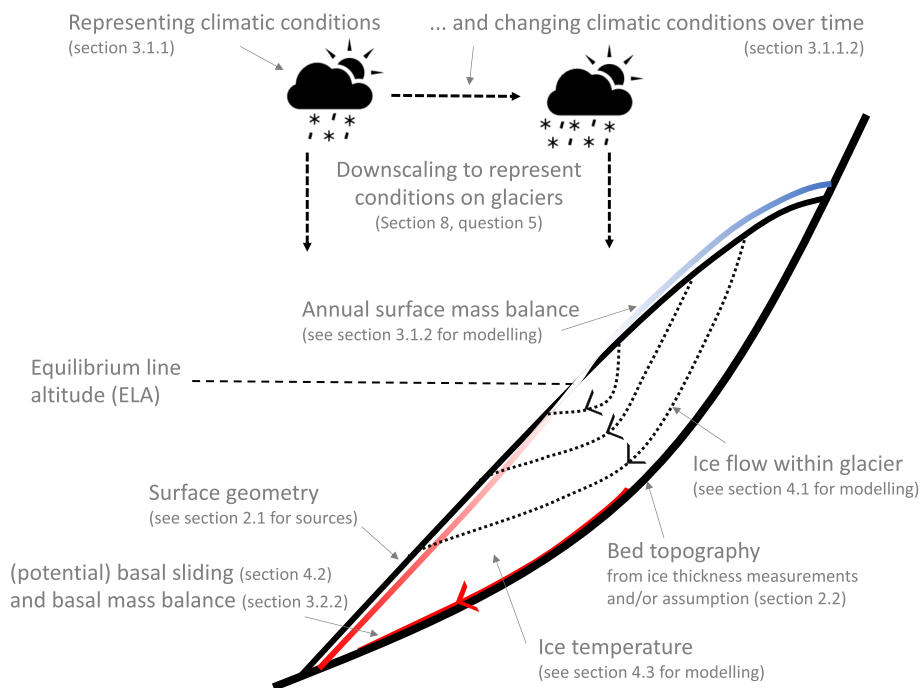


Figure 3. Schematic cross-sectional representation of glacier geometry and some of the major processes that drive the glacier evolution. The red and blue lines schematically represent net ablation (below the equilibrium line altitude [ELA]) and net accumulation (above the ELA).

vertical velocities is decoupled from the ice-dynamical equations, and the vertical velocities can be determined directly via mass conservation. For more insights on higher-order approaches, we refer to studies in which these models are introduced (e.g., Blatter, 1995; Brinkerhoff & Johnson, 2013; Fürst et al., 2011; Pattyn, 2003).

4.1.2.2. Shallow Ice Approximation

A more simplified approach is to rely on the “shallowness” of glaciers, that is, the fact that the glacier thickness is typically much smaller than the horizontal extent (glacier width and length; Figure 4b). In this approach, termed the Shallow Ice Approximation (SIA; e.g., Hutter, 1983; Morland, 1984), horizontal stress gradients are assumed to be negligible compared to vertical gradients of horizontal shear stress. In the SIA, the momentum balance equations can be reduced to simple expressions in which vertical shear stresses are related directly to local gravitational driving stresses. As a result, the stresses can be calculated directly from the slope and thickness at each point. For detailed and accessible accounts on the SIA (including equations and derivation), we refer to for example, Fowler and Ng (2020, pp. 19–22) and Greve and Blatter (2009, pp. 77–83).

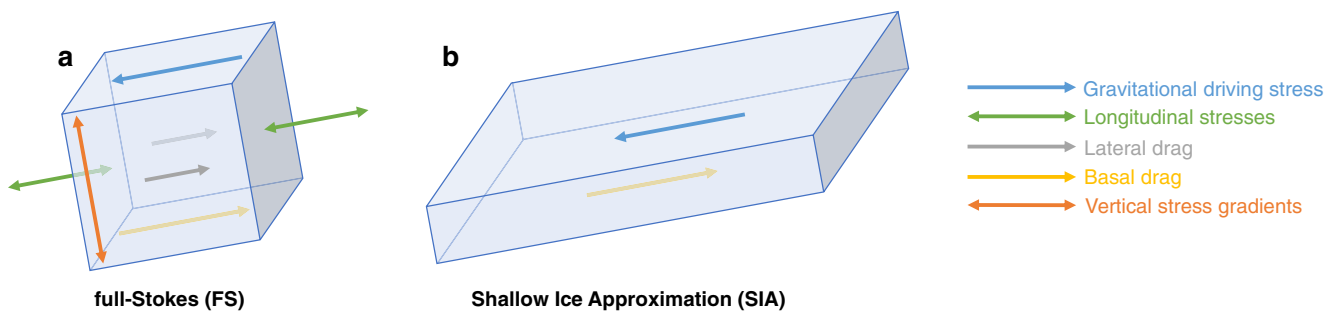


Figure 4. (a) Stresses represented in full-Stokes models and (b) simplified models that rely on the Shallow Ice Approximation (SIA). The schematic representation for the SIA (panel b) indicates an ice body that is wider and longer in comparison to the full-Stokes case (panel a). Different types of higher-order models exist, which tend to include most stresses shown in panel a (full-Stokes models). Figure inspired by graphical representation on www.antarcticglaciers.org.

4.1.2.3. Strength and Limitations of Simplified Approaches

Given its computational efficiency, the SIA has been widely used in IDGES. Most flowline approaches (detailed in Section 5.1.1) use the SIA, and also several 3-D IDGES have used the SIA to describe the ice flow within a glacier (detailed in Section 5.1.2). However, the approach was originally developed for the interior of ice sheets and whether the inherent assumptions made in applying the SIA are justified for glaciers have been the topic of discussion over the past decades, as described in the following examples. Le Meur et al. (2004) used a SIA finite difference model and compared the outcome with results from a finite element full-Stokes model. They found that the largest discrepancy in modeled geometry occurs for steep slopes, and that this effect is more important than effects related to the vertical-to-horizontal scale ratio. Le Meur et al. (2004) define a slope of less than 20% to be acceptable for applying the SIA to mountain glaciers. Leysinger Vieli and Gudmundsson (2004) also used an idealized glacier setup and found that a SIA model roughly produces the same advance and retreat rates (for a given mass balance distribution) compared to more complex approaches. These simulations suggest that for cases where the integrated response to changes in mass balance is assessed (as opposed to short-term changes), using a SIA model is justifiable. Egholm et al. (2011) studied the flow of idealized glaciers over steep terrain while showing the limitations of SIA to model the ice flow velocities accurately. To overcome these limitations, they suggest using a method of intermediate complexity, referred to as an integrated second-order SIA, which accounts for higher-order effects but still provides the computational efficiency compared to full-Stokes model. Zhang et al. (2015) also compared the evolution of idealized glaciers under varying model complexities with a special focus on the effect of various thermal conditions. They found that for temperate ice zones (ice at the pressure melting point), or when basal sliding is important, significant differences between simulated ice flow can occur depending on the model complexity.

The effect of the ice-flow model complexity has also been investigated for real glacier and ice cap geometries, with a calibrated and evaluated setup. Various studies on ice caps suggest that the inclusion of higher-order stresses matters for detailed representation of ice flow, for instance to reproduce closely observed surface velocities (e.g., Marshall et al., 2005; Zekollari et al., 2017). However, these studies also show that the added value of using higher-order and full-Stokes solutions is limited for transient simulations (differences in modeled volume and area are typically <5% when compared to SIA simulations), and that in such cases using the SIA is sufficient (Åkesson et al., 2017; Marshall et al., 2005; Zekollari, Lecavalier, et al., 2017). The limited importance of detailed ice-flow model physics when modeling long-term glacier evolution was also found for several studies on the evolution of mountain glaciers. Albrecht et al. (2000) were able to reproduce a very similar transiently modeled glacier geometry for Storglaciären (Sweden) with a SIA model compared to a higher-order model. In a study on Haig Glacier (Canada), Adhikari and Marshall (2013) showed that the inclusion of a full-Stokes representation is important for detailed modeling of surface velocities during glacier advance. However, when modeling glacier retreat, the differences (SIA vs. full-Stokes) in modeled volume and area change were found only to be on the order of few percent or less. Similar findings were obtained by Zhao et al. (2014) in a study on Gurenhekou Glacier (Tibet). They suggest that it is important to include longitudinal stress gradients for diagnostic analyses (i.e., without time dimension) but that the added value is very limited for prognostic studies when considering volume and area changes.

4.2. Basal Sliding

Basal sliding is strongly linked to basal temperatures and the presence of water at the ice-bed interface. Typically, glaciers are assumed to slide over the bed where the temperature is at pressure melting point (temperate zones), whereas for cold regions (ice temperature below the pressure melting point) the ice is typically assumed to be frozen to the bed. The locations of temperate and cold basal zones within a glacier can be determined by explicitly modeling the thermodynamics of glaciers (Section 4.3). An alternative, simpler approach consists of determining an elevation below which basal sliding occurs, that is, assuming the ice to be frozen to the bed in the upper part of the glacier (Table 1, refs 24). In some IDGES, basal motion is explicitly set to zero over the entire glacier domain through a no-slip basal boundary condition (Table 1, refs 25).

Most IDGES use general sliding laws that account for bed properties and other (potentially time-dependent) features, such as basal hydrology. A widely used method is to use a Weertman-type sliding law, in which the basal sliding is directly linked to the basal drag (Weertman, 1964). The most common approach consists of relating

the sliding to the third power of the basal drag (Table 1, refs 26). In some of these IDGES, the basal drag to the third power is divided by a pressure term (the overburden load, the effective pressure, or combinations of these), making the relationship between basal sliding and drag in fact a quadratic relationship (Table 1, refs 27). Some IDGES directly use a quadratic relationship between basal drag and velocity (e.g., Rowan et al., 2015; Ziemen et al., 2016), but also here a division by the effective pressure sometimes occurs (Rowan et al., 2015). Finally, a series of IDGES directly relies on a linear relationship between basal drag and sliding (Table 1, refs 28).

Other approaches determine basal sliding through the shallow-shelf approximation (SSA), which was originally developed for ice shelves for which longitudinal stresses dominate and for which basal shear stresses are assumed to be zero (SSA; Bueler and Brown (2009); see Fowler and Ng (2020, pp. 205–208) for a clear introduction to this). This is the case, for instance, in IDGES that use the Parallel Ice Sheet Model (PISM), which is an open-source modeling framework for ice sheets and glaciers (Schmidt et al., 2020; Ziemen et al., 2016). Another series of approaches in IDGES determines components of the basal motion explicitly, for instance by parameterizing the basal ice flow as a function of spatially and temporally evolving subglacial water pressure (e.g., Flowers et al., 2005, 2007; Marshall et al., 2005), or by accounting for till properties and deformation (e.g., Schmidt et al., 2020).

In some IDGES, basal sliding is only included in the treatment of internal deformation (Table 1, refs 29), or imposed as a fraction of the calculated surface speed (e.g., Huss et al., 2007). A justification for these approaches is that both sliding and internal deformation are strongly linked to the glacier thickness and surface slope (e.g., Dehecq et al., 2019; Flowers et al., 2007; Gudmundsson, 1999; Zekollari et al., 2013). As a consequence, good agreement between observed and modeled surface velocities can often be achieved even when neglecting basal sliding (e.g., Hooke et al., 1989; Zekollari et al., 2013). Moreover, as direct observations on sliding processes are very sparse, the use of complex approaches to represent processes occurring at the glacier base may not always be justifiable. For more details about basal processes occurring under ice masses and how to represent these in mathematical models, we refer to for example, Hooke (2005, chapter 7), Cuffey and Paterson (2010, chapter 7), Fowler and Ng (2020, chapter 3.1), and Greve and Blatter (2009, pp. 157–163).

4.3. Thermodynamics

The ice temperature has a large influence on the dynamics of glaciers, as it directly influences the stiffness of the ice (see e.g., Table 3.3 in Cuffey and Paterson (2010)) and thereby its deformation (see Section 4.1.1) and determines where basal sliding occurs (Section 4.2).

In many IDGES, glaciers are assumed to be isothermal, with all the ice being at the pressure melting point (i.e., at or just below 0°C). This is the case for most IDGES that focus on glacier evolution in the European Alps (Table 1, refs 30), Scandinavia (Table 1, refs 31), Iceland (Table 1, refs 32), the Himalayas (e.g., Adhikari & Huybrechts, 2009; Engelhardt et al., 2017; Gantayat et al., 2017), and the Canadian Rocky Mountains (e.g., Adhikari & Marshall, 2013).

For representing temperatures within cold and polythermal glaciers, approaches of varying complexity have been used in IDGES. A simple approach is to impose a depth-dependent temperature profile (e.g., Schäfer et al., 2015; Wang et al., 2019), or, in the case of thin glaciers, even assume the temperature to remain constant with depth (Réveillet et al., 2015). Such approaches are reasonable when the focus of the study is not on thermodynamics, as errors introduced through these simplifications are relatively small compared to other model uncertainties (e.g., Schäfer et al., 2015). A more comprehensive method to represent the thermodynamics in IDGES is based on the conservation of energy and accounts for heat fluxes due to advection of ice, diffusion of heat, and strain heating (Table 1, refs 33). In such approaches, the thermodynamics at the glacier base are controlled by the geothermal heat flux (Table 1, refs 34). Typically, latent heat released by the refreezing of meltwater is also accounted for. This refreezing typically occurs at the glacier surface or at shallow depths, but in some cases meltwater can also penetrate into the glacier before eventually refreezing englacially or subglacially (e.g., Gilbert et al., 2020; Schäfer et al., 2014; Zekollari, Huybrechts, et al., 2017). To ensure energy conservation, one can also use an enthalpy formulation, which facilitates the representation of phase transitions (Aschwanden et al., 2012), as used for instance in recent IDGES by Gilbert et al. (2017, 2020). For a comprehensive review on ice thermodynamics, refer to for example, Hooke (2005, chapter 6), Cuffey and Paterson (2010, chapter 9), or Fowler and Ng (2020, chapter 2).

5. Numerical Representation of Glacier Evolution

5.1. Spatial Dimensions

5.1.1. Flowline Modeling

The simplest approach to account for ice flow processes is to represent the glacier geometry along a flowline (Figure 5). Indeed, the first efforts to model the temporal evolution of glaciers relied on such flowline modeling (Table 1, refs 35). These pioneering studies, which provided some of the first quantitative insights on glacier fluctuations and the driving mechanisms behind these changes, facilitated a widespread adoption of flowline modeling in the late 1980s and 1990s (Table 1, refs 36). Flowline approaches are computationally efficient (Section 5.4) and can therefore be used to perform a wide range of simulations, hence their persistent popularity (e.g., Engelhardt et al., 2017; Gantayat et al., 2017; Leclercq et al., 2012). To represent glaciers with more complex shapes, some IDGES split the glacier domain into several independent flowlines (Table 1, refs 37). An extensive summary of IDGES relying on flowline approaches is provided in Table 2.

In many IDGES, the determination of flowlines is performed manually, typically by following a trajectory that is perpendicular to the elevation contours and centrally located between the nearest glacier edges. Such an approach is feasible when working on individual glaciers and has the advantage that it can incorporate field knowledge (Table 1, refs 38). More recently, automated techniques have been developed, which are typically designed to determine flowlines for larger samples of glaciers, but which can nevertheless be used at the single-glacier scale (e.g., Kienholz et al., 2014; Le Moine & Gsell, 2015; Machguth & Huss, 2014; Maussion et al., 2019).

In flowline studies, the cross section parameterization of the glacier is of large importance. This representation is necessary to ensure that a thinning of the glacier leads to a decreasing width and, consequently, modifies the area at a given elevation. As such, the cross section representation is not only relevant to ice flow, but it also influences the glacier SMB. Different methods exist to represent the glacier cross section, where the use of a geometrical



Figure 5. Overview of various glacier geometry representations used in numerical models, including scaling-based relationships (blue), flowline approaches (orange) and 3-D modeling (yellow). The Morteratsch Glacier complex is chosen as an example (picture by Günter Seggebaing, June 2005). The first geometry (starting from left) corresponds to an early twenty-first century representation of the glacier, while the evolution in a future climate is derived from a hypothetical glacier evolution. The 3-D glacier representations (yellow box) are generated with the TopoZeko toolbox (Zekollari, 2017).

representation is the most common approach. Mostly, the glacier is represented as a trapezoid (Table 1, refs 39), although some studies also use a power-law or parabolic fit (e.g., Huybrechts et al., 1989; Kruss, 1984; Mackintosh et al., 2002). In some cases, the cross section is even represented explicitly at every grid point by taking into account the observed local cross section (e.g., Huss et al., 2007; Sugiyama et al., 2007).

Most flowline models use the SIA, in which the forces acting on the ice are directly related to the local ice thickness and surface slope (Section 4.1.2). However, in some cases friction from the side walls, which can be important for valley glaciers, is accounted for through a multiplication factor, typically referred to as a shape factor (e.g., Anderson et al., 2008; De Smedt & Pattyn, 2003; Schlosser, 1997). Additionally, other non-local stresses (e.g., longitudinal) are sometimes included in flowlines studies, for example, through correction factors, or in some cases, even by explicitly including these stresses when solving the force balance (Table 1, refs 40).

5.1.2. 3-D Models

A 3-D setup is computationally more demanding compared to a flowline setup but allows better accounting for specific geometrical settings and how ice flow reacts to these. Moreover, a 3-D setup often allows for a more sophisticated calibration and evaluation (Section 6).

Whereas series of 3-D diagnostic glacier studies (e.g., Gudmundsson, 1999; Hubbard et al., 1998) and time-dependent ice sheet studies (e.g., Greve, 1997; Huybrechts, 1990) were performed in the 1990s, the use of 3-D approaches for IDGES only started appearing from the early 2000s onwards. Some of these 3-D approaches use the SIA (Table 1, refs 41). These 3-D SIA models are sometimes referred to as 2-D or 2.5D, as the ice flow at a single location represents the entire ice column (i.e., vertical integration).

More sophisticated approaches exist, in which non-local stresses are also included in 3-D IDGES. These stresses can be accounted for by applying perturbations or corrections to the SIA (e.g., Marshall et al., 2005; Rowan et al., 2015; Wijngaard et al., 2019), through hybrid SIA-SSA approaches (e.g., Schmidt et al., 2020; Ziemen et al., 2016) or by explicitly solving for higher-order/full-Stokes stresses (Table 1, refs 42). For a detailed overview on 3-D IDGES, refer to Table 3.

5.2. Spatial Discretization and Resolution

The various differential equations used in IDGES are typically resolved by models that use finite difference or finite element approaches.

5.2.1. Finite Differences

Finite differences are used for virtually all flowline models and for many 3-D models (Table 1, refs 43). In these finite difference studies, the spatial domain is discretized on a regular grid, which can have a strongly varying resolution depending on the study (see Tables 2 and 3). In the earliest flowline models, for instance, the grid resolution was typically on the order of (a few) hundred meters (Table 1, refs 44). The first generation of 3-D IDGES also typically operated at a lower horizontal resolution, on the order of 100 m (Albrecht et al., 2000; Giesen & Oerlemans, 2010). More recently, high-resolution IDGES have emerged with horizontal resolutions of only a few tens of meters, which for small- to medium-sized glaciers results in a domain on the order of 10,000–100,000 grid points (Table 1, refs 45).

5.2.2. Finite Elements

Finite element methods used in IDGES rely on various mesh forms: for example, tetrahedrons (e.g., Jouvet & Huss, 2019; Jouvet et al., 2009, 2011) or triangular elements (Table 1, refs 46). Finite element methods are more complex to implement than finite difference approaches, but have the advantage that the mesh can be adapted to specific needs: for example, having a high resolution for dynamic and quickly changing outlet glaciers of ice caps, whereas the interior can be described with larger elements of lower resolution. Typical sizes for the elements are on the order of a few tens of meters (Table 1, refs 47). In most IDGES, the grid elements are fixed in time (Table 1, refs 48), and often various meshes are used depending on the model component: for example, a reference grid can be used to solve the stress balance equations, but the continuity equation is then solved on a smaller grid (e.g., Jouvet et al., 2009).

Finite element approaches are typically used in 3-D studies that solve for higher-order/full-Stokes stresses (Table 1, refs 49). However, some 3-D SIA studies (sometimes referred to as 2-D or 2.5-D, see Section 5.1.2) also use finite element methods (e.g., Aðalgeirsdóttir et al., 2011; Hannesdóttir et al., 2015).

5.3. Glacier Evolution

5.3.1. Mass Conservation

In IDGES, the time evolution of glaciers is based on the conservation of mass. This conservation is typically obtained by combining ice flow and SMB processes through a type of continuity equation for ice thickness or based on the “evolution of the free surface”. In such relationships, ice is usually represented as an incompressible non-Newtonian material, with imposed densities of for example, 850 kg m^{-3} (Adhikari & Huybrechts, 2009), 870 kg m^{-3} (e.g., De Smedt & Pattyn, 2003), 890 kg m^{-3} (e.g., Le Meur et al., 2004), 900 kg m^{-3} (Table 1, refs 50), 910 kg m^{-3} (Table 1, refs 51), up to the theoretical maximum of 917 kg m^{-3} (Table 1, refs 52). Typically, the entire mass is considered to be ice, while in reality some parts of the glacier are also covered with snow and firn. However, only assuming ice to be present generates a relatively small error, which can be accepted given many other uncertainties in the model and boundary conditions (Albrecht et al., 2000).

5.3.2. Explicit Versus Implicit Schemes

To model the change in glacier geometry, various numerical schemes are used in IDGES. Explicit (forward) schemes take information at a given time step and use this to determine the state at a later step through an analytical solution. Such explicit schemes are relatively straightforward to implement and are known to work well when solving the continuity equation if small time steps are used. Explicit schemes have been used in many flowline studies (Table 1, refs 53) and have also been applied in 3-D IDGES (Table 1, refs 54).

Implicit methods use information on both a current and a future state to determine the state of a system at a later time, which makes them less straightforward to incorporate (requiring matrix solvers) compared to explicit methods (solving tridiagonal matrices, Table 1, refs 55). However, implicit schemes allow using larger time steps, and in some cases even become unconditionally stable, meaning that the method will not become unstable even with very large time steps. Implicit methods are computationally more demanding, meaning that the calculation of every individual time step will take longer compared to an explicit approach. Moreover, too large a time step cannot be used, as otherwise the geometry change over the time step becomes too large, leading to a poor approximation of the solution.

5.3.3. Time Stepping

In general, the time step at which the glacier geometry is updated is set as large as possible in order to reduce the computational time, while ensuring numerical stability. This time step is typically constant in IDGES, and varies from (sub)daily (ca. $0.00025\text{--}0.003$ a), through (half-)weekly ($0.01\text{--}0.025$ a), (half-)monthly, half-yearly ($0.05\text{--}0.5$ a), to annual time steps (Table 1, refs 56–59). As the glacier geometry can strongly change throughout simulations, it is also beneficial in some cases to use a dynamic time step, which changes during the simulation. For small ice thickness and low velocities, large time steps can be used, while smaller time steps need to be used when flow velocities are high. To estimate the required time step, a Courant–Friedrichs–Lewy type of criterion can be used as a rule of thumb, which estimates the largest possible time step as a function of the spatial resolution and the ice flow velocity (Courant et al., 1928). Despite the advantages of using a dynamic time step, the approach is not widely used in IDGES (e.g., Anderson et al., 2008; Rowan et al., 2015).

In many IDGES, various model components are updated at lower time-frequency compared to the glacier evolution (Figure 6). For instance, the mass balance forcing might be updated once a year (Table 1, refs 60), which is typically sufficient if the interest is in the evolution of a glacier over decadal to centennial time scales (e.g., Albrecht et al., 2000). Despite the yearly update, the mass balance itself is often calculated at a much higher frequency, typically with time steps on the order of minutes to days (Table 1, refs 61). Other model components that influence the glacier evolution are usually updated once a year, such as the ice thermodynamics (Gilbert et al., 2020) and the bed isostasy (Marshall et al., 2005). In some cases, the update of model components can even

be at larger time steps, such as the coupling between the hydrological conditions and ice dynamics, which was set at 5 years in IDGES by Flowers et al. (2005, 2007) and Marshall et al. (2005).

5.4. Computational Resources

The increase of computational capacity over the last decades has allowed the development of IDGES with increased complexity in terms of geometric representation (e.g., 3-D), mass balance modeling (e.g., energy balance modeling) and ice flow modeling (e.g., including higher-order and full-Stokes stresses). In early IDGES, the computational capacity was a limiting factor (e.g., mentioned explicitly in Kruss and Smith (1982) and Gruell (1992)). Although direct comparisons are difficult to make, a qualitative estimate of the increase in computational power over the last two to three decades suggests that calculations with flowline models may have gained about one to two orders of magnitude in speed on individual computers (Figure 7). Oerlemans (1997b), for instance, mentioned a calculation time of 10 min to calculate 1,000 years of evolution on a Macintosh Power PC 7100-66 (coded in FORTRAN-77) when simulating the evolution of Nigardsbreen (Norway) with a flowline model. In recent studies by Zekollari et al. (2019, 2020), Compagno, Eggs, et al. (2021), and Compagno, Zekollari, et al. (2021), in which the evolution of glaciers in the European Alps and Scandinavia was calculated with a flowline approach, in general it took only a handful of seconds to calculate the evolution of an individual glacier over multicentennial timescales (with MATLAB, on 2015 MacBook Pro with 2.2 GHz Intel Core i7 and 16 GB RAM).

With new computational resources, especially using computer clusters, the application of higher-order and full-Stokes ice flow modeling in IDGES has become increasingly possible (e.g., explicitly mentioned in Réveillet et al. (2015)). However, it must be noted that such calculations are still relatively time consuming, which tends to limit possibilities for model calibration and for evaluating the model sensitivity to specific parameters. Often, calculation times on the order of days for 3-D higher-order/full-Stokes centennial-scale simulations performed on single machines must be accounted for (Figure 7). For instance, Jouvet et al. (2009, 2011) needed several

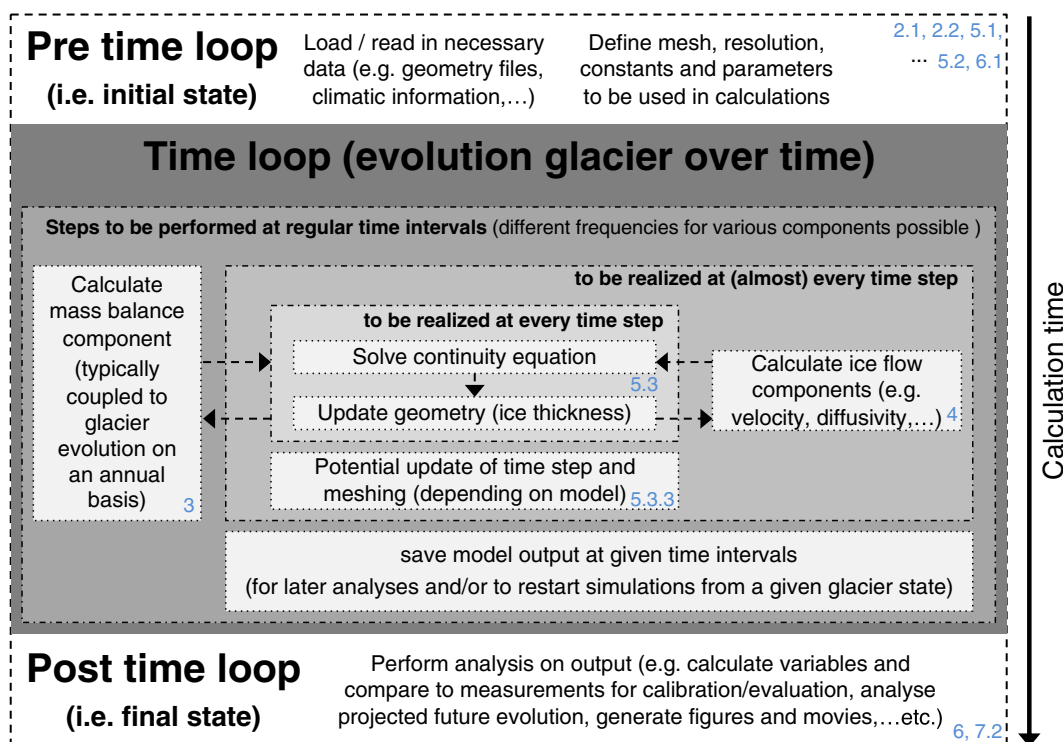


Figure 6. Schematic overview of various steps when numerically modeling the ice-dynamical evolution of glaciers, with a subdivision between the steps that need to occur before the glacier evolution, those occurring while the glacier geometry evolves, and those to be performed after the simulations. The blue numbers correspond to the subsections numbering.

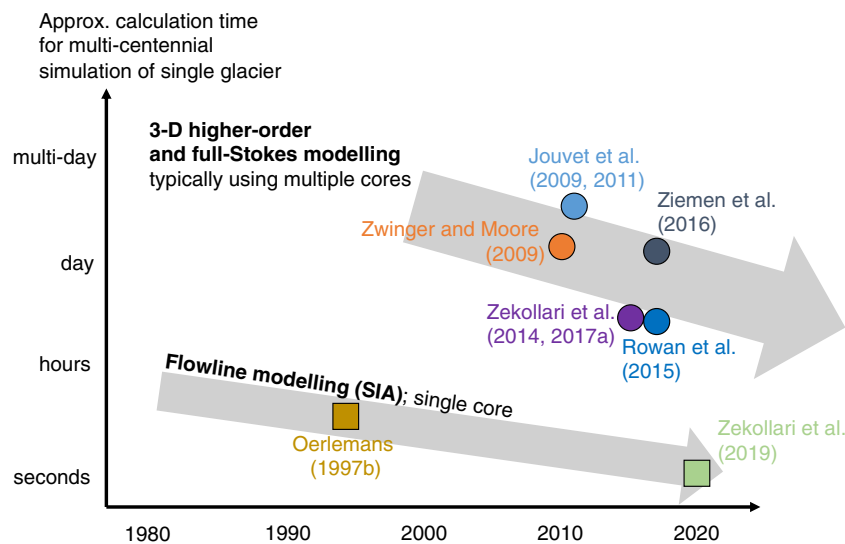


Figure 7. Schematic representation of the typical calculation time needed over the past decades to model the temporal evolution of glaciers. Most studies do not explicitly include information about the computational resources, and the few publications that do strongly vary in terms of resolution, domain size and number of cores used. Consequently, the schematic representation has a qualitative character.

days for multidecadal simulations of Rhone Glacier (Switzerland), and about 1–2 days for a period of 100 years when calculating the evolution of Aletsch Glacier (Switzerland). Zwinger and Moore (2009) needed around 1 day to simulate the multidecadal evolution (53 years) of Midtre Lovénbreen (Svalbard) with a dual core processor. These calculation times are now reducing as computational power increases, and important increases in speed can be obtained when running in parallel on computer clusters with multiple cores. Rowan et al. (2015) used a 12-core central processing unit, requiring around 8–12 hr for 1,000-year simulations of Khumbu Glacier (Nepal), while Ziemer et al. (2016) used 64 CPUs for modeling the evolution of the Juneau Icefield with PISM, which took about 36 hr for the multicentennial spin-up and simulations (Figure 7).

6. Initializing, Calibrating, and Evaluating a Glacier Evolution Model

6.1. Model Initialization

When simulating the temporal evolution of glaciers, a major challenge relates to model initialization, which can have a large impact on the modeled glacier evolution. This is a well-known problem in glaciology, as illustrated by recent intercomparisons specifically focusing on the initialization of ice sheets models (Goelzer et al., 2018; Seroussi et al., 2019).

In IDGES, three main initialization techniques have typically been used. The first approach consists of starting simulations from an observed state (Table 1, refs 62). This is the most straightforward approach, but the discretization to a numerical environment and the uncertainties related to this will cause a non-physical initial (dynamical) shock. As a result, a part of the modeled initial glacier evolution will not be driven by the forcing but will instead be an artificial “adaptation” of the modeled glacier geometry to the numerical environment. Moreover, a start from an observed state is problematic for thermo-mechanically coupled glacier evolution models, as the thermodynamic state of a glacier strongly depends on past climatic conditions, mass balance and glacier evolution. In general, the initial model shock becomes less relevant for longer time scales, thus justifying a start from the observed state in such cases. An alternative approach is to start from a relaxed version of the observed geometry, where the time over which the relaxation occurs needs to be long enough to reduce the initial model shock, but not too long to avoid the relaxed geometry being too different from the observed state (e.g., Réveillet et al., 2015; Schäfer et al., 2015; Ziemer et al., 2016). This typically results in relaxation times on the order of a few years (Réveillet et al., 2015; Schäfer et al., 2015), although some IDGES have relied on more complex multi-stage initializations in which the geometry is relaxed in a controlled way (Ziemer et al., 2016).

A second approach consists of assuming that the starting geometry is in steady state (Table 1, refs 63). In such approaches, by continuously applying a constant climate forcing, the glaciers evolve in a steady state geometry that is similar to the observed state. The downside of this approach is that, in reality, glaciers are never entirely in equilibrium with climatic conditions. This approximation will thus have an influence on the initial glacier evolution (e.g., delayed response in glacier length changes as the glacier adjusts to the non steady-state conditions). However, this effect reduces with time and is acceptable if the main focus of the IDGES is on longer timescales. An advantage of using a modeled initial state is that the initialization procedure can be used to calibrate some of the model parameters (e.g., ice flow parameters), which can then be used for the transient simulations performed in the IDGES (see also Section 6.2).

As a third initialization approach, the final state of an historical glacier evolution simulation can be used as the initial state of a transient run (e.g., glacier evolution from a present-day state until 2100). This approach has been used in a wide range of IDGES (Table 1, refs 64). In many of these IDGES, the historical runs are forced with a time-varying mass balance perturbation in order to reproduce past observed glacier states through a so-called “dynamic calibration” (Table 1, refs 65). This initialization method can be quite elaborate in terms of setup and computational requirements, but it has the advantage that the initial transient glacier state can be closely reproduced, while also allowing for calibration of some of the model parameters.

6.2. Model Calibration

When calibrating model parameters in IDGES, a distinction is typically made between the calibration of SMB components (Section 6.2.1) and the calibration of ice flow components (Section 6.2.2). Occasionally, both model components are considered in a coupled setup (Section 6.2.3).

6.2.1. Surface Mass Balance

6.2.1.1. Observations for Model Calibration

The calibration of mass balance parameters in IDGES is performed to reproduce a wide range of observations. In some cases, the goal is to reproduce the observed glacier evolution, or the geodetic mass balance derived from this. Such values can be obtained from geodetic products derived from satellite observations (e.g., Braun et al., 2019; Brun et al., 2017; Hugonet et al., 2021). Various IDGES have used such geodetic observations as a target to calibrate the mass balance component (Table 1, refs 66). As internal and basal mass balance processes are typically neglected in IDGES (Section 3.2.2), calibrating the mass balance component to match geodetic mass balances will lump these processes into the SMB model calibration.

Other IDGES calibrate the mass balance components to reproduce directly mass balances observed in-situ or ELA observations, which are typically derived from stake or snowline measurements (Table 1, refs 67). Other approaches focus on reproducing water discharge measurements downstream from glacier (e.g., Johannesson, 1997; Jouvet et al., 2009), or calibrating the mass balance model for the integrated mass balance to be zero for a period for which the glacier is close to equilibrium (Johannesson, 1997).

An alternative SMB calibration approach consists of focusing on the output of the glacier evolution model, which is itself driven by the mass balance forcing. Examples in IDGES include efforts to calibrate the SMB by reproducing observed length changes (e.g., Allison & Kruss, 1977; Anderson et al., 2008; Sugiyama et al., 2007) or to match the geometry at a given date (Table 1, refs 68).

6.2.1.2. Model Input and Parameters for Calibration

The most widely used approach when calibrating the IDGES SMB model is to modify the parameters that are used in the SMB model or to modify the parameters that define the imposed SMB profile. These parameters typically consist of PDD factors, albedo values, and various terms in the radiation balance (Table 1, refs 69).

Another approach consists of modifying the input of the mass balance models. One of the largest unknowns in the mass balance forcing of glaciers is solid precipitation. The latter often has large spatial variability and is difficult to constrain without direct observations. A common approach in IDGES is to take this uncertainty into account by modifying the precipitation either manually, through scaling, by imposing an altitudinal gradient, or through applying a uniform correction (Table 1, refs 70). Alternatively, some IDGES have also modified the temperature

forcing, by adding a correction on this quantity or by imposing a gradient as part of the calibration process (e.g., Anderson et al., 2008; Flowers et al., 2005; Gilbert et al., 2020).

6.2.2. Ice Flow

6.2.2.1. Observations for Model Calibration

One of the most common approaches for the flow model calibration in IDGES is to reproduce observed surface velocities (Table 1, refs 71). This works relatively well in general, even for simplified approaches (e.g., SIA), as long as the observed velocities do not exhibit short-lived variations or small-scale variability. An important consideration when calibrating the flow model with observations is to ensure that the modeled glacier geometry is similar to the real glacier geometry from which the surface velocities are observed. As ice flow controls the glacier evolution, the calibration of the flow parameters is sometimes also performed by matching observed changes in glacier length or glacier volume (Table 1, refs 72). Another approach consists of matching the observed glacier geometry (Table 1, refs 73).

6.2.2.2. Model Input and Parameters for Calibration

In most IDGES, the ice flow is determined by a combination of internal deformation (Section 4.1) and basal sliding (Section 4.2). The internal deformation is controlled by the rate factor, which determines the stiffness of the ice. As such, it has a large influence on the modeled glacier geometry: a low value represents stiffer ice and will result in a larger ice thickness, whereas a high value corresponds to a higher viscosity (i.e., smaller stiffness), which results in a lower ice thickness. The quantity is thus widely used as a calibration parameter in IDGES (Table 1, refs 74).

A comprehensive overview of rate factors used for temperate glaciers in IDGES suggests that typical values vary between 0.4 and $1.3 \times 10^{-16} \text{ Pa}^{-3} \text{ a}^{-1}$ (Q1 and Q3 values based on 48 published studies; median and mean of 0.75 and $0.89 \times 10^{-16} \text{ Pa}^{-3} \text{ a}^{-1}$, respectively, Figure 8). This includes values that were directly derived in the IDGES as a part of the calibration procedure, as well as commonly used values in IDGES that are derived from lab experiments, field observations or other numerical modeling. In general, the values agree well with the widely used value of $0.76 \times 10^{-16} \text{ Pa}^{-3} \text{ a}^{-1}$ suggested by Cuffey and Paterson (2010) for temperate ice based on calibrated numerical models, and confirm that the values obtained from lab experiments or field observations are typically higher than those from numerical simulations (Figure 8). Directly comparing rate factors from different studies is difficult, as they often represent other processes: some include basal sliding, shape factors or correction factors to account for example, longitudinal and transverse stresses, etc., while others do not.

The basal sliding or (basal) friction parameter is another widely used quantity for calibrating the ice flow model component in IDGES. This quantity, which is sometimes calibrated together with the ice flow, determines the amount of sliding occurring as a function of the basal stresses, thereby exerting an important control on the glacier geometry (Table 1, refs 75) (Figure 9). Typically, a single value for the sliding parameter is calibrated and imposed for the entire glacier, where the unit of the sliding parameter is directly related to the sliding law used (Figure 9). Some IDGES do however vary the sliding parameter spatially as part of the calibration procedure (Table 1, refs 76).

6.2.3. Mixed Approaches and Other Parameters

In some IDGES, the ice flow and mass balance parameters are calibrated simultaneously (e.g., Flowers et al., 2007; Schmeits & Oerlemans, 1997; Wijngaard et al., 2019). Such approaches are generally very comprehensive, as they allow the determination of interactions between various processes on the glacier evolution.

Besides the ice flow and mass balance parameters, other model parameters can also be calibrated to match observations. For instance, the bed topography can be used as a tuneable quantity, rather than being considered as a static model input. In some IDGES, the bed elevation has been modified to minimize differences between the modeled and the observed historical glacier changes (Table 1, refs 6), or as a tool to produce a realistic transiently modeled present-day glacier geometry (e.g., Engelhardt et al., 2017; Gantayat et al., 2017). Depending on the specific setting, other model components can be calibrated as well, for example, matching observed englacial temperatures by modifying thermodynamic model parameters (Zekollari, Huybrechts, et al., 2017).

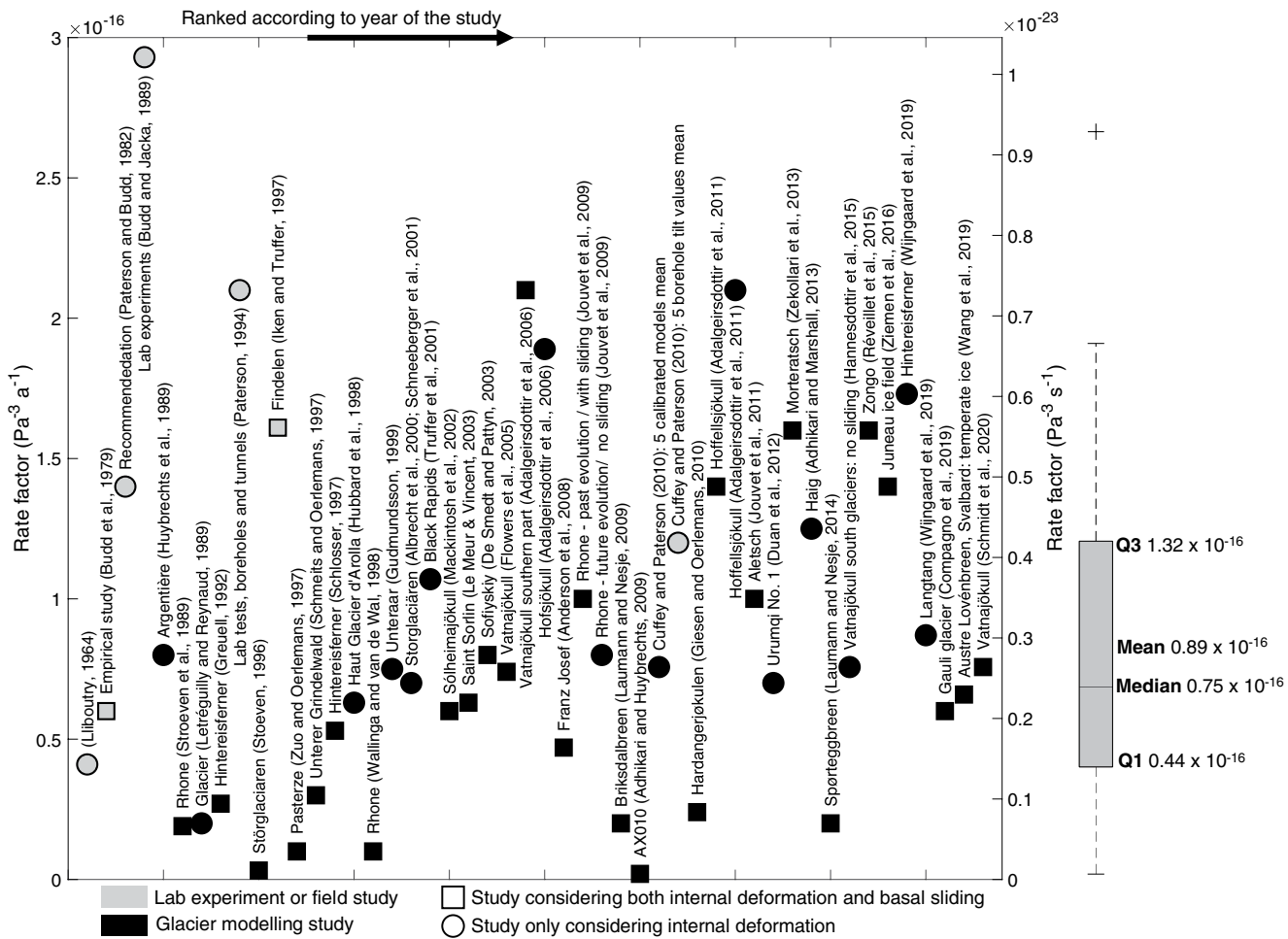


Figure 8. Overview of rate factors used in ice-dynamical glacier evolution studies (IDGES), based on 48 studies from the literature (Tables 2 and 3). The bar on the right side indicates the 25% percentile (Q1), the 50% percentile (median), the 75% percentile (Q3), and the mean value. Notice that it is not always possible to compare these values directly, as some studies include basal sliding, shape factors and/or correction factors (e.g., to account for longitudinal and transverse stresses), while others do not. The values given here take into account the enhancement factor (e.g., Wang et al., 2019) and multiplication factors related to longitudinal stresses (Wijngaard et al., 2019). Some of the rate factors in this figure originate from lab experiments, field studies and diagnostic glacier modeling efforts (Budd & Jacka, 1989; Budd et al., 1979; Cuffey & Paterson, 2010; Gudmundsson, 1999; Iken & Truffer, 1997; Lliboutry, 1964; Paterson, 1981, 1994; Paterson & Budd, 1982; Zekollari et al., 2013), and were used directly in IDGES: that is, IDGES were the calibration of rate factor is not explicitly performed.

6.3. Model Evaluation

To reduce the uncertainty in the simulated glacier evolution, it is important to evaluate model performance. This evaluation needs to be independent from the calibration process: for example, if velocity or mass balance observations have been used for model calibration, these quantities should not be used to assess the performance.

On the one hand, the model evaluation can be based on individual model components, which include comparisons between observed and modeled SMB (Table 1, refs 77), surface velocities (Table 1, refs 78), englacial temperatures (e.g., Gilbert et al., 2020; Li et al., 2017), basal conditions (Zwinger & Moore, 2009), and isochrones (Zwinger & Moore, 2009). On the other hand, the modeled glacier geometry that results from the interaction between mass balance and ice flow processes, can be compared to observations (Table 1, refs 79). Finally, changes in glacier volume, area, and length have also been used to evaluate the model performance (Table 1, refs 80).

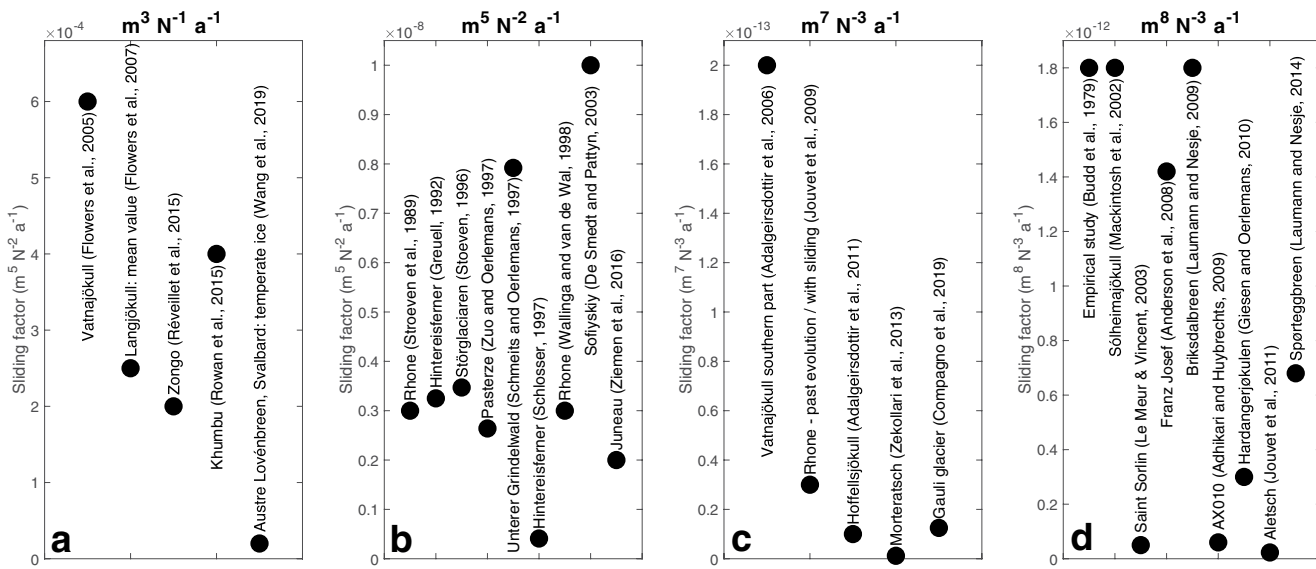


Figure 9. Overview of sliding parameters used in ice-dynamical glacier evolution studies. The values are ordered based on their units (a) $m^3 N^{-1} a^{-1}$ ($= Pa^{-1} m a^{-1}$), (b) $m^5 N^{-2} a^{-1}$ ($= Pa^{-2} m a^{-1}$), (c) $m^7 N^{-3} a^{-1}$ ($= Pa^{-3} m a^{-1}$), and (d) $m^8 N^{-3} a^{-1}$ ($= Pa^{-3} m^2 a^{-1}$). In each panel, the studies are ordered based on the year in which the study appeared. All entries in this figure are included in Tables 2 and 3.

7. Challenges and Outlook

7.1. From Case Studies to Large-Scale Ice-Dynamical Glacier Evolution Modeling

Until recently, modeling a large number of glaciers required simplified techniques in which ice flow processes were not explicitly represented. These approaches include the use of parameterizations based on the accumulation-area ratio (e.g., Schaeffli et al., 2007), representations of the glacier evolution in which the ELA is shifted (e.g., Paul et al., 2007; Zemp et al., 2006), minimal and linear glacier models (e.g., Oerlemans, 2012), approaches in which the glacier volume is scaled as a function of glacier area and/or length (e.g., Marzeion et al., 2012; Radić & Hock, 2011, 2014) and methods in which the projected glacier changes are based on typical patterns of observed ice surface elevation glacier changes (e.g., Huss & Hock, 2015). Many of these methods are valid over relatively short time scales (a few years). However, applying such approaches over time scales of decades to centuries is not recommended, as these methods fail to represent large changes in glacier geometry and the related ice-dynamical adjustments accurately. It is thus a major advantage to apply methods in which both SMB and ice flow processes are explicitly accounted for. By including these physical processes, important feedback mechanisms (e.g., related to the surface elevation and SMB) can be represented. Moreover, an ice-dynamical representation allows for an improved representation of processes such as debris-cover evolution (e.g., Compagno et al., 2022) and mass transfer to glacier tongues of marine-terminating glaciers (e.g., Recinos et al., 2019), which is important for modeling glacier calving realistically.

A new generation of regional to global models now also explicitly includes ice flow and SMB processes. These large-scale IDGES largely rely on the same types of techniques that have been used for decades to model the temporal evolution of individual glaciers (Figure 10). 3-D approaches can be applied at regional scales directly (i.e., individual glaciers not modeled separately; e.g., Clarke et al. (2015)), but such approaches suffer from the general difficulty of reproducing the observed ice-covered area (i.e., failing to get the ice in the correct places). These mismatches are relatively limited when considering relative changes in regional glacier volume (on the order of a few %), but for detailed analysis and in regions with many small glaciers, such a 3-D regional approach is not ideal. So far, large-scale ice-dynamical glacier models have therefore focused mainly on flowline approaches (Compagno, Eggs, et al., 2021; Compagno, Zekollari, et al., 2021; Marzeion et al., 2020; Maussion et al., 2019; Zekollari et al., 2019). The fact that such approaches can now be applied at regional to global scales owes much to the increase in computational capacity and an ever-increasing amount of observations available for model input and calibration/evaluation at regional to global scales: for example, glacier outlines (RGI Consortium, 2017), ice thickness reconstructions (Farinotti, Huss, et al., 2019; Millan et al., 2022), debris cover

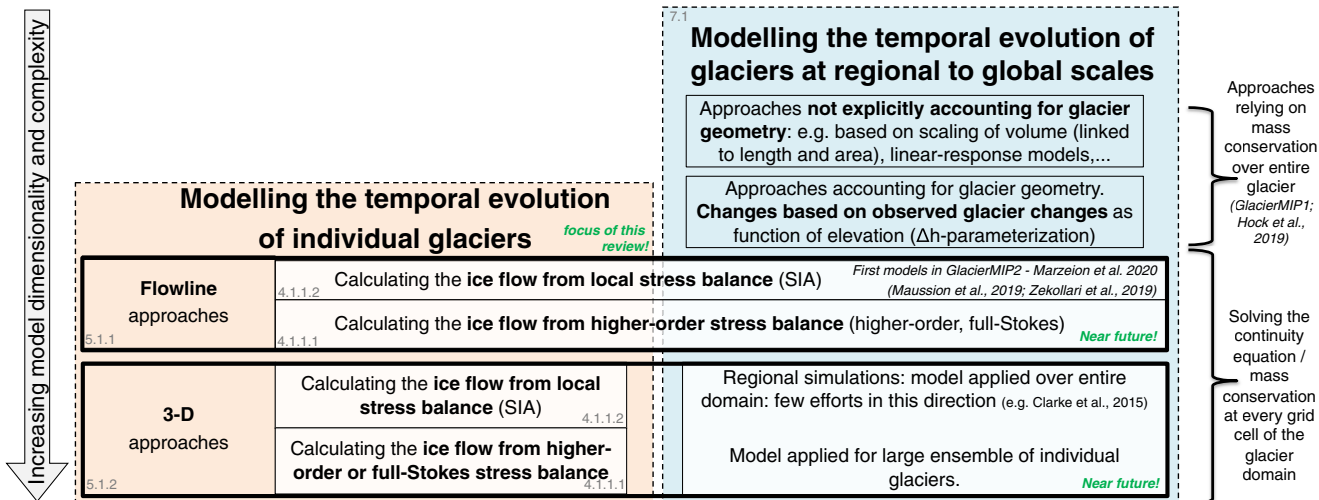


Figure 10. Schematic evolution of dimensionality and ice-dynamical representation in ice-dynamical glacier evolution studies (IDGES) performed on individual glaciers (left side, orange box) and large-scale IDGES (at regional and global scales, right side, blue box). The links between studies performed on individual glaciers and those performed at large scales highlight how techniques that were typically used for individual glaciers are now starting to be applied in large-scale IDGES. Gray numbers refer to the numbering of the sections in which the respective topics are addressed.

and thickness maps (Herreid & Pellicciotti, 2020; Rounce et al., 2021; Scherler et al., 2018), and geodetic mass balances of individual glaciers (e.g., Hugonet et al., 2021).

7.2. Main Achievements and Importance of Detailed IDGES on Individual Glaciers

Detailed IDGES on individual glaciers provide important insights into physical processes that drive glacier changes (Section 7.2.2), help us to understand the consequences of these changes (Section 7.2.3) and allow us to disentangle the delayed response of glaciers to changing climatic conditions (Section 7.2.4). As such, detailed IDGES will remain important in the future, allowing us to incorporate these findings when performing glacier modeling at regional to global scales (Section 7.2.1).

7.2.1. Informing and Evaluating Large-Scale Glacier Modeling Efforts

Modeling the evolution of individual glaciers with ice-dynamical approaches can be used to inform and improve large-scale modeling efforts (Section 7.1). Such modeling efforts on individual glaciers have been used to test the validity of simplified large-scale approaches: for example, Huss et al. (2010) proposed a retreat parameterization that formed the basis for the later global modeling of glaciers by Huss and Hock (2015, 2018), and they compared simulations obtained with this simplified approach to detailed 3-D full-Stokes simulations.

To date, comparing the simulations obtained from various large-scale glacier evolution models has been difficult owing to differences in model input, initialization and forcing. In fact, the recent Glacier Model Intercomparison Projects, GlacierMIP (Hock et al., 2019; Marzeion et al., 2020), have compared the modeled glacier evolution at regional scales, whereas information on the evolution of individual glaciers was not part of the analysis. By comparing the evolution of individual glaciers, more detailed insights could be obtained, for example, how the model choice may affect the rate at which glaciers evolve. Finally, detailed modeling efforts (e.g., with energy balance approaches, with 3-D higher-order/full-Stokes) will remain important to evaluate further the simplifications performed in large-scale models (e.g., relying on PDD, or using the SIA).

7.2.2. Improved Understanding of Physical Processes That Drive Glacier Changes

By modeling the evolution of individual glaciers, new insights can be obtained into the mechanisms and physical processes driving these changes. IDGES have, for instance, been used to increase our understanding of how glacier dynamics and evolution are affected by:

1. (The lack of) glacier calving (e.g., Laumann & Nesje, 2009; Oerlemans, 1986).
2. Debris cover distribution and evolution (Table 1, refs 22).

3. Subglacial hydrology, and how the glacier evolution can in turn affect the subglacial hydrology (e.g., Flowers et al., 2005; Marshall et al., 2005).
4. The relationship between SMB and surface elevation, and how the corresponding positive feedback mechanism (i.e., decrease in SMB leading to decrease in surface elevation, increasing the local surface temperatures, which in turn decreases the SMB further) should be accounted for when the SMB calculation does not include the effects of changes in glacier geometry (Table 1, refs 81).
5. Water percolation and its influence on the thermal structure of glaciers (e.g., Gilbert et al., 2020; Zekollari, Huybrechts, et al., 2017).

In the coming years, IDGES on individual glaciers that include a physics-based calving approach or that have an improved representation of the evolution of debris cover, melt ponds and ice cliffs on glaciers, will provide new insights and allow for a better representation of these processes in large-scale IDGES (Section 7.2.1). Many of the above-described processes have already been included in individual studies (Buri et al., 2016; Miles et al., 2016), but not yet in large-scale IDGES. In addition, other mechanisms, such as the link between glacier sliding and basal hydrology (e.g., De Fleurian et al., 2018), and a time-evolving representation of glacier surges (vs. steady state approaches and simplified models used so far, e.g., Oerlemans and Van Pelt (2015) and van Geffen and Oerlemans (2017)) could be explored further through high-resolution higher-order/full-Stokes IDGES.

7.2.3. Glacier Change Impact Analysis

Modeling the temporal evolution of individual glaciers is of large importance to predict the impact of glacier change. For instance, glaciers act as natural water reservoirs and can thus have a strong influence on the changes in runoff in downstream areas. Individual IDGES have studied the effect of glacier changes on river runoff (Table 1, refs 82). In most of these studies it is assumed that all meltwater that leaves the glacier enters the river, but more sophisticated approaches have also accounted for interactions with the groundwater reservoir (e.g., Flowers et al., 2005, 2007). Glacier dynamics and geometry are also known to have a strong effect on subglacial erosion and sediment deposition: such effects can be studied from idealized settings (e.g., Delaney & Adhikari, 2020), but IDGES have been used for this purpose too (e.g., Flowers et al., 2007). When glaciers are subject to strong changes, they can cause various types of natural hazards: some of the earlier IDGES for instance examined the potential risks linked to a possible readvance of glaciers (e.g., Bindschadler, 1983; Letréguilly & Reynaud, 1989). A more recent example is the work by Gilbert et al. (2017), who link changes in the geometry Barnes Ice Cap (Canada) to a potentially catastrophic drainage of ice-dammed lakes.

It is clear that in order to project future glacier change impacts, detailed IDGES will remain important. These will include studies to estimate some of the above-mentioned impacts (runoff, erosion and natural hazards), but could also be considered for various other purposes, for example, focusing on future hydropower generation in deglacierizing glacier basins (e.g., Farinotti, Round, et al., 2019), or for reconstructing the trajectory of objects within a glacier over time (e.g., Compagno et al., 2019; Jouvet et al., 2020).

7.2.4. Glaciers as Climate Change Indicators and Their Time-Lagged Response

Climatic conditions determine the mass balance of glaciers, which in turn affect the evolution of their geometry and dynamics. Glacier evolution models are important for describing the complex non-linear and time-lagged relationship between climatic conditions and glacier dynamical changes. Today, most of the Earth's glaciers are out of balance with the local climate conditions, and IDGES can be used to examine the glacier responses to this imbalance. This may be realized through stabilization experiments, that is, experiments that calculate the glacier evolution is under stationary climate conditions. Based on such stabilization experiments, a comprehensive overview of glacier response time has been obtained from individual IDGES, suggesting typical glacier response times on the order of decades to centuries (Table 1, refs 83; Figure 11).

The relationship between the changes in climatic conditions and glacier geometry can also be used to infer past climatic conditions from glacier changes. Here again, ice-dynamical glacier evolution models can represent the lagged response between changes in climate forcing and the resulting changes in geometry. Some IDGES have reconstructed past climatic conditions over multi-millennial timescales, but several applications at decadal to centennial time scales also exist (Table 1, refs 84). Large-scale modeling efforts have also aimed to extract past climatic information from glacier simulations (e.g., Goosse et al., 2018; Parkes & Goosse, 2020), and such studies will directly benefit from future insights obtained from IDGES on individual glaciers (see also Section 7.2.1).

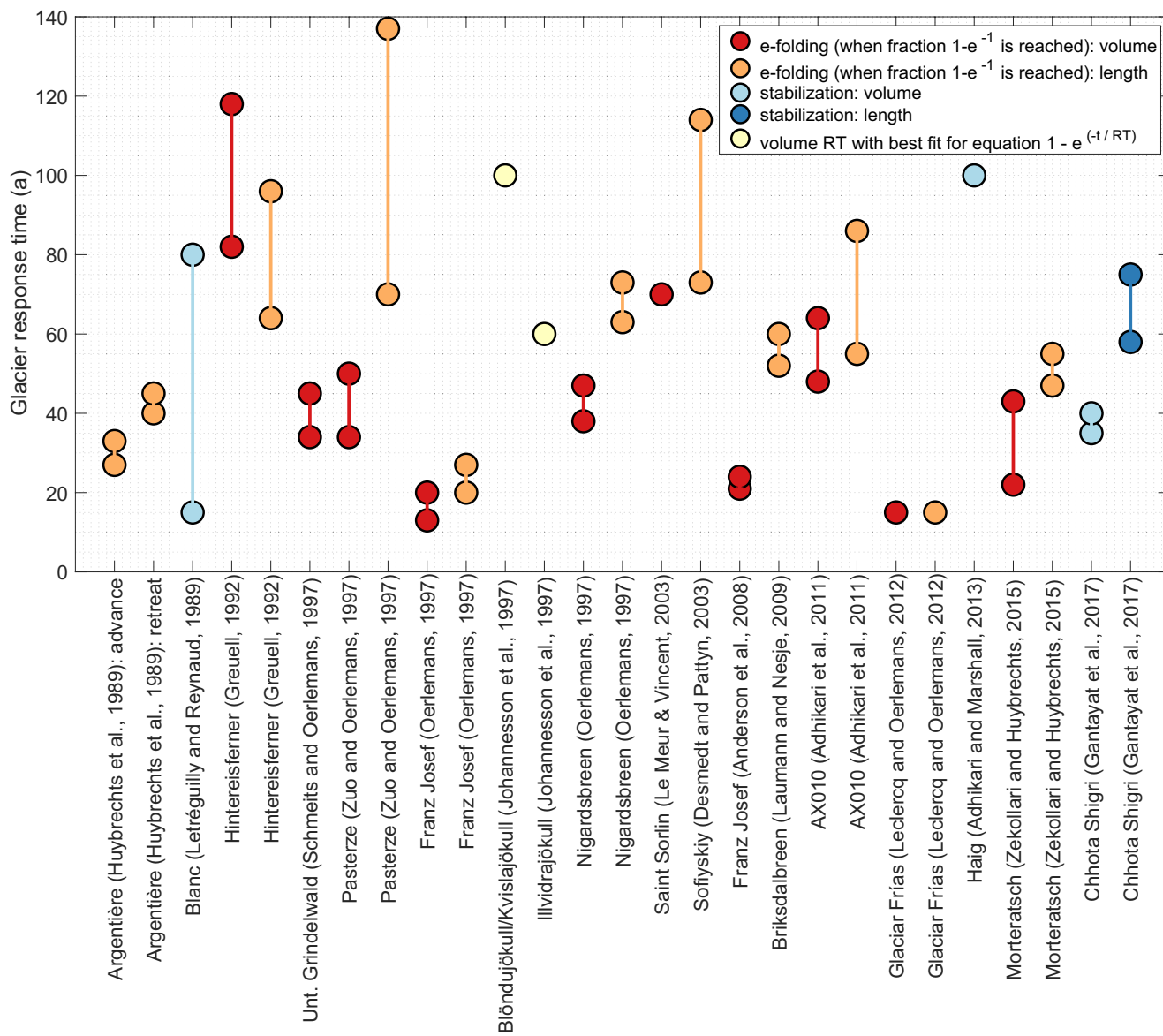


Figure 11. Response time derived for various types of glaciers from ice-dynamical glacier evolution studies (IDGES). Three definitions of response times are used in IDGES: (i) the time needed to reach $1 - e^{-1}$ of the total change ($= 63.2\%$), (ii) the response time (τ) that yields the best fit to the volume/length change (V/L), following the relationship $\Delta V/L = \Delta V/L_\infty (1 - e^{-t/\tau})$, and (iii) the time needed to have a (full) stabilization of the volume/length. The response time for medium-sized to large mountain glaciers is typically on the order of decades to centuries. Studies are ordered according to the year of publication.

In the coming years, IDGES will remain important for quantifying the time-lagged response of glaciers as a result of the existing imbalance between glacier geometry and the local climatic conditions. Moreover, IDGES will also help us to unravel further the factors that determine this lagged glacier response, such as the roles of glacier size, surface slope, SMB gradient, and ice thickness (e.g., Harrison et al., 2001; Jóhannesson et al., 1989; Lüthi & Bauder, 2010). Studies on individual glaciers will also allow us to gain insights into the role of anthropogenic forcing: that is, performing attribution studies on observed glacier changes (e.g., Wijngaard et al., 2019), which have the potential to provide new insights (e.g., reflecting ice-dynamical changes and their role on glacier evolution) and eventually replace simplified approaches that have so far been used in attribution studies (e.g., Marzeion et al., 2014; Roe et al., 2021; Vargo et al., 2020).

8. Concluding Recommendations

Based on this review, we formulate a list of recommendations to follow when designing an IDGES. These recommendations are made for ice-dynamical studies focusing on individual glaciers and highlight the limitations and strengths of various modeling strategies. Most of these recommendations are also applicable to large-scale IDGES, a field that is strongly evolving and increasingly incorporating concepts originally developed for IDGES dealing with individual glaciers (Section 7.1). The recommendations are formulated as a set of questions and answers, leading to a schematic decision-making chart (Figure 12). The recommendations encompass many of the subjects treated in this review, thereby acting as a conclusion on the evolution of IDGES over the past decades and the expected future directions for this field of research.

1. Which glacier to model?

An IDGES is sometimes performed because a specific interest in a glacier exists for geotechnical reasons: for example, a hydropower application or to study the effect of an artificial surface covering on future evolution. However, in many cases a glacier is also modeled to illustrate a process (e.g., evolution of supraglacial debris over time, effect of subglacial hydrology on glacier flow, detailed analyses of glacier response time). In such cases, the choice of the glacier to be simulated should be dependent on the data availability. Having detailed data at hand is important to reduce the uncertainty in the model input, and to allow for an elaborate model calibration and evaluation.

We recommend paying particular attention to data availability, and to treat the compilation of data as an integral part of the study design (see decision-making chart in Figure 12, where the observations are prominently featured). Ideally, detailed and high-resolution field data (e.g., ice thickness and SMB measurements) should be available. These can be complemented by remotely sensed observations and related large-scale products (e.g., Farinotti, Huss, et al., 2019; Hugonet et al., 2021; RGI Consortium, 2017). If detailed data are not available (e.g., if the bed topography is unknown or no SMB measurements are available), it is likely not worth performing

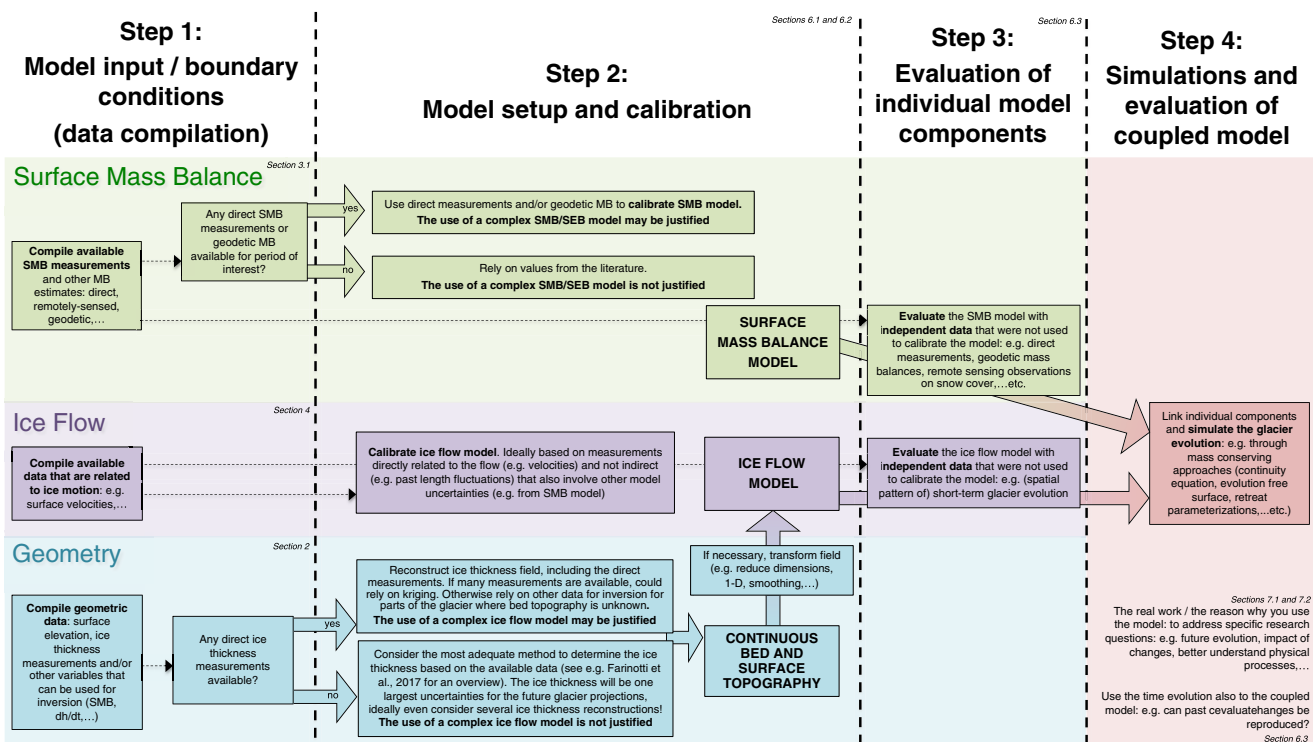


Figure 12. Schematic overview of steps to follow when deciding on model setup and experimental design for glacier evolution modeling. The procedure is meant as a general example and, depending on the available data and goal of the study, it may be advisable to deviate from this. Also note that a few aspects that can be important for specific cases (e.g., studies including glaciers with important frontal mass balance and debris cover) are not accounted for in this diagram.

an IDGES on this glacier, as the large uncertainties will hinder a useful interpretation of the model results. In such cases, it is best to identify other glaciers with better data availability, or even to consider using an idealized glacier geometry for which analyzing the effect of physical processes and their representation is often more straightforward.

2. How complex should the approach be in terms of mass balance and ice flow modeling?

The increase in computational resources allows for more complex methods to be used when simulating ice flow and SMB processes (Figure 13). The use of a sophisticated SMB model can be advantageous if detailed meteorological observations and abundant direct SMB measurements are available for model evaluation (Figure 12). Even if these data are available, simplified SMB approaches (e.g., solely using temperature as a proxy for melt) can sometimes perform as well as complex approaches (Gabbi et al., 2014; Réveillet et al., 2018). Using higher-order/full-Stokes solutions is advantageous, as the vertical scale is often not negligible compared to the typical horizontal scale (while this is the central assumption behind the SIA, see Section 4.1.2). Moreover, more complex ice flow approaches tend to represent ice flow better when the bed topography is irregular and over steep terrain. Therefore, we generally recommend using a higher-order/FS model, ideally in 3D, when modeling the evolution of a glacier. However, such sophisticated approaches are computationally expensive, and may in some cases have only limited additional value compared to SIA models.

In general, differences in ice flow model complexity result in different ice dynamics and glacier evolution over short time scales (e.g., Le Meur et al., 2004; Zekollari, Huybrechts, et al., 2017) but these differences reduce over mid- to long-term time scales, over which mass balance processes dominate (e.g., Le Meur et al., 2004; Leysinger Vieli & Gudmundsson, 2004; Wallinga & van de Wal, 1998; Zekollari, Lecavalier, et al., 2017). If the time scale of interest exceeds several decades, it may therefore be worth focusing on the SMB representation and using a simpler approach for ice flow. This will reduce computational costs, allowing for more simulations to be performed (e.g., important to understand the sensitivity of results to model parameters, see question 9). Moreover, if large uncertainties exist in the model input (e.g., if the bed topography was not measured) or in other model components (e.g., if no SMB measurements are available), the added value of using a complex ice flow model will be limited. This is because the large errors and uncertainties introduced by other model components will dominate and be larger than differences that result from increased model complexity. Also, when choosing how to represent basal motion, one should question whether a complex approach is needed, given that generally little is known about the mechanisms that govern motion at the glacier bed to constrain and/or evaluate model results.

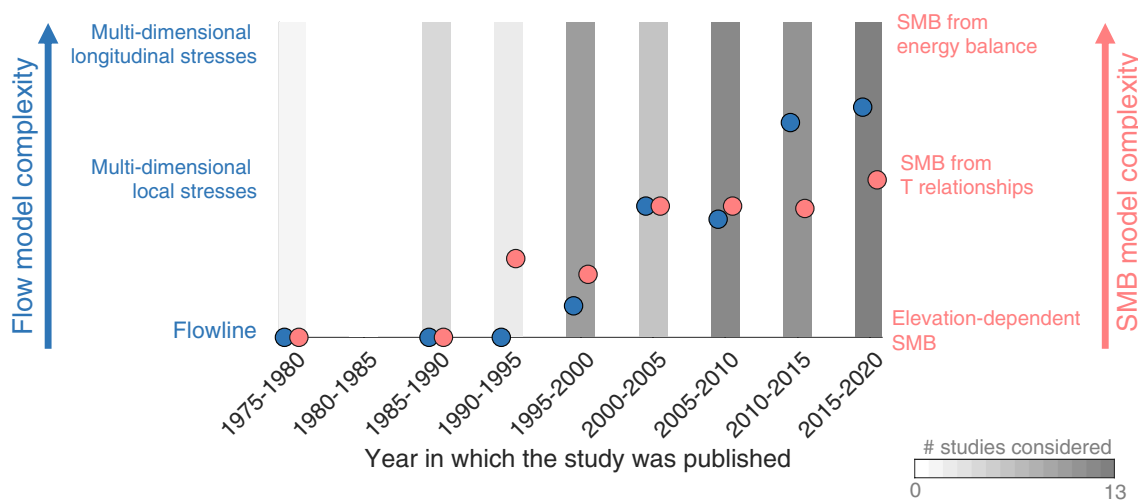


Figure 13. Schematic representation of the evolution of model complexity used in ice-dynamical glacier evolution studies (IDGES). Model complexity is determined separately for the ice flow component (blue; 1 = flowline model; 2 = 3-D Shallow Ice Approximation; and 3 = 3-D higher-order/full-Stokes) and the surface mass balance (SMB) component (red; 1 = imposed SMB without ablation/accumulation distinction; 2 = positive degree day approach; and 3 = energy-balance approach). Values are based on the 59 studies included in Tables 2 and 3, and the graph shows values calculated over 5-year time periods. The lower and upper limits of the vertical bars correspond to mean values of 1 and 3, respectively. A linear interpolation applies in between.

In summary, it is not always recommended to opt for the most complex modeling approaches (Emanuel, 2020). One should consider how the model complexity affects the glacier evolution on the time scales of interest, how to take into account the data availability, and how to consider the uncertainty in both model input and other model components (Figure 12). As Nye (1948) stated: “better to think exactly with simplified ideas than to reason inexactly with complex ones”.

3. Which kind of numerical scheme, implementation and resolution to use? Should I program this myself, or should I use an existing model?

When choosing the numerical scheme and the temporal resolution, it is very important to consider both the model stability and mass conservation. Large time steps reduce the total simulation time needed to ensure numerical stability. Explicit numerical methods tend to be easier to implement and are computationally cheaper compared to implicit methods. However, as explicit methods are less stable than implicit ones, smaller time steps need to be used, which increases the simulation time. As a first approach to ice-dynamical glacier evolution modeling, we recommend using explicit methods and finite difference schemes owing to their simplicity, thereby considering model stability. Subsequently, more sophisticated approaches (e.g., using staggered grids) and implicit methods can be considered.

Regardless of the chosen setup, we recommend utilizing a time step that evolves over time. Although the time step is typically constant in IDGES, by allowing the time step to vary over the simulation period, considerable computational time can be saved. This is particularly the case when the glacier geometry strongly changes: with little ice and low flow velocities, larger time steps can be considered for the time evolution, while shorter time steps need to be considered when ice flow is higher.

4. Which values should be used for model parameters?

Generally, it is recommended to derive model parameters as an integral part of the IDGES rather than relying on parameters taken from other studies. The definition of important model parameters (e.g., melt parameters in SMB and rate factor for ice flow) typically occurs as a part of the model calibration. When tuning model parameters for ice flow, we recommend considering the range that has been found in previous IDGES (Figures 8 and 9). This range is relatively wide, showing that the specific glacier setting and model setup can have a large influence on the flow parameters. In turn, this indicates that working with reference values from other studies can be problematic if no elaborate evaluation is performed. For cases where calibration of model parameters is not possible, we highly recommend performing a thorough model evaluation (Section 6.3).

5. Which climate forcing should be used and how to apply it?

It is important to consider carefully the climatic forcing, as this will directly determine the SMB and thus the glacier evolution over time. When considering both past and future climatic conditions, one can sometimes use continuous series, for example, from climate simulations that span the entire period of interest. However, in many cases it is more suitable to use observations or reanalysis products for the past and projected climatic conditions for the future. In such cases, homogenization of both time series is important. This is usually obtained by applying a bias correction, ensuring consistency over a common time period (see e.g., Huss & Hock, 2015, p. 4). It is also recommended to use the latest available climate model outputs, which are typically at higher spatial resolution and account for more physical processes: for example, if designing a study now, instead of using for instance ERA-Interim reanalyses data and Coupled Model Intercomparison Project Phase 5 (CMIP5) GCM output forced with RCPs, one should now rather select ERA5 reanalyses data and CMIP6 GCM output forced with SSPs.

In most cases a downscaling of the climatic data to the glacier level is needed, which is a complex task (e.g., Behrangi et al., 2018; Maussion et al., 2014; Roth et al., 2018; Vionnet et al., 2019). Techniques of various complexity have been used for downscaling climatic data in IDGES (Table 1, refs 85). If no direct meteorological observations are available on the glacier level, we recommend downscaling the climatic forcing by reproducing the observed (geodetic) mass balance, thereby reducing potential biases due to the considered climatic input (Compagno, Zekollari, et al., 2021).

6. How should the simulations be initialized?

The model initialization needs to be designed with care, as it can have large effects on the modeled glacier evolution. When doing so, it is important to consider the trade-offs between various initialization options. If the main focus of the study is on the short- to mid-term glacier evolution (annual to decadal time scale), it is important to represent detailed features closely: that is, the starting geometry should be very close to the observations. However, when starting from a state close to the observation, one should pay particular attention to the initial (dynamical) model adjustment. This non-physical shock can be reduced by relaxing the observed model geometry, but this will come at the cost of increasing the discrepancy between present-day modeled state and observations.

If the focus is on the multi-decadal to centennial glacier evolution, it might be more advisable to start from a modeled transient state that is calibrated and/or evaluated based on the past glacier evolution. For such cases, a larger discrepancy between modeled and observed glacier geometry is generally acceptable. Here, we recommend using a large ensemble of simulations, through which the model settings to match past and present-day glacier observations can be determined. If the bed topography is based on inversion techniques (for instance to match surface velocities, e.g., Millan et al. (2022), or by relying on adjoints methods, e.g., Mosbeux et al. (2016)), it is recommended to use the same glacier model for the inversion and for the glacier evolution. This will allow starting from a glacier state very close to observations while reducing model shock.

7. What to consider when calibrating a glacier evolution model?

Typically, when calibrating glacier models, an explicit distinction is made between the calibration of the SMB (Section 6.2.1) and the ice dynamical (Section 6.2.2) components. This is a recommended approach (Figure 12), as it allows the determination of these respective effects: for example, the ice flow model can be tuned to match observed velocities, while the SMB component can be tuned to reproduce *in situ* measurements. However, because the two components interact, it is suggested also to consider glacier evolution during calibration. This can be realized by first determining ice flow and SMB parameters that provide good results for the individual components, and then narrowing the selection based on the comparison against observed geometry changes. An alternative is to use the observed glacier evolution to evaluate the calibrated model, ensuring that the calibrated parameters allow for a good fit with observed changes.

When searching for parameters that closely reproduce observations, it is important to cover the parameter space fully. In practice, this translates into running a large ensemble of simulations, and it is therefore important to use a model with the appropriate complexity. To explore the parameter space efficiently, and to allow for a detailed analysis of the uncertainty introduced by the various parameters, one can, for instance, use Bayesian techniques (e.g., Rounce et al., 2020).

In virtually all IDGES, the calibrated model parameters are assumed to be time independent: that is, the parameters are derived for a given time period and then kept constant. With increasing data availability for model calibration and evaluation, it will likely become possible to start experimenting with time-varying model parameters (e.g., Huss et al. (2009) and Bolibar et al. (2022) question the validity of PDD models with time-independent parameters). We suggest keeping this in mind when designing a study and to potentially investigate how this may affect the model outcome.

8. How should the model performance be evaluated?

Ensuring that the data used to evaluate model performance are independent of the data used to calibrate the model is of central importance (Figure 12). Ideally, both modeled glacier quantities (e.g., surface velocities and SMB) and glacier evolution (resulting from the interaction of various features) should be compared against field and/or remotely sensed observations (Figure 12). In some cases, the simulated glacier dynamics and evolution can also be compared to other model output, for example, from simulations from a more complex model.

When designing and creating a new model or modifying an existing one, it is also recommended to test model performance in an idealized setup, and to compare the output to benchmark experiments (e.g., Pattyn et al., 2008) and/or analytical solutions (e.g., Bueler et al., 2007; Jarosch et al., 2013; Jouvet et al., 2009).

9. How sensitive is the simulated glacier evolution to the model setup?

When presenting the simulated glacier evolution, we recommend providing insights into how sensitive the modeled glacier evolution is to model parameters, and how the uncertainty in the model input affects the results. Ideally, this translates into providing the glacier evolution as a probability distribution instead of as a single result, which characterizes how the results may shift depending on the uncertainty in the model setup (e.g., Brinkerhoff et al., 2017; Eis et al., 2021; Rounce et al., 2020). Such probabilistic approaches (e.g., Edwards et al., 2021) are more useful for decision-making than traditional deterministic forecasts without uncertainty information.

An elaborate sensitivity analysis can, in many cases, be linked directly to the model calibration (question 7). Again, choosing a suitable model complexity is crucial to allow for large ensemble simulations. Some IDGES have performed such elaborate sensitivity analyses (e.g., Flowers et al., 2007; Gilbert et al., 2020; Jouvet et al., 2011; Marshall et al., 2005; Wijngaard et al., 2019), and we recommend following the example of such studies.

10. How to communicate the outcome of an IDGES?

Providing details about model setup is important when communicating the outcome of an IDGES. This information will allow other scientists to understand the model outcome, contextualize the results, and will help during the design of other IDGES. Studies that can be considered as examples in this context are: Marshall et al. (2005), Flowers et al. (2007), Giesen and Oerlemans (2010), Rowan et al. (2015), Wijngaard et al. (2019), and Gilbert et al. (2020). In general, providing tables with the main parameters used is of great help to the reader. Combined with mathematical descriptions of the methods, and providing code and data, this will allow increased transparency and reproducibility of simulations. A large-scale ice-dynamical glacier model that sets the standard in terms of transparency, openness and documentation, is the Open Global Glacier Model (Maussion et al., 2019).

Finally, when communicating the results of an IDGES, we strongly encourage practitioners to provide answers to questions that may be obvious to the writer, but not to the reader: for example, Why was this particular glacier modeled? Why was a specific model used and not another? What are the main findings and takeaways from the study? What are the implications of the modeled glacier evolution? How can the simulated glacier evolution be generalized to other studies? Etc.

Glossary

Glacier:

body of permanent ice that moves under its own weight. Dome-shaped glaciers that largely cover the underlying landscape are sometimes referred to as “ice caps,” and are also considered in this review. In contrast, we do not consider the Greenland and Antarctic ice sheet in this study.

Glacier evolution model:

numerical computer model that simulates the evolution of a glacier over time.

Large-scale glacier evolution studies:

studies in which the temporal evolution of a glacier ensemble is simulated (e.g., at regional to global scale).

Ice flow:

the transfer of ice within a glacier through gravitational forces (i.e., “moving under its own weight”). The mass transfer occurs through two main processes: internal deformation and basal sliding.

Mass balance:

process of adding and/or removing mass to the glacier surface (surface mass balance), inside the glacier (internal mass balance), at the glacier base (basal mass balance), and at the glacier front (frontal mass balance).

Volume-scaling method:

method in which the glacier volume and its evolution are estimated by using a relationship between glacier volume and glacier area, length or both. These methods do not have an explicit representation of glacier geometry.

Ice-dynamical model:

model in which the mass transfer of a glacier through ice flow is explicitly accounted for.

Ice-dynamical glacier evolution study (IDGES):

study in which an ice-dynamical model is used to model the glacier evolution over time. In this review, we specifically focus on IDGES performed over individual glaciers.

Flowline model:

model in which the evolution along the glacier's central region (flowline) is simulated. By imposing a geometrical shape for the glacier cross section, the modeled evolution along the flowlines is extended. Flowline models are typically referred to as 1-D models.

3-D model:

model in which the glacier and the ice flow are modeled through an explicit representation of both horizontal directions. In some cases, vertically integrated models (i.e., models that do not represent the vertical ice flow) are referred to as 2-D or 2.5-D models.

Force balance:

ice flow models describe the forces acting on glaciers and their spatial distribution through a force balance. In a full-Stokes approach, all forces are accounted for, while other approaches rely on simplifications that reduce computational costs. Examples of the latter include the Shallow Ice Approximation (SIA) and the Shallow-Shelf Approximation (SSA).

Circulation model:

type of climate model. Distinction is typically made between regional climate models (RCMs) and global circulation models (GCMs). A GCM typically represents processes occurring in the atmosphere, ocean and cryosphere, as well as interactions between them. An RCM is typically run at higher resolution and is usually nested in a GCM. An Earth System Model distinguishes itself from a GCM, as it also includes cycling in terrestrial and marine ecosystems, as well as related feedbacks.

Data Availability Statement

No new data were created for this research article.

References

- Adhikari, S., & Huybrechts, P. (2009). Numerical modelling of historical front variations and the 21st-century evolution of glacier AX010, Nepal Himalaya. *Annals of Glaciology*, 50(52), 27–34. <https://doi.org/10.3189/172756409789624346>
- Adhikari, S., & Marshall, S. J. (2011). Improvements to shear-deformational models of glacier dynamics through a longitudinal stress factor. *Journal of Glaciology*, 57(206), 1003–1016. <https://doi.org/10.3189/002214311798843449>
- Adhikari, S., & Marshall, S. J. (2012). Parameterization of lateral drag in flowline models of glacier dynamics. *Journal of Glaciology*, 58(212), 1119–1132. <https://doi.org/10.3189/2012JoG12018>
- Adhikari, S., & Marshall, S. J. (2013). Influence of high-order mechanics on simulation of glacier response to climate change: Insights from Haig Glacier, Canadian Rocky Mountains. *The Cryosphere*, 7(5), 1527–1541. <https://doi.org/10.5194/tc-7-1527-2013>
- Adhikari, S., Marshall, S. J., & Huybrechts, P. (2011). On characteristic timescales of glacier AX010 in the Nepalese Himalaya. *Bulletin of Glaciological Research*, 29, 19–29. <https://doi.org/10.5331/bgr.29.19>
- Åkesson, H., Nisancioğlu, K. H., Giesen, R. H., & Morlighem, M. (2017). Simulating the evolution of Hardangerjøkulen ice cap in southern Norway since the mid-Holocene and its sensitivity to climate change. *The Cryosphere*, 11(1), 281–302. <https://doi.org/10.5194/tc-11-281-2017>
- Albrecht, O., Jansson, P., & Blatter, H. (2000). Modelling glacier response to measured mass-balance forcing. *Annals of Glaciology*, 31, 91–96. <https://doi.org/10.3189/172756400781819996>
- Allison, I., & Kruss, P. (1977). Estimation of recent climate change in Irian Jaya by numerical modeling of its tropical glaciers. *Arctic and Alpine Research*, 9(1), 49–60. <https://doi.org/10.2307/1550408>
- Anderson, B., Lawson, W., & Owens, I. (2008). Response of Franz Josef Glacier Ka Roimata o Hine Hukatere to climate change. *Global and Planetary Change*, 63(1), 23–30. <https://doi.org/10.1016/j.gloplacha.2008.04.003>
- Anderson, S., & Radić, V. (2020). Identification of local water resource vulnerability to rapid deglaciation in Alberta. *Nature Climate Change*, 10(10), 933–938. <https://doi.org/10.1038/s41558-020-0863-4>
- Aschwanden, A., Bueler, E., Khroulev, C., & Blatter, H. (2012). An enthalpy formulation for glaciers and ice sheets. *Journal of Glaciology*, 58(209), 441–457. <https://doi.org/10.3189/2012JoG11J088>

- Aðalgeirsdóttir, G., Gudmundsson, G. H., & Björnsson, H. (2000). The response of a glacier to a surface disturbance: A case study on Vatnajökull ice cap, Iceland. *Annals of Glaciology*, 31, 104–110. <https://doi.org/10.3189/172756400781819914>
- Aðalgeirsdóttir, G., Guðmundsson, S., Björnsson, H., Pálsson, F., Jóhannesson, T., Hannesson, H., et al. (2011). Modelling the 20th and 21st century evolution of Hoffellsjökull glacier, SE-Vatnajökull, Iceland. *The Cryosphere*, 5(4), 1961–1975. <https://doi.org/10.5194/tc-5-961-2011>
- Aðalgeirsdóttir, G., Jóhannesson, T., Björnsson, H., Pálsson, F., & Sigurðsson, O. (2006). Response of Hofsjökull and southern Vatnajökull, Iceland, to climate change. *Journal of Geophysical Research*, 111(3), F03001. <https://doi.org/10.1029/2005JF000388>
- Balco, G. (2020). Glacier change and paleoclimate applications of cosmogenic-nuclide exposure dating. *Annual Review of Earth and Planetary Sciences*, 48(1), 1–28. <https://doi.org/10.1146/annurev-earth-081619-052609>
- Behrangi, A., Gardner, A., Reager, J. T., Fisher, J. B., Yang, D., Huffman, G. J., & Adler, R. F. (2018). Using GRACE to estimate snowfall accumulation and assess gauge undercatch corrections in high latitudes. *Journal of Climate*, 31(21), 8689–8704. <https://doi.org/10.1175/JCLI-D-18-0163.1>
- Biemans, H., Siderius, C., Lutz, A. F., Ahmad, B., Hassan, T., von Bloh, W., et al. (2019). Importance of snow and glacier meltwater for agriculture on the Indo-Gangetic Plain. *Nature Sustainability*, 2(7), 594–601. <https://doi.org/10.1038/s41893-019-0305-3>
- Bindschadler, R. (1983). The predicted behavior of Griesgletscher, Wallis, Switzerland, and its possible threat to a Nearby Dam. *Annals of Glaciology*, 4, 295. <https://doi.org/10.3189/S0260305500005632>
- Bindschadler, R., Harrison, W. D., Raymond, C. F., & Crosson, R. (1977). Geometry and dynamics of a surge-type glacier. *Journal of Glaciology*, 18(79), 181–194. <https://doi.org/10.1017/s002214300021298>
- Blatter, H. (1995). Velocity and stress fields in grounded glaciers: A simple algorithm for including deviatoric stress gradients. *Journal of Glaciology*, 41(138), 333–344. <https://doi.org/10.3189/S00221430001621X>
- Bolibar, J., Rabatel, A., Gouttevin, I., Galiez, C., Condom, T., & Sauquet, E. (2020). Deep learning applied to glacier evolution modelling. *The Cryosphere*, 14(2), 565–584. <https://doi.org/10.5194/tc-14-565-2020>
- Bolibar, J., Rabatel, A., Gouttevin, I., Zekollari, H., & Galiez, C. (2022). Nonlinear sensitivity of glacier mass balance to future climate change unveiled by deep learning. *Nature Communications*, 13(1), 409. <https://doi.org/10.1038/s41467-022-28033-0>
- Boulton, G. S., & Hindmarsh, R. C. A. (1987). Sediment deformation beneath glaciers: Rheology and geological consequences. *Journal of Geophysical Research*, 92(B9), 9059–9082. <https://doi.org/10.1029/JB092iB09p09059>
- Braithwaite, R. J. (1995). Positive degree-day factors for ablation on the Greenland ice-sheet studied by energy balance modeling. *Journal of Glaciology*, 41(137), 153–160. <https://doi.org/10.1017/s0022143000017846>
- Braun, M. H., Malz, P., Sommer, C., Farias-Barahona, D., Sauter, T., Casassa, G., et al. (2019). Constraining glacier elevation and mass changes in South America. *Nature Climate Change*, 9(2), 130–136. <https://doi.org/10.1038/s41558-018-0375-7>
- Brinkerhoff, D., Truffer, M., & Aschwanden, A. (2017). Sediment transport drives tidewater glacier periodicity. *Nature Communications*, 8(1), 90. <https://doi.org/10.1038/s41467-017-00095-5>
- Brinkerhoff, D. J., & Johnson, J. V. (2013). Data assimilation and prognostic whole ice sheet modelling with the variationally derived, higher order, open source, and fully Parallel Ice Sheet Model VarGlaS. *The Cryosphere*, 7(4), 1161–1184. <https://doi.org/10.5194/tc-7-1161-2013>
- Brown, L. E., Khamis, K., Wilkes, M., Blaen, P., Brittain, J. E., Carrivick, J. L., et al. (2018). Functional diversity and community assembly of river invertebrates show globally consistent responses to decreasing glacier cover. *Nature Ecology and Evolution*, 2(2), 325–333. <https://doi.org/10.1038/s41559-017-0426-x>
- Brun, F., Berthier, E., Wagnon, P., Kääb, A., & Treichler, D. (2017). A spatially resolved estimate of High Mountain Asia glacier mass balances from 2000 to 2016. *Nature Geoscience*, 10(9), 668–673. <https://doi.org/10.1038/NGEO2999>
- Budd, W. F. (1975). A first simple model for periodically self-surging glaciers. *Journal of Glaciology*, 14(70), 3–21. <https://doi.org/10.1017/s002214300013344>
- Budd, W. F., & Jacka, T. H. (1989). A review of ice rheology for ice sheet modelling. *Cold Regions Science and Technology*, 16(2), 107–144. [https://doi.org/10.1016/0165-232x\(89\)90014-1](https://doi.org/10.1016/0165-232x(89)90014-1)
- Budd, W. F., & Jenssen, D. (1975). Numerical modelling of glacier systems. *IAHS-AISH Publication*, 104, 257–291.
- Budd, W. F., Keage, P. L., & Blundy, N. A. (1979). Empirical studies of ice sliding. *Journal of Glaciology*, 23(89), 157–170. <https://doi.org/10.3189/s0022143000029804>
- Budd, W. F., & McInnes, B. J. (1974). Modeling periodically surging glaciers. *Science*, 186(4167), 925–927. <https://doi.org/10.1126/science.186.4167.925>
- Bueler, E., & Brown, J. (2009). Shallow shelf approximation as a “sliding law” in a thermomechanically coupled ice sheet model. *Journal of Geophysical Research*, 114(3), 1–21. <https://doi.org/10.1029/2008JF001179>
- Bueler, E., Brown, J., & Lingle, C. (2007). Exact solutions to the thermomechanically coupled shallow-ice approximation: Effective tools for verification. *Journal of Glaciology*, 53(182), 499–516. <https://doi.org/10.3189/002214307783258396>
- Buri, P., Pellicciotti, F., Steiner, J. F., Miles, E. S., & Immerzeel, W. W. (2016). A grid-based model of backwasting of supraglacial ice cliffs on debris-covered glaciers. *Annals of Glaciology*, 57(71), 199–211. <https://doi.org/10.3189/2016AoG71A059>
- Cauvy-Fraunié, S., & Dangles, O. (2019). A global synthesis of biodiversity responses to glacier retreat. *Nature Ecology and Evolution*, 3(12), 1675–1685. <https://doi.org/10.1038/s41559-019-1042-8>
- Ciraci, E., Velicogna, I., & Swenson, S. (2020). Continuity of the mass loss of the world’s glaciers and ice caps from the GRACE and GRACE follow-on missions. *Geophysical Research Letters*, 47(9), e2019GL086926. <https://doi.org/10.1029/2019GL086926>
- Clarke, G. K. C., Jarosch, A. H., Anslow, F. S., Radić, V., & Menounos, B. (2015). Projected deglaciation of western Canada in the twenty-first century. *Nature Geoscience*, 8(5), 372–377. <https://doi.org/10.1038/ngeo2407>
- Compagno, L., Eggs, S., Huss, M., Zekollari, H., & Farinotti, D. (2021). Brief communication: Do 1.0, 1.5, or 2.0°C matter for the future evolution of Alpine glaciers? *The Cryosphere*, 15(6), 2593–2599. <https://doi.org/10.5194/tc-15-2593-2021>
- Compagno, L., Huss, M., Miles, E. S., McCarthy, M. J., Zekollari, H., Dehecq, A., et al. (2022). Modelling supraglacial debris-cover evolution from the single glacier to the regional scale: An application to High Mountain Asia. *The Cryosphere*, 1–33. <https://doi.org/10.5194/tc-2021-233>
- Compagno, L., Jouvet, G., Bauder, A., Funk, M., Church, G., Leinss, S., & Luthi, M. P. (2019). Modeling the re-appearance of a crashed airplane on Gauligletscher, Switzerland. *Frontiers of Earth Science*, 7(July), 170. <https://doi.org/10.3389/feart.2019.00170>
- Compagno, L., Zekollari, H., Huss, M., & Farinotti, D. (2021). Limited impact of climate forcing products on future glacier evolution in Scandinavia and Iceland. *Journal of Glaciology*, 1–17. <https://doi.org/10.1017/jog.2021.24>
- Cook, K. L., Andermann, C., Gimbert, F., Adhikari, B. R., & Hovius, N. (2018). Glacial lake outburst floods as drivers of fluvial erosion in the Himalaya. *Science*, 362(6410), 53–57. <https://doi.org/10.1126/science.aat4981>
- Copland, L., Harbor, J., & Sharp, M. (1997). Borehole video observation of englacial and basal ice conditions in a temperate valley glacier. *Annals of Glaciology*, 24, 277–282. <https://doi.org/10.1017/s0260305500012301>

- Courant, R., Friedrichs, K., & Lewy, H. (1928). Über die partiellen Differenzengleichungen der mathematischen Physik. *Mathematische Annalen*, 100(1), 32–74. <https://doi.org/10.1007/bf01448839>
- Cuffey, K. M., & Paterson, W. S. B. (2010). *The physics of glaciers*. Butterworth-Heinemann. [https://doi.org/10.1016/0016-7185\(71\)90086-8](https://doi.org/10.1016/0016-7185(71)90086-8)
- De Fleurian, B., Werder, M. A., Beyer, S., Brinkerhoff, D. J., Delaney, I., Dow, C. F., et al. (2018). SHMIP the subglacial hydrology model inter-comparison project. *Journal of Glaciology*, 64(248), 1–20. <https://doi.org/10.1017/jog.2018.78>
- Dehecq, A., Gourmelen, N., Gardner, A. S., Brun, F., Goldberg, D., Nienow, P. W., et al. (2019). Twenty-first century glacier slowdown driven by mass loss in High Mountain Asia. *Nature Geoscience*, 12(1), 22–27. <https://doi.org/10.1038/s41561-018-0271-9>
- Delaney, I., & Adhikari, S. (2020). Increased subglacial sediment discharge in a warming climate: Consideration of ice dynamics, glacial erosion, and fluvial sediment transport. *Geophysical Research Letters*, 47(7). <https://doi.org/10.1029/2019GL085672>
- Demiroglu, O. C., Dannevig, H., & Aall, C. (2018). Climate change acknowledgement and responses of summer (glacier) ski visitors in Norway. *Scandinavian Journal of Hospitality and Tourism*, 18(4), 419–438. <https://doi.org/10.1080/15022250.2018.1522721>
- De Smedt, B., & Pattyn, F. (2003). Numerical modelling of historical front variations and dynamic response of Sofiyiskiy glacier, Altai Mountains, Russia. *Annals of Glaciology*, 37, 143–149. <https://doi.org/10.3189/172756403781815654>
- Duan, K. Q., Yao, T. D., Wang, N. L., & Liu, H. C. (2012). Numerical simulation of Urumqi Glacier No. 1 in the eastern Tianshan, central Asia from 2005 to 2070. *Chinese Science Bulletin*, 57(34), 4505–4509. <https://doi.org/10.1007/s11434-012-5469-4>
- Edwards, T. L., Nowicki, S., Marzeion, B., Hock, R., Goelzer, H., Seroussi, H., et al. (2021). Projected land ice contributions to 21st century sea level rise. *Nature*, 593(7857), 74–82. <https://doi.org/10.1038/s41586-021-03302-y>
- Egholm, D. L., Knudsen, M. F., Clark, C. D., & Lesemann, J. E. (2011). Modeling the flow of glaciers in steep terrains: The integrated second-order shallow ice approximation (iSOSIA). *Journal of Geophysical Research*, 116(2), 1–16. <https://doi.org/10.1029/2010JF001900>
- Einhorn, B., Eckert, N., Chaix, C., Ravanel, L., Deline, P., Gardent, M., et al. (2015). Climate change and natural hazards in the Alps. *Journal of Alpine Research*, 103(2), 1–38. <https://doi.org/10.4000/rga.2878>
- Eis, J., van der Laan, L., Maussion, F., & Marzeion, B. (2021). Reconstruction of past glacier changes with an ice-flow glacier model: Proof of concept and validation. *Frontiers of Earth Science*, 9. <https://doi.org/10.3389/feart.2021.595755>
- Emanuel, K. (2020). The relevance of theory for contemporary research in atmospheres, oceans, and climate. *AGU Advances*, 1(2), e2019AV000129. <https://doi.org/10.1029/2019AV000129>
- Engelhardt, M., Leclercq, P., Eidhammer, T., Kumar, P., Landgren, O., & Rasmussen, R. (2017). Meltwater runoff in a changing climate (1951–2099) at Chhota Shigri Glacier, western Himalaya, northern India. *Annals of Glaciology*, 58(75pt1), 47–58. <https://doi.org/10.1017/aog.2017.13>
- Faillat, J., Funk, M., & Vincent, C. (2015). Avalanche glacier instabilities: Review on processes and early warning perspectives. *Reviews of Geophysics*, 53(2), 203–224. <https://doi.org/10.1002/2014RG000466>
- Farinotti, D., Brinkerhoff, D. J., Clarke, G. K. C., Fürst, J. J., Frey, H., Gantayat, P., et al. (2017). How accurate are estimates of glacier ice thickness? Results from ITMIX, the Ice Thickness Models Intercomparison eXperiment. *The Cryosphere*, 11(2), 949–970. <https://doi.org/10.5194/tc-11-949-2017>
- Farinotti, D., Brinkerhoff, D. J., Fürst, J. J., Gantayat, P., Gillet-Chaulet, F., Huss, M., et al. (2021). Results from the Ice Thickness Models Intercomparison eXperiment phase 2 (ITMIX2). *Frontiers of Earth Science*, 8. <https://doi.org/10.3389/feart.2020.571923>
- Farinotti, D., Huss, M., Fürst, J. J., Landmann, J., Machguth, H., Maussion, F., & Pandit, A. (2019). A consensus estimate for the ice thickness distribution of all glaciers on Earth. *Nature Geoscience*, 12(3), 168–173. <https://doi.org/10.1038/s41561-019-0300-3>
- Farinotti, D., Round, V., Huss, M., Compagno, L., & Zekollari, H. (2019). Large hydropower and water storage potential in future glacier-free basins. *Nature*, 575(7782), 341–344. <https://doi.org/10.1038/s41586-019-1740-z>
- Fell, S. C., Carrivick, J. L., Kelly, M. G., Fireder, L., & Brown, L. E. (2018). Declining glacier cover threatens the biodiversity of alpine river diatom assemblages. *Global Change Biology*, 24(12), 5828–5840. <https://doi.org/10.1111/gcb.14454>
- Fettweis, X., Hofer, S., Krebs-Kanzow, U., Amory, C., Aoki, T., Berends, C., et al. (2020). GrSMBMIP: Intercomparison of the modelled 1980–2012 surface mass balance over the Greenland Ice Sheet. *The Cryosphere*, 2020(January), 1–35. <https://doi.org/10.5194/tc-2019-321>
- Fitzpatrick, N., Radić, V., & Menounos, B. (2017). Surface energy balance closure and turbulent flux parameterization on a mid-latitude mountain glacier, Purcell Mountains, Canada. *Frontiers of Earth Science*, 5, 1–20. <https://doi.org/10.3389/feart.2017.00067>
- Flowers, G. E., Björnsson, H., Geirsdóttir, Á., Miller, G. H., & Clarke, G. K. C. (2007). Glacier fluctuation and inferred climatology of Langjökull ice cap through the Little Ice Age. *Quaternary Science Reviews*, 26(19–21), 2337–2353. <https://doi.org/10.1016/j.quascirev.2007.07.016>
- Flowers, G. E., Marshall, S. J., Björnsson, H., & Clarke, G. K. C. (2005). Sensitivity of Vatnajökull ice cap hydrology and dynamics to climate warming over the next 2 centuries. *Journal of Geophysical Research*, 110(2), F02011. <https://doi.org/10.1029/2004JF000200>
- Fowler, A., & Ng, F. (2020). *Glaciers and Ice Sheets in the climate system: The Karlsruhe summer school lecture notes*. Springer.
- Frederikse, T., Landerer, F., Caron, L., Adhikari, S., Parkes, D., Humphrey, V. W., et al. (2020). The causes of sea-level rise since 1900. *Nature*, 584(7821), 393–397. <https://doi.org/10.1038/s41586-020-2591-3>
- Fürst, J. J., Rybak, O., Goelzer, H., De Smedt, B., De Groen, P., & Huybrechts, P. (2011). Improved convergence and stability properties in a three-dimensional higher-order ice sheet model. *Geoscientific Model Development*, 4(4), 1133–1149. <https://doi.org/10.5194/gmd-4-1133-2011>
- Gabbi, J., Carenzo, M., Pellicciotti, F., Bauder, A., & Funk, M. (2014). A comparison of empirical and physically based glacier surface melt models for long-term simulations of glacier response. *Journal of Glaciology*, 60(224), 1199–1207. <https://doi.org/10.3189/2014JoG14J011>
- Gantayat, P., Kulkarni, A. V., Srinivasan, J., & Schmeits, M. J. (2017). Numerical modelling of past retreat and future evolution of Chhota Shigri glacier in Western Indian Himalaya. *Annals of Glaciology*, 58(75pt2), 136–144. <https://doi.org/10.1017/aog.2017.21>
- Gerbaux, M., Genton, C., Etchevers, P., Vincent, C., & Dedieu, J. P. (2005). Surface mass balance of glaciers in the French Alps: Distributed modeling and sensitivity to climate change. *Journal of Glaciology*, 51(175), 561–572. <https://doi.org/10.3189/172756505781829133>
- Giesen, R. H., & Oerlemans, J. (2010). Response of the ice cap Hardangerjökulen in southern Norway to the 20th and 21st century climates. *The Cryosphere*, 4(2), 191–213. <https://doi.org/10.5194/tc-4-191-2010>
- Gilbert, A., Flowers, G. E., Miller, G. H., Refsnider, K., Young, N. E., & Radic, V. (2017). The projected demise of Barnes Ice Cap: Evidence of an unusually warm 21st century Arctic. *Geophysical Research Letters*, 44(6), 2810–2816. <https://doi.org/10.1002/2016GL072394>
- Gilbert, A., Simisalo, A., Gurung, T., Fujita, K., Maharjan, S., Sherpa, T., & Fukuda, T. (2020). The influence of water percolation through crevasses on the thermal regime of a Himalayan mountain glacier. *The Cryosphere*, 14(4), 1273–1288. <https://doi.org/10.5194/tc-14-1273-2020>
- Glen, J. W. (1955). The creep of polycrystalline ice. *Proceedings of the Royal Society A: Mathematical, Physical & Engineering Sciences*, 228(1175), 519–538. <https://doi.org/10.1098/rspa.1955.0066>
- Goelzer, H., Nowicki, S. M. J., Edwards, T. L., Beckley, M., Abe-Ouchi, A., Aschwanden, A., et al. (2018). Design and results of the ice sheet model initialisation experiments initMIP-Greenland: An ISMIP6 intercomparison. *The Cryosphere*, 12(4), 1433–1460. <https://doi.org/10.5194/tc-12-1433-2018>

- Goelzer, H., Robinson, A., Seroussi, H., & van de Wal, R. S. W. (2017). Recent progress in Greenland Ice Sheet modelling. *Current Climate Change Reports*, 3(4), 291–302. <https://doi.org/10.1007/s40641-017-0073-y>
- Goodman, D. J., King, G. C. P., Millar, D. H. M., & DeqRobin, G. (1979). Pressure-melting effects in basal ice of temperate glaciers: Laboratory studies and field observations under glacier d'Argentiere. *Journal of Glaciology*, 23(89), 259–271. <https://doi.org/10.1017/S0022143000029889>
- Goosse, H., Barriat, P.-Y., Dalaiden, Q., Klein, F., Marzeion, B., Maussion, F., et al. (2018). Testing the consistency between changes in simulated climate and Alpine glacier length over the past millennium. *Climate of the Past*, 14, 1119–1133. <https://doi.org/10.5194/cp-2018-48>
- Greuell, W. (1992). Hintereisferner, Austria: Mass-balance reconstruction and numerical modelling of the historical length variations. *Journal of Glaciology*, 38(129), 233–244. <https://doi.org/10.3189/0022143000003646>
- Greve, R. (1997). Application of a polythermal three-dimensional ice sheet model to the Greenland Ice Sheet: Response to steady-state and transient climate scenarios. *Journal of Climate*, 10(5), 901–918. [https://doi.org/10.1175/1520-0442\(1997\)010<0901:AOAPTD>2.0.CO;2](https://doi.org/10.1175/1520-0442(1997)010<0901:AOAPTD>2.0.CO;2)
- Greve, R., & Blatter, H. (2009). *Dynamics of ice sheets and glaciers*. Springer Science & Business Media.
- Gudmundsson, G. H. (1999). A three-dimensional numerical model of the confluence area of Unteraargletscher, Bernese Alps, Switzerland. *Journal of Glaciology*, 45(150), 219–230. <https://doi.org/10.3189/002214399793377086>
- Guðmundsson, S., Björnsson, H., Jóhannesson, T., Ádalgeirsdóttir, G., Pálsson, F., & Sigurðsson, O. (2009). Similarities and differences in the response to climate warming of two ice caps in Iceland. *Hydrology Research*, 40(5), 495–502. <https://doi.org/10.2166/nh.2009.210>
- Haeberli, W., & Weingartner, R. (2020). In full transition: Key impacts of vanishing mountain ice on water-security at local to global scales. *Water Security*, 11, 100074. <https://doi.org/10.1016/j.wasec.2020.100074>
- Hanna, E., Pattyn, F., Navarro, F., Favier, V., Goelzer, H., van den Broeke, M. R., et al. (2020). Mass balance of the ice sheets and glaciers – Progress since AR5 and challenges. *Earth-Science Reviews*, 201, 102976. <https://doi.org/10.1016/j.earscirev.2019.102976>
- Hannesdóttir, H., Aoalgeirsdóttir, G., Jóhannesson, T., Guomundsson, S., Crochet, P., Ágústsson, H., et al. (2015). Downscaled precipitation applied in modelling of mass balance and the evolution of southeast Vatnajökull, Iceland. *Journal of Glaciology*, 61(228), 799–813. <https://doi.org/10.3189/2015JoG15J024>
- Harris, I., Osborn, T. J., Jones, P., & Lister, D. (2020). Version 4 of the CRU TS monthly high-resolution gridded multivariate climate dataset. *Scientific Data*, 7(1), 1–18. <https://doi.org/10.1038/s41597-020-0453-3>
- Harrison, S., Kargel, J. S., Huggel, C., Reynolds, J., Shugar, D. H., Betts, R. A., et al. (2018). Climate change and the global pattern of moraine-dammed glacial lake outburst floods. *The Cryosphere*, 12(4), 1195–1209. <https://doi.org/10.5194/tc-12-1195-2018>
- Harrison, W. D., Elsberg, D. H., Echelmeyer, K. A., & Krimmel, R. M. (2001). On the characterization of glacier response by a single time-scale. *Journal of Glaciology*, 47(159), 659–664. <https://doi.org/10.3189/172756501781831837>
- Herreid, S., & Pellicciotti, F. (2020). The state of rock debris covering Earth's glaciers. *Nature Geoscience*, 13(9), 621–627. <https://doi.org/10.1038/s41561-020-0615-0>
- Hindmarsh, R. C. A. (2004). A numerical comparison of approximations to the Stokes equations used in ice sheet and glacier modeling. *Journal of Geophysical Research*, 109(F1), F01012. <https://doi.org/10.1029/2003JE000065>
- Hindmarsh, R. C. A. (2018). Ice sheet and glacier modelling. In *Past glacial environments* (2nd ed., pp. 605–661). Elsevier Ltd. <https://doi.org/10.1016/B978-0-08-100524-8.00019-1>
- Hock, R. (2003). Temperature index melt modelling in mountain areas. *Journal of Hydrology*, 282(1–4), 104–115. [https://doi.org/10.1016/S0022-1694\(03\)00257-9](https://doi.org/10.1016/S0022-1694(03)00257-9)
- Hock, R., Bliss, A., Marzeion, B., Giesen, R. H., Hirabayashi, Y., Huss, M., et al. (2019). GlacierMIP – A model intercomparison of global-scale glacier mass-balance models and projections. *Journal of Glaciology*, 65(251), 453–467. <https://doi.org/10.1017/jog.2019.22>
- Hooke, R. L. B. (2005). *Principles of glacier mechanics* (2nd ed.). Cambridge University Press.
- Hooke, R. L. B., Holmlund, P., Nilsson, M., & Stroeven, A. (1989). A 3 year record of seasonal variations in surface velocity, Storglaciären, Sweden. *Journal of Glaciology*, 35(120), 235–247. <https://doi.org/10.3189/s002214300004561>
- Hubbard, A. (2000). The verification and significance of three approaches to longitudinal stresses in high-resolution models of glacier flow. *Geografiska Annaler – Series A: Physical Geography*, 82(4), 471–487. <https://doi.org/10.1111/j.0435-3676.2000.00135.x>
- Hubbard, A. L., Blatter, H., Nienow, P., Mair, D., & Hubbard, B. (1998). Comparison of a three-dimensional model for glacier flow with field data from Haut Glacier d'Arolla, Switzerland. *Journal of Glaciology*, 44(147), 368–378. <https://doi.org/10.3198/1998JoG44-147-368-378>
- Hugonet, R., McNabb, R., Berthier, E., Menounos, B., Nuth, C., Girod, L., et al. (2021). Accelerated global glacier mass loss in the early twenty-first century. *Nature*, 592(7856), 726–731. <https://doi.org/10.1038/s41586-021-03436-z>
- Huss, M., Bauder, A., Funk, M., & Hock, R. (2008). Determination of the seasonal mass balance of four Alpine glaciers since 1865. *Journal of Geophysical Research*, 113(F1), F01015. <https://doi.org/10.1029/2007F000803>
- Huss, M., & Farinotti, D. (2012). Distributed ice thickness and volume of all glaciers around the globe. *Journal of Geophysical Research*, 117(4), F04010. <https://doi.org/10.1029/2012JF002523>
- Huss, M., Funk, M., & Ohmura, A. (2009). Strong Alpine glacier melt in the 1940s due to enhanced solar radiation. *Geophysical Research Letters*, 36(23), L23501. <https://doi.org/10.1029/2009GL040789>
- Huss, M., & Hock, R. (2015). A new model for global glacier change and sea-level rise. *Frontiers of Earth Science*, 3, 1–22. <https://doi.org/10.3389/feart.2015.00054>
- Huss, M., & Hock, R. (2018). Global-scale hydrological response to future glacier mass loss. *Nature Climate Change*, 8(2), 135–140. <https://doi.org/10.1038/s41558-017-0049-x>
- Huss, M., Jouvet, G., Farinotti, D., & Bauder, A. (2010). Future high-mountain hydrology: A new parameterization of glacier retreat. *Hydrology and Earth System Sciences*, 14(5), 815–829. <https://doi.org/10.5194/hess-14-815-2010>
- Huss, M., Sugiyama, S., Bauder, A., & Funk, M. (2007). Retreat scenarios of Unteraargletscher, Switzerland, using a combined ice-flow mass-balance model. *Arctic Antarctic and Alpine Research*, 39(3), 422–431. [https://doi.org/10.1657/1523-0430\(06-036](https://doi.org/10.1657/1523-0430(06-036)
- Hutter, K. (1983). *Theoretical glaciology*. Reidel Publ. Co.
- Huybrechts, P. (1990). A 3-D model for the Antarctic Ice Sheet: A sensitivity study on the glacial-interglacial contrast. *Climate Dynamics*, 5(2), 79–92. <https://doi.org/10.1007/BF00207423>
- Huybrechts, P., de Nooze, P., & Declerq, H. (1989). Numerical modelling of glacier d'Argentière and its historic front variations. In J. Oerlemans (Ed.), *Glacier fluctuations and climatic change* (pp. 373–389). Kluwer Academic Publishers. https://doi.org/10.1007/978-94-015-7823-3_24
- Iken, A., & Truffer, M. (1997). The relationship between subglacial water pressure and velocity of Findelengletscher, Switzerland, during its advance and retreat. *Journal of Glaciology*, 43(144), 328–338. <https://doi.org/10.1017/CBO9781107415324.004>
- Immerzeel, W. W., Lutz, A. F., Andrade, M., Bahl, A., Biemans, H., Bolch, T., et al. (2020). Importance and vulnerability of the world's water towers. *Nature*, 577(7790), 364–369. <https://doi.org/10.1038/s41586-019-1822-y>

- IPCC. (2021). *Climate Change 2021: The Physical Science Basis. Contribution of Working Group I to the Sixth Assessment Report of the Intergovernmental Panel on Climate Change*. (In V. Masson-Delmotte, P. Zhai, A. Pirani, S. L. Connors, C. Péan, S. Berger, et al., Eds.). Cambridge University Press.
- Iverson, N. R., Hooyer, T. S., Fischer, U. H., Cohen, D., Moore, P. L., Jackson, M., et al. (2007). Soft-bed experiments beneath Engabreen, Norway: Regelation, infiltration, basal slip and bed deformation. *Journal of Glaciology*, 53(182), 323–340. <https://doi.org/10.3189/002214307783258431>
- Jarosch, A. H., Schoof, C. G., & Anslow, F. S. (2013). Restoring mass conservation to shallow ice flow models over complex terrain. *The Cryosphere*, 7(1), 229–240. <https://doi.org/10.5194/tc-7-229-2013>
- Jóhannesson, T. (1997). The response of two Icelandic glaciers to climatic warming computed with a degree-day glacier mass-balance model coupled to a dynamic glacier model. *Journal of Glaciology*, 43(143), 321–327. <https://doi.org/10.3189/s0022143000003270>
- Jóhannesson, T., Pálmasón, B., Hjartarson, Á., Jarosch, A. H., Magnússon, E., Belart, J. M. C., & Gudmundsson, M. T. (2020). Non-surface mass balance of glaciers in Iceland. *Journal of Glaciology*, 66(258), 685–697. <https://doi.org/10.1017/jog.2020.37>
- Jóhannesson, T., Raymond, C. F., & Waddington, E. D. (1989). A simple method for determining the response time of glaciers. In *Glacier fluctuations and climatic change* (pp. 343–352). Kluwer Academic Publishers.
- Jouvet, G., & Huss, M. (2019). Future retreat of great Aletschgletscher. *Journal of Glaciology*, 65(253), 869–872. <https://doi.org/10.1017/jog.2019.52>
- Jouvet, G., Huss, M., Blatter, H., Picasso, M., & Rappaz, J. (2009). Numerical simulation of Rhonegletscher from 1874 to 2100. *Journal of Computational Physics*, 228(17), 6426–6439. <https://doi.org/10.1016/j.jcp.2009.05.033>
- Jouvet, G., Huss, M., Funk, M., & Blatter, H. (2011). Modelling the retreat of Grosser Aletschgletscher, Switzerland, in a changing climate. *Journal of Glaciology*, 57(206), 1033–1045. <https://doi.org/10.3189/002214311798843359>
- Jouvet, G., Röllin, S., Sahli, H., Corcho, J., Gnägi, L., Compagni, L., et al. (2020). Mapping the age of ice of Gauligletscher combining surface radionuclide contamination and ice flow modeling. *The Cryosphere*, 14(11), 4233–4251. <https://doi.org/10.5194/tc-14-4233-2020>
- Kääb, A., Leiss, S., Gilbert, A., Bühl, Y., Gascoin, S., Evans, S. G., et al. (2018). Massive collapse of two glaciers in western Tibet in 2016 after surge-like instability. *Nature Geoscience*, 11(2), 114–120. <https://doi.org/10.1038/s41561-017-0039-7>
- Kienholz, C., Rich, J. L., Arendt, A. A., & Hock, R. (2014). A new method for deriving glacier centerlines applied to glaciers in Alaska and northwest Canada. *The Cryosphere*, 8(2), 503–519. <https://doi.org/10.5194/tc-8-503-2014>
- Kruss, P. (1983). Climate change in East Africa: A numerical simulation from the 100 years of terminus record of Lewis glacier, mount Kenya. *Zeitschrift für Gletscherkunde und Glazialgeologie*, 19(1), 43–60.
- Kruss, P. D. (1984). Terminus response of Lewis Glacier, Mount Kenya, Kenya, to sinusoidal net-balance forcing. *Journal of Glaciology*, 30(105), 212–217. <https://doi.org/10.1017/s0022143000005943>
- Kruss, P. D., & Smith, I. N. (1982). Numerical modelling of the Vernagtferner and its fluctuations. *Zeitschrift für Gletscherkunde und Glazialgeologie*, 18(492), 93–106.
- Lapazaran, J. J., Otero, J., Martín-Español, A., & Navarro, F. J. (2016). On the errors involved in ice-thickness estimates II: Errors in digital elevation models of ice thickness. *Journal of Glaciology*, 62(236), 1021–1029. <https://doi.org/10.1017/jog.2016.94>
- Laumann, T., & Nesje, A. (2009). The impact of climate change on future frontal variations of Briksdalsbreen, western Norway. *Journal of Glaciology*, 55(193), 789–796. <https://doi.org/10.3189/002214309790152366>
- Laumann, T., & Nesje, A. (2014). Spørteggbreen, western Norway, in the past, present and future: Simulations with a two-dimensional dynamical glacier model. *The Holocene*, 24(7), 842–852. <https://doi.org/10.1177/0959683614530446>
- Laurent, L., Buoncristiani, J.-F., Pohl, B., Zekollari, H., Farinotti, D., Huss, M., et al. (2020). The impact of climate change and glacier mass loss on the hydrology in the Mont-Blanc massif. *Scientific Reports*, 10(1), 10420. <https://doi.org/10.1038/s41598-020-67379-7>
- Leclercq, P. W., Pitte, P., Giesen, R. H., Masiokas, M. H., & Oerlemans, J. (2012). Modelling and climatic interpretation of the length fluctuations of Glaciar Frías (north Patagonian Andes, Argentina) 1639–2009 AD. *Climate of the Past*, 8(5), 1385–1402. <https://doi.org/10.5194/cp-8-1385-2012>
- Le Meur, E., Gagliardini, O., Zwinger, T., & Ruokolainen, J. (2004). Glacier flow modelling: A comparison of the Shallow Ice Approximation and the full-stokes solution. *Comptes Rendus Physique*, 5(7), 709–722. <https://doi.org/10.1016/j.crhy.2004.10.001>
- Le Meur, E., Gerbaux, M., Schäfer, M., & Vincent, C. (2007). Disappearance of an Alpine glacier over the 21st century simulated from modeling its future surface mass balance. *Earth and Planetary Science Letters*, 261(3–4), 367–374. <https://doi.org/10.1016/j.epsl.2007.07.022>
- Le Meur, E., & Vincent, C. (2003). A two-dimensional shallow ice-flow model of Glacier de Saint-Sorlin, France. *Journal of Glaciology*, 49(167), 527–538. <https://doi.org/10.3189/172756503781830421>
- Le Moine, N., & Gsell, P. (2015). A graph-based approach to glacier flowline extraction: An application to glaciers in Switzerland. *Computers & Geosciences*, 85, 91–101. <https://doi.org/10.1016/j.cageo.2015.09.010>
- Letréguilly, A., & Reynaud, L. (1989). Past and forecast fluctuations of glacier Blanc (French Alps). *Annals of Glaciology*, 13, 159–163. <https://doi.org/10.3189/s0260305500007813>
- Leysinger Vieli, G. J.-M. C., & Gudmundsson, G. H. (2004). On estimating length fluctuations of glaciers caused by changes in climatic forcing. *Journal of Geophysical Research*, 109(F01007), F01007. <https://doi.org/10.1029/2003JF000027>
- Li, Y., Tian, L., Yi, Y., Moore, J. C., Sun, S., & Zhao, L. (2017). Simulating the evolution of Qiangtang No. 1 glacier in the central Tibetan Plateau to 2050. *Arctic Antarctic and Alpine Research*, 49(1), 1–12. <https://doi.org/10.1657/aaar0016-008>
- Lliboutry, L. (1964). *Traité de glaciologie. Tome 1: Glace, neige, hydrologie nivale*. Masson et Cie.
- Lüthi, M. P., & Bauder, A. (2010). Analysis of Alpine glacier length change records with a macroscopic glacier model. *Geographica Helvetica*, 65(2), 92–102. <https://doi.org/10.5194/gh-65-92-2010>
- Lutz, A. F., Maat, H. W., Wijngaard, R. R., Biemans, H., Syed, A., Shrestha, A. B., et al. (2019). South Asian river basins in a 1.5°C warmer world. *Regional Environmental Change*, 19(3), 833–847. <https://doi.org/10.1007/s10113-018-1433-4>
- Machguth, H., & Huss, M. (2014). The length of the world's glaciers – A new approach for the global calculation of center lines. *The Cryosphere*, 8(5), 1741–1755. <https://doi.org/10.5194/tc-8-1741-2014>
- Mackintosh, A., Anderson, B. M., & Pierrehumbert, R. T. (2017). Reconstructing climate from glaciers. *Annual Review of Earth and Planetary Sciences*, 45(1), 649–680. <https://doi.org/10.1146/annurev-earth-063016-020643>
- Mackintosh, A., Dugmore, A. J., & Hubbard, A. L. (2002). Holocene climatic changes in Iceland: Evidence from modelling glacier length fluctuations at Sólheimajökull. *Quaternary International*, 91(1), 39–52. [https://doi.org/10.1016/S1040-6182\(01\)00101-X](https://doi.org/10.1016/S1040-6182(01)00101-X)
- Marshall, S. J., Björnsson, H., Flowers, G. E., & Clarke, G. K. C. (2005). Simulation of Vatnajökull ice cap dynamics. *Journal of Geophysical Research*, 110(F3), F03009. <https://doi.org/10.1029/2004JF000262>
- Martín-Español, A., Lapazaran, J. J., Otero, J., & Navarro, F. J. (2016). On the errors involved in ice-thickness estimates III: Error in volume. *Journal of Glaciology*, 62(236), 1030–1036. <https://doi.org/10.1017/jog.2016.95>

- Marzeion, B., Cogley, J. G., Richter, K., & Parkes, D. (2014). Attribution of global glacier mass loss to anthropogenic and natural causes. *Science*, 345(6199), 919–921. <https://doi.org/10.1126/science.1254702>
- Marzeion, B., Hock, R., Anderson, B., Bliss, A., Champollion, N., Fujita, K., et al. (2020). Partitioning the uncertainty of ensemble projections of global glacier mass change. *Earth's Future*, 8(7), e2019EF001470. <https://doi.org/10.1029/2019EF001470>
- Marzeion, B., Jarosch, A. H., & Hofer, M. (2012). Past and future sea-level change from the surface mass balance of glaciers. *The Cryosphere*, 6(6), 1295–1322. <https://doi.org/10.5194/tc-6-1295-2012>
- Maussion, F., Butenko, A., Champollion, N., Dusch, M., Eis, J., Fourteau, K., et al. (2019). The Open Global Glacier Model (OGGM) v1.1. *Geoscientific Model Development*, 12(3), 909–931. <https://doi.org/10.5194/gmd-12-909-2019>
- Maussion, F., Scherer, D., Mölg, T., Collier, E., Curio, J., & Finkelburg, R. (2014). Precipitation seasonality and variability over the Tibetan Plateau as resolved by the high Asia reanalysis. *Journal of Climate*, 27(5), 1910–1927. <https://doi.org/10.1175/JCLI-D-13-00282.1>
- Meier, M. F. (1984). Contribution of small glaciers to global sea level. *Science*, 226(4681), 1418–1421. <https://doi.org/10.1126/science.226.4681.1418>
- Miles, E. S., Pellicciotti, F., Willis, I. C., Steiner, J. F., Buri, P., & Arnold, N. S. (2016). Refined energy-balance modelling of a supraglacial pond, Langtang Kholo, Nepal. *Annals of Glaciology*, 57(71), 29–40. <https://doi.org/10.3189/2016AoG71A421>
- Millan, R., Mouginot, J., Rabatel, A., & Morlighem, M. (2022). Ice velocity and thickness of the world's glaciers. *Nature Geoscience*, 15(2), 124–129. <https://doi.org/10.1038/s41561-021-00885-z>
- Milner, A. M., Khamis, K., Battin, T. J., Brittain, J. E., Barrand, N. E., Olafsson, S., et al. (2017). Glacier shrinkage driving global changes in downstream systems. *Proceedings of the National Academy of Sciences of the United States of America*, 114(37), 9770–9778. <https://doi.org/10.1073/pnas.1619807114>
- Morland, L. W. (1984). Thermomechanical balances of ice sheet flows. *Geophysical & Astrophysical Fluid Dynamics*, 29(1–4), 237–266. <https://doi.org/10.1080/03091928408248191>
- Mosbeux, C., Gillet-Chaulet, F., & Gagliardini, O. (2016). Comparison of adjoint and nudging methods to initialise ice sheet model basal conditions. *Geoscientific Model Development*, 9(7), 2549–2562. <https://doi.org/10.5194/gmd-9-2549-2016>
- Mottram, R., Hansen, N., Kittel, C., van Wessem, M., Agosta, C., Amory, C., et al. (2020). What is the surface mass balance of Antarctica? An intercomparison of regional climate model estimates. *The Cryosphere Discussions*, 2020(January), 1–42. <https://doi.org/10.5194/tc-2019-333>
- Nick, F. M., Vieli, A., Andersen, M. L., Joughin, I., Payne, A. J., Edwards, T. L., et al. (2013). Future sea-level rise from Greenland's main outlet glaciers in a warming climate. *Nature*, 497(7448), 235–238. <https://doi.org/10.1038/nature12068>
- Nye, J. F. (1948). The flow of glaciers. *Nature*, 161(4099), 819–821. <https://doi.org/10.1038/161819a0>
- Nye, J. F. (1957). The distribution of stress and velocity in glaciers and ice-sheets. *Proceedings of the Royal Society A: Mathematical, Physical & Engineering Sciences*, 239(1216), 113–133. <https://doi.org/10.1098/rspa.1957.0026>
- Oerlemans, J. (1986). An attempt to simulate historic front variations of Nigardsbreen, Norway. *Theoretical and Applied Climatology*, 37(3), 126–135. <https://doi.org/10.1007/BF00867846>
- Oerlemans, J. (1992). Climate sensitivity of glaciers in southern Norway: Application of an energy-balance IIodel to Nigardsbreen, Hellstugubreen and Alfotbreen. *Journal of Glaciology*, 38(129), 223–232. <https://doi.org/10.3189/s002214300003634>
- Oerlemans, J. (1997a). Climate sensitivity of Franz Josef glacier, New Zealand, as Revealed by numerical modeling. *Arctic and Alpine Research*, 29(2), 233–239. <https://doi.org/10.2307/1552052>
- Oerlemans, J. (1997b). A flowline model for Nigardsbreen, Norway: Projection of future glacier length based on dynamic calibration with the historic record. *Annals of Glaciology*, 24, 382–389. <https://doi.org/10.1017/s0260305500012489>
- Oerlemans, J. (2012). Linear modelling of glacier length fluctuations. *Geografiska Annaler – Series A: Physical Geography*, 94(2), 183–194. <https://doi.org/10.1111/j.1468-0459.2012.00469.x>
- Oerlemans, J., Anderson, B., Hubbard, A. L., Huybrechts, P., Jóhannesson, T., Knap, W. H., et al. (1998). Modelling the response of glaciers to climate warming. *Climate Dynamics*, 14(4), 267–274. <https://doi.org/10.1007/s003820050222>
- Oerlemans, J., & Van Pelt, W. J. J. (2015). A model study of Abrahamsenbreen, a surging glacier in northern Spitsbergen. *The Cryosphere*, 9(2), 767–779. <https://doi.org/10.5194/tc-9-767-2015>
- Parkes, D., & Goosse, H. (2020). Modelling regional glacier length changes over the last millennium using the Open Global Glacier Model. *The Cryosphere*, 14(9), 3135–3153. <https://doi.org/10.5194/tc-14-3135-2020>
- Parkes, D., & Marzeion, B. (2018). Twentieth-century contribution to sea-level rise from uncharted glaciers. *Nature*, 563(7732), 551–554. <https://doi.org/10.1038/s41586-018-0687-9>
- Paterson (1981). *The physics of glaciers*. Pergamon Press.
- Paterson, W. S. B. (1994). *The physics of glaciers*. Pergamon.
- Paterson, W. S. B., & Budd, W. F. (1982). Flow parameters for ice sheet modeling. *Cold Regions Science and Technology*, 6(2), 175–177. [https://doi.org/10.1016/0165-232X\(82\)90010-6](https://doi.org/10.1016/0165-232X(82)90010-6)
- Patty, F. (2003). A new three-dimensional higher-order thermomechanical ice sheet model: Basic sensitivity, ice stream development, and ice flow across subglacial lakes. *Journal of Geophysical Research*, 108(B8), B82382. <https://doi.org/10.1029/2002JB002329>
- Patty, F., Favier, L., Sun, S., & Durand, G. (2017). Progress in numerical modeling of Antarctic ice-sheet dynamics. *Current Climate Change Reports*, 3(3), 174–184. <https://doi.org/10.1007/s40641-017-0069-7>
- Patty, F., Perichon, L., Aschwanden, A., Breuer, B., De Smedt, B., Gagliardini, O., et al. (2008). Benchmark experiments for higher-order and full-Stokes ice sheet models (ISMIP-HOM). *The Cryosphere*, 2, 95–108. <https://doi.org/10.5194/tcd-2-111-2008>
- Paul, F., Maisch, M., Rothenbühler, C., Hoelzle, M., & Haeberli, W. (2007). Calculation and visualisation of future glacier extent in the Swiss Alps by means of hypsographic modelling. *Global and Planetary Change*, 55(4), 343–357. <https://doi.org/10.1016/j.gloplacha.2006.08.003>
- Pellicciotti, F., Brock, B., Strasser, U., Burlando, P., Funk, M., & Corripio, J. (2005). An enhanced temperature-index glacier melt model including the shortwave radiation balance: Development and testing for Haut Glacier d'Arolla, Switzerland. *Journal of Glaciology*, 51(175), 573–587. <https://doi.org/10.3189/172756505781829124>
- Pritchard, H. D. (2019). Asia's shrinking glaciers protect large populations from drought stress. *Nature*, 569(7758), 649–654. <https://doi.org/10.1038/s41586-019-1240-1>
- Purdie, H., Hughes, J., Stewart, E., & Espiner, S. (2020). Journal of outdoor Recreation and tourism implications of a changing alpine environment for geotourism: A case study from Aoraki/Mount Cook, New Zealand. *Journal of Outdoor Recreation and Tourism*, 29, 100235. <https://doi.org/10.1016/j.jort.2019.100235>
- Radić, V., & Hock, R. (2011). Regionally differentiated contribution of mountain glaciers and ice caps to future sea-level rise. *Nature Geoscience*, 4(2), 91–94. <https://doi.org/10.1038/ngeo1052>
- Radić, V., & Hock, R. (2014). Glaciers in the Earth's hydrological cycle: Assessments of glacier mass and runoff changes on global and regional scales. *Surveys in Geophysics*, 35(3), 813–837. <https://doi.org/10.1007/s10712-013-9262-y>

- Rea, B. R., & Whalley, W. B. (1994). Subglacial observations from øksfjordjøkelen, north Norway. *Earth Surface Processes and Landforms*, 19(7), 659–673. <https://doi.org/10.1002/esp.3290190706>
- Recinos, B., Maussion, F., Rothenpieler, T., & Marzeion, B. (2019). Impact of frontal ablation on the ice thickness estimation of marine-terminating glaciers in Alaska. *The Cryosphere*, 13(10), 2657–2672. <https://doi.org/10.5194/tc-13-2657-2019>
- Réveillet, M., Rabaté, A., Gillet-Chaulet, F., & Soruco, A. (2015). Simulations of changes to Glaciar Zongo, Bolivia (16°S), over the 21st century using a 3-D full-Stokes model and CMIP5 climate projections. *Annals of Glaciology*, 56(70), 89–97. <https://doi.org/10.3189/2015AoG70A113>
- Réveillet, M., Six, D., Vincent, C., Rabaté, A., Dumont, M., Lafayesse, M., et al. (2018). Relative performance of empirical and physical models in assessing the seasonal and annual glacier surface mass balance of Saint-Sorlin Glacier (French Alps). *The Cryosphere*, 12(4), 1367–1386. <https://doi.org/10.5194/tc-12-1367-2018>
- RGI Consortium. (2017). *Randolph Glacier Inventory – A dataset of global glacier outlines: Version 6.0: Technical report, Global Land Ice Measurements from space*. Digital Media. <https://doi.org/10.7265/N5-RGI-60>
- Riegler, G., Hennig, S. D., & Weber, M. (2015). WorldDEM—A novel global foundation layer. *International Archives of the Photogrammetry, Remote Sensing and Spatial Information Sciences – ISPRS Archives*, 40(3W2), 183–187. <https://doi.org/10.5194/isprarchives-XL-3-W2-183-2015>
- Roe, G., Christian, J. E., & Marzeion, B. (2021). On the attribution of industrial-era glacier mass loss to anthropogenic climate change. *The Cryosphere*, 15(4), 1889–1905. <https://doi.org/10.5194/tc-15-1889-2021>
- Roe, G. H., Baker, M. B., & Herla, F. (2017). Centennial glacier retreat as categorical evidence of regional climate change. *Nature Geoscience*, 10(2), 95–99. <https://doi.org/10.1038/ngeo2863>
- Roth, A., Hock, R., Schuler, T. V., Bieniek, P. A., Pelto, M., & Aschwanden, A. (2018). Modeling winter precipitation over the Juneau Icefield, Alaska, using a linear model of orographic precipitation. *Frontiers of Earth Science*, 6, 20. <https://doi.org/10.3389/feart.2018.00020>
- Rounce, D. R., Hock, R., McNabb, R. W., Millan, R., Sommer, C., Braun, M. H., et al. (2021). Distributed global debris thickness estimates reveal debris significantly impacts glacier mass balance. *Geophysical Research Letters*, 48(8). <https://doi.org/10.1029/2020gl091311>
- Rounce, D. R., Khurana, T., Short, M., Hock, R., Shean, D., & Brinkerhoff, D. J. (2020). Quantifying parameter uncertainty in a large-scale glacier evolution model with a Bayesian model: Application to High Mountain Asia. *Journal of Glaciology*, 66, 175–187. <https://doi.org/10.1017/jog.2019.91>
- Rowan, A. V., Egholm, D. L., Quincey, D. J., & Glasser, N. F. (2015). Modelling the feedbacks between mass balance, ice flow and debris transport to predict the response to climate change of debris-covered glaciers in the Himalaya. *Earth and Planetary Science Letters*, 430, 427–438. <https://doi.org/10.1016/j.epsl.2015.09.004>
- Salim, E., Ravanel, L., Deline, P., & Gauchon, C. (2021). A review of melting ice adaptation strategies in the glacier tourism context. *Scandinavian Journal of Hospitality and Tourism*, 21(2), 229–246. <https://doi.org/10.1080/15022250.2021.1879670>
- Schaefer, M., Machguth, H., Falvey, M., Casassa, G., & Rignot, E. (2015). Quantifying mass balance processes on the Southern Patagonia Icefield. *The Cryosphere*, 9(1), 25–35. <https://doi.org/10.5194/tc-9-25-2015>
- Schaefli, B., Hingray, B., & Musy, A. (2007). Climate change and hydropower production in the Swiss Alps: Quantification of potential impacts and related modelling uncertainties. *Hydrology and Earth System Sciences*, 11(3), 1191–1205. <https://doi.org/10.5194/hess-11-1191-2007>
- Schaefli, B., Manso, P., Fischer, M., Huss, M., & Farinotti, D. (2019). The role of glacier retreat for Swiss hydropower production. *Renewable Energy*, 132, 615–627. <https://doi.org/10.1016/j.renene.2018.07.104>
- Schäfer, M., Gillet-Chaulet, F., Gladstone, R., Pettersson, R., Pohjola, V. A., Strozzi, T., & Zwinger, T. (2014). Assessment of heat sources on the control of fast flow of Vestfonna ice cap, Svalbard. *The Cryosphere*, 8(5), 1951–1973. <https://doi.org/10.5194/tc-8-1951-2014>
- Schäfer, M., & Le Meur, E. (2007). Improvement of a 2-D SIA ice-flow model: Application to Glacier de Saint-Sorlin, France. *Journal of Glaciology*, 53(183), 713–722. <https://doi.org/10.3189/002214307784409234>
- Schäfer, M., Möller, M., Zwinger, T., & Moore, J. C. (2015). Dynamic modelling of future glacier changes: Mass-balance/elevation feedback in projections for the Vestfonna ice cap, Nordaustlandet, Svalbard. *Journal of Glaciology*, 61(230), 1121–1136. <https://doi.org/10.3189/2015JoG14J184>
- Scherler, D., Wulf, H., & Gorelick, N. (2018). Global assessment of supraglacial debris cover extents. *Geophysical Research Letters*, 45(21), 4–11. <https://doi.org/10.1029/2018GL080158>
- Schlosser, E. (1997). Numerical simulation on fluctuations of Hintereisferner, Ötztal Alps, since AD 1850. *Annals of Glaciology*, 24, 199–202. <https://doi.org/10.1017/s0260305500012179>
- Schmeits, M. J., & Oerlemans, J. (1997). Simulation of the historical variations in length of Unterer Grindelwaldgletscher, Switzerland. *Journal of Glaciology*, 43(143), 152–164. <https://doi.org/10.3189/s0022143000002914>
- Schmidt, L. S., Aðalgeirsdóttir, G., Pálsson, F., Langen, P. L., Guðmundsson, S., & Björnsson, H. (2020). Dynamic simulations of Vatnajökull ice cap from 1980 to 2300. *Journal of Glaciology*, 66(255), 97–112. <https://doi.org/10.1017/jog.2019.90>
- Schneeberger, C., Albrecht, O., Blatter, H., Wild, M., & Hock, R. (2001). Modelling the response of glaciers to a doubling in atmospheric CO₂: A case study of Storglaciären, northern Sweden. *Climate Dynamics*, 17(11), 825–834. <https://doi.org/10.1007/s003820000147>
- Seroussi, H., Nowicki, S., Simon, E., Ouchi, A. A., Albrecht, T., Brondex, J., et al. (2019). initMIP-Antarctica: An ice sheet model initialization experiment of ISMIP6. *The Cryosphere Discussions*, 1–44. <https://doi.org/10.5194/tc-2018-271>
- Sicart, J. E., Hock, R., Ribstein, P., Litt, M., & Ramirez, E. (2011). Analysis of seasonal variations in mass balance and meltwater discharge of the tropical Zongo Glacier by application of a distributed energy balance model. *Journal of Geophysical Research*, 116(D13), D13105. <https://doi.org/10.1029/2010JD015105>
- Smith, I. N., & Budd, W. F. (1979). The derivation of past climatic changes from observed changes of glaciers. *IAHS Publication*, 131, 31–52.
- Steinemann, S. (1958). Experimentelle Untersuchungen zur Plastizität von Eis. *Beiträge Zur Geologie Der Schweiz – Hydrologie*, 10, 1–72. <https://doi.org/10.3929/ethz-a-000096707>
- Steiner, D., Pauling, A., Nussbaumer, S. U., Nesje, A., Luterbacher, J., Wanner, H., & Zumbühl, H. J. (2008). Sensitivity of European glaciers to precipitation and temperature – Two case studies. *Climatic Change*, 90(4), 413–441. <https://doi.org/10.1007/s10584-008-9393-1>
- Steiner, D., Walter, A., & Zumbühl, H. J. (2005). The application of a non-linear back-propagation neural network to study the mass balance of Grosse Aletschgletscher, Switzerland. *Journal of Glaciology*, 51(173), 313–323. <https://doi.org/10.3189/172756505781829421>
- Stewart, E. J., Wilson, J., Espiner, S., Purdie, H., & Dawson, J. (2017). Implications of climate change for glacier tourism. *Tourism Geographies*, 6688(October), 377–398. <https://doi.org/10.1080/14616688.2016.1198416>
- Stroeven, A., van de Wal, R., & Oerlemans, J. (1989). Historic front variations of the Rhone Glacier: Simulation with an ice flow model. In J. Oerlemans (Ed.), *Glacier fluctuations and climate change* (pp. 391–405). Kluwer Academic Publishers.
- Stroeven, A. P. (1996). The robustness of one-dimensional, time-dependent, ice-flow models: A case study from Storglaciären, northern Sweden. *Geografiska Annaler – Series A: Physical Geography*, 78(2/3), 133–146. <https://doi.org/10.2307/520975>
- Sugiyama, S., Bauder, A., Zahno, C., & Funk, M. (2007). Evolution of Rhonegletscher, Switzerland, over the past 125 years and in the future: Application of an improved flowline model. *Annals of Glaciology*, 46, 268–274. <https://doi.org/10.3189/172756407782871143>

- Todd, J., Christoffersen, P., Zwinger, T., Räback, P., & Benn, D. I. (2019). Sensitivity of a calving glacier to ice-ocean interactions under climate change: New insights from a 3-D full-Stokes model. *The Cryosphere*, 13(6), 1681–1694. <https://doi.org/10.5194/tc-13-1681-2019>
- Ultee, L., & Bassis, J. N. (2017). A plastic network approach to model calving glacier advance and retreat. *Frontiers of Earth Science*, 5(March), 1–12. <https://doi.org/10.3389/feart.2017.00024>
- Untersteiner, N., & Nye, J. F. (1968). Computations of the possible future behaviour of Berendon Glacier, Canada. *Journal of Glaciology*, 7(50), 205–213. <https://doi.org/10.1017/s0022143000031002>
- van Dongen, E. C. H., Åström, J. A., Jouvet, G., Todd, J., Benn, D. I., & Funk, M. (2020). Numerical modeling shows increased fracturing due to melt-undercutting prior to major calving at Bowdoin Glacier. *Frontiers of Earth Science*, 8(July), 1–12. <https://doi.org/10.3389/feart.2020.00253>
- van Geffen, S., & Oerlemans, J. (2017). The 1982/83 surge and antecedent quiescent phase of Variegated Glacier: Revising the original dataset for application in flow line models. *Journal of Glaciology*, 63(241), 772–782. <https://doi.org/10.1017/jog.2017.43>
- Vargo, L. J., Anderson, B. M., Dadić, R., Horgan, H. J., Mackintosh, A. N., King, A. D., & Lorrey, A. M. (2020). Anthropogenic warming forces extreme annual glacier mass loss. *Nature Climate Change*, 10(9), 856–861. <https://doi.org/10.1038/s41558-020-0849-2>
- Veh, G., Korup, O., & Walz, A. (2020). Hazard from Himalayan glacier lake outburst floods. *Proceedings of the National Academy of Sciences of the United States of America*, 117(2), 907–912. <https://doi.org/10.1073/pnas.1914898117>
- Vincent, C., Kappenberger, G., Valla, F., Bauder, A., Funk, M., & Le Meur, E. (2004). Ice ablation as evidence of climate change in the Alps over the 20th century. *Journal of Geophysical Research – D: Atmospheres*, 109(10), D10104. <https://doi.org/10.1029/2003JD003857>
- Vincent, C., Soruco, A., Azam, M. F., Basantes-Serrano, R., Jackson, M., Kjøllmoen, B., et al. (2018). A Nonlinear statistical model for extracting a climatic signal from glacier mass balance measurements. *Journal of Geophysical Research: Earth Surface*, 123(9), 2228–2242. <https://doi.org/10.1029/2018JF004702>
- Vincent, C., Vallon, M., Reynaud, L., & Le Meur, E. (2000). Dynamic behaviour analysis of glacier de Saint Sorlin, France, from 40 years of observations, 1957–97. *Journal of Glaciology*, 46(154), 499–506. <https://doi.org/10.3189/172756500781833052>
- Vionnet, V., Six, D., Auger, L., Dumont, M., Lafayse, M., Quéno, L., et al. (2019). Sub-kilometer precipitation datasets for snowpack and glacier modeling in Alpine terrain. *Frontiers of Earth Science*, 7, 182. <https://doi.org/10.3389/feart.2019.00182>
- Wallinga, J., & van de Wal, R. S. W. (1998). Sensitivity of Rhonegletscher, Switzerland, to climate change: Experiments with a one-dimensional flowline model. *Journal of Glaciology*, 44(147), 383–393. <https://doi.org/10.3189/s0022143000002719>
- Wang, Z., Lin, G., & Ai, S. (2019). How long will an Arctic mountain glacier survive? A case study of Austre Lovénbreen, Svalbard. *Polar Research*, 38, 3519. <https://doi.org/10.33265/polar.v38.3519>
- Watson, C. S., & King, O. (2018). Everest's thinning glaciers: Implications for tourism and mountaineering. *Geology Today*, 34(1), 18–25. <https://doi.org/10.1111/gto.12215>
- Weertman, J. (1964). The theory of glacier sliding. *Journal of Glaciology*, 5(39), 287–303. <https://doi.org/10.3189/s0022143000029038>
- Wijngaard, R. R., Steiner, J. F., Kraaijenbrink, P. D. A., Klug, C., Adhikari, S., Banerjee, A., et al. (2019). Modeling the response of the Langtang Glacier and the Hintereisferner to a changing climate since the little ice age. *Frontiers of Earth Science*, 7, 143. <https://doi.org/10.3389/feart.2019.00143>
- Wouters, B., Gardner, A. S., & Moholdt, G. (2019). Global glacier mass loss during the GRACE satellite mission (2002–2016). *Frontiers of Earth Science*, 7, 96. <https://doi.org/10.3389/feart.2019.00096>
- Yurkov, A. M., Sannino, C., & Turchetti, B. (2019). *Makrilia fibulata* sp. nov., a psychrotolerant yeast from temperate and cold habitats. *Antonie van Leeuwenhoek*, 113(4), 499–510. <https://doi.org/10.1007/s10482-019-01359-4>
- Zekollari, H. (2017). TopoZeko: A MATLAB function for 3-D and 4-D topographical visualization in geosciences. *Software*, 6, 285–292. <https://doi.org/10.1016/j.softx.2017.10.004>
- Zekollari, H., Fürst, J. J., & Huybrechts, P. (2014). Modelling the evolution of Vadret da Morteratsch, Switzerland, since the Little Ice Age and into the future. *Journal of Glaciology*, 60(224), 1208–1220. <https://doi.org/10.3189/2014JoG14J053>
- Zekollari, H., Huss, M., & Farinotti, D. (2019). Modelling the future evolution of glaciers in the European Alps under the EURO-CORDEX RCM ensemble. *The Cryosphere*, 13(4), 1125–1146. <https://doi.org/10.5194/tc-13-1125-2019>
- Zekollari, H., Huss, M., & Farinotti, D. (2020). On the imbalance and response time of glaciers in the European Alps. *Geophysical Research Letters*, 47(2). <https://doi.org/10.1029/2019GL085578>
- Zekollari, H., & Huybrechts, P. (2015). On the climate-geometry imbalance, response time and volume-area scaling of an Alpine glacier: Insights from a 3-D flow model applied to Vadret da Morteratsch, Switzerland. *Annals of Glaciology*, 56(70), 51–62. <https://doi.org/10.3189/2015AoG70A921>
- Zekollari, H., & Huybrechts, P. (2018). Statistical modelling of the surface mass balance variability of the Morteratsch Glacier, Switzerland: Strong control of early melting season meteorological conditions. *Journal of Glaciology*, 64(244), 275–288. <https://doi.org/10.1017/jog.2018.18>
- Zekollari, H., Huybrechts, P., Fürst, J. J., Rybak, O., & Eisen, O. (2013). Calibration of a higher-order 3-D ice-flow model of the Morteratsch glacier complex, Engadin, Switzerland. *Annals of Glaciology*, 54(63), 343–351. <https://doi.org/10.3189/2013AoG63A434>
- Zekollari, H., Huybrechts, P., Noël, B., van de Berg, W. J., & van den Broeke, M. R. (2017). Sensitivity, stability and future evolution of the world's northernmost ice cap, Hans Tausen Iskappe (Greenland). *The Cryosphere*, 11(2), 805–825. <https://doi.org/10.5194/tc-11-805-2017>
- Zekollari, H., Lecavalier, B. S., & Huybrechts, P. (2017). Holocene evolution of Hans Tausen Iskappe (Greenland) and implications for the palaeoclimatic evolution of the high Arctic. *Quaternary Science Reviews*, 168, 182–193. <https://doi.org/10.1016/j.quascirev.2017.05.010>
- Zemp, M., Haeberli, W., Hoelzle, M., & Paul, F. (2006). Alpine glaciers to disappear within decades? *Geophysical Research Letters*, 33(13), L13504. <https://doi.org/10.1029/2006GL026319>
- Zemp, M., Huss, M., Thibert, E., Eckert, N., McNabb, R., Huber, J., et al. (2019). Global glacier mass balances and their contributions to sea-level rise from 1961 to 2016. *Nature*, 568(7752), 368–386. <https://doi.org/10.1038/s41586-019-1071-0>
- Zhang, T., Ju, L., Leng, W., Price, S., & Gunzburger, M. (2015). Thermomechanically coupled modelling for land-terminating glaciers: A comparison of two-dimensional, first-order and three-dimensional, full-Stokes approaches. *Journal of Glaciology*, 61(228), 702–712. <https://doi.org/10.3189/2015JoG14J220>
- Zhao, L., Tian, L., Zwinger, T., Ding, R., Zong, J., Ye, Q., & Moore, J. C. (2014). Numerical simulations of Gurenhekou Glacier on the Tibetan Plateau. *Journal of Glaciology*, 60(219), 71–82. <https://doi.org/10.3189/2014JoG13J126>
- Ziemer, F. A., Hock, R., Aschwanden, A., Khroulev, C., Kienholz, C., Melkonian, A., & Zhang, J. (2016). Modeling the evolution of the Juneau Icefield using the Parallel Ice Sheet Model (PISM). *Journal of Glaciology*, 62(231), 199–214. <https://doi.org/10.1017/jog.2016.13>
- Zuo, Z., & Oerlemans, J. (1997). Numerical modelling of the historic front variation and the future behaviour of the Pasterze Glacier, Austria. *Annals of Glaciology*, 24, 234–241. <https://doi.org/10.1017/s026030500012234>
- Zwinger, T., & Moore, J. C. (2009). Diagnostic and prognostic simulations with a full Stokes model accounting for superimposed ice of Midtre Lovénbreen, Svalbard. *The Cryosphere*, 3(2), 217–229. <https://doi.org/10.5194/tc-3-217-2009>